POLITECNICO DI TORINO

Course of Master's Degree in Civil Engineering

Master's Degree Thesis

Probabilistic robustness capacity curves of R.C. structures in seismic zone

Supervisor
Prof. Paolo Castaldo
Dott. Ing. Diego Gino

Student
Bartolomeo Minutella

March 2020

Abstract

Catastrophic consequences, both in terms of human and material losses on high interest structures, caused by exceptional events, brought AEC sector experts to show growing interest towards structural safety in last decades. In particular, a new concept of structural *robustness* was defined: robustness is intended in a more specific sense as the capability to support extreme loads due to exceptional events trying to prevent disproportioned collapse. Several researches have already been done, and a lot of efforts are still spent by scientific community with the objective to better understand the problem and to propose solutions regarding the structural robustness theme.

The *probabilistic analysis* approach, integrates in this continuously developing context trying to define a more accurate structural design process which implies increasing efficiency in the whole realization process (from the design to the construction), respecting the established safety thresholds and looking also at the principle of economic sustainability.

The combination of these two issues, of paramount importance for structural engineers, lead to the adoption of a probabilistic analysis approach for the evaluation of the structural robustness and thus of the structural capacity of a building, with the final aim to define the *reliability* of a structure. Therefore, this master's degree thesis represents another piece of this complex and articulated mosaic, that researchers are trying to build one tessera after other.

In this work, probabilistic robustness analysis is performed on a 2D R.C. multistorey plane frame in seismic zone. After the preliminary design stage with the classical semi-probabilistic approach, a random *sampling* is conducted both on *material properties* and *actions*. The sampling was made using the *Latin hypercube simulation* (*LHS*) technique which is a particular Monte Carlo sampling method; therefore, 100 different structural models were generated from the random values of each sampled variable. Then, a displacement-control *push-down* analysis was conducted on each of the 100 models on Atena2D software, through a non-linear analysis, imposing a controlled displacement to the top of the central column of the ground floor which was removed. The resulting load-displacement capacity curves were thus exploited to determine the *dynamic amplification factor* (*DAF*), by using the energetic theory proposed by Izzuddin and others.

Acknowledgements

Questo lavoro di tesi sugella la fine di un intenso percorso di crescita sia da un punto di vista umano quanto didattico. Era il Marzo del 2014 quando misi per la prima volta piede al Politecnico, dopo sei anni ne sto uscendo una persona diversa e credo più matura. Sono fiero di aver creduto in me stesso sin dal primo giorno e di non aver mai pensato di stare al posto sbagliato, ho vissuto la mia vita da fuorisede e da studente di ingegneria con grande grinta, frutto di un'innata passione che mi ha sempre spinto a guardare oltre l'ostacolo circostanziale.

Ciò che mi porterò dietro, a valle di tutta questa esperienza, non sarà solo un Titolo, che chi mi conosce sa bene cosa voglia dire per me, ma saranno anche i rapporti tessuti e quelli maturati durante questo percorso. Ognuno di loro, nel bene o nel male, chi più chi meno, ha scandito la mia vita negli ultimi anni, mi sembra doveroso per cui ringraziarli.

Le prime persone che voglio ringraziare sono Luca e Ludovico, definirli coinquilini penso possa solo sminuire il nostro rapporto. Se c'è una cosa di cui sono certo è che senza di loro non sarebbe di certo stato tutto lo stesso. Auguro a tutti nella vita di incontrare delle persone che vi capiscano e vi facciano stare così bene. Leonardo, non un semplice complice di giochi quotidiani, sono contento di quello che sta diventando e credo di poterne andare anche un po' fiero. Gandolfo, una delle persone che ha alimentato la mia crescita accademica più di chiunque altro.

Ringrazio quindi tutta la famiglia di via Morghen che negli anni ho visto crescere, trasformarsi e cambiare pelle di continuo, così come tutto l'universo di persone che attorno ad essa hanno gravitato a vario titolo, credetemi sarebbe letteralmente impossibile poterli citare tutti senza dimenticarne qualcuno.

Tutti i miei amici, vicini e lontani, con i quali negli anni ho preservato e, nella maggior parete dei casi, maturato rapporti unici; loro sanno che a me piace definirli Fratelli, per me sono questo, sono parte della mia vita. Un doveroso ringraziamento a tal proposito devo rivolgerlo a Domenico G. per la grossa mano fornitami per la stesura di questa tesi di Laurea.

Il mio non più collega ma amico Gabriele M., come ho già detto in svariate occasioni, la sua lungimiranza è spesso stato un faro nella nebbia universitaria, la nostra complicità una cosa indescrivibile. Elena che mi sopportato soprattutto negli ultimi anni e al fianco della quale ho lavorato meglio che con chiunque altro in tutta la mia carriera universitaria e non, è anche grazie al nostro reciproco aiuto se questo lavoro oggi trova una degna conclusione. Tutti i miei colleghi per la grande stima avuta nei miei confronti, sempre.

Tutti gli amici conosciuti a Leuven durante il mio periodo Erasmus in Belgio, Gabriele N., Lorenzo e tutti gli altri. Lasciare casa non è mai facile, lasciarla per la seconda volta vi assicuro che può solo essere peggio. Li ringrazio per avermi inconsapevolmente aiutato e risollevato in uno dei periodi forse più bui degli ultimi anni.

Il Professore Paolo Castaldo e Il Dott. Diego Gino, perché quando incontri due persone così preparate e allo stesso tempo così umane, in un percorso del genere, puoi solo sentirti una persona fortunata.

La mia famiglia, perché ha sempre creduto in me e mi ha sempre spronato a fare di più, mi scuso con loro per la difficoltà a mantenere i rapporti a distanza, ma chi mi conosce sa cosa significa per me sapere di avere delle persone che ti vogliono bene in tal misura anche se a migliaia di chilometri di distanza. Mia sorella Irene, con la quale ho maturato negli anni un legame inossidabile e una complicità crescente, mi ha sempre fatto capire cosa voglia dire studiare e cosa sia il sacrificio, di queste glie ne sarò sempre grato.

Infine, non negando l'emozione nello scrivere queste ultime righe, vorrei ringraziare mia Madre e mio Padre, per quello che sono e soprattutto per quello che mi auguro sarò. Mi hanno sempre supportato sin dal primo giorno, con la dovuta fermezza e la saggezza che li contraddistingue, mi hanno sempre fatto capire l'importanza di ogni decisione presa, lasciandomi però sempre libero di poter correre liberamente i miei rischi. Sono orgoglioso di loro così come spero lo siano loro di me. Tutto questo lo devo principalmente a loro. Grazie Mamma e Papà.

Infine un saluto al mio caro zio Cataldo.

Ai miei nonni,
Bartolo e Giuseppe

Contents

List of Tables

List of Figures

Chapter 1

Introduction

1.1 Background

Structural design has always followed evolution of society and has always been conditioned by it. At the same time progress both in design and in construction procedures, have influenced the life of human beings. Therefore, the idea of structure cannot be limited to the concept of a simple building; structure means also safety, family, work, in simple word structures are an inextricable part of our life.

Duty of a structural engineer is to guarantee an appropriate design process which can answer to community needs, being always in line with the times. For this reason, continuous efforts are spent by engineers to update the way in which a structure is conceived and then realized. Probability based design approach seems to represent a reliable methodology to rich the best solution in terms of practical and economical efforts for structural design. Probability, in AEC (Architecture, Engineering and Construction) sector , assumes a particular acceptation, is indeed not intended as relative frequency but as the degrees of belief in relation to the various uncertainties, and suitable to decision making processes [1]. Although the stochastic approach require a broad data set, that in any case cannot describe exactly the real entity of used materials and applied loads, it can guarantee a more detailed analysis of structural systems, returning a more reliable final result and more efficient than that obtained with the deterministic approach using safety factors [2].

Nowadays developments are needed when dealing with extreme events that were not considered, or only partially, up to last decades in performing structural analysis. Especially in case of extraordinary events of both natural or anthropic origin, like explosions, fires, avalanches or terroristic attacks that often cannot be previously predicted. All this type of events can determine critical conditions for a structure that often cannot bear these exceptional loads for which it was not designed. In particular, the static conditions of equilibrium result to be locally not satisfied triggering a chain of events that in some cases can leads to the partial or total disproportioned collapse of a structure. Terrible events like the disaster of 11 September 2001, which caused the total collapse of the so-called Twin Towers and thousands of victims Figure 1.1, or the Ronan Point Tower explosion in 1968 represented a shock for the entire building community, not only for the material consequences due to the structural collapse of the buildings, but mostly for human loss.

The concept of Structural Robustness has born to take care of this new aspect of increasing importance in structural design process, in particular for buildings that represent centres of large economic and social interest. Thus, design a Robust structure, means guarantee stability in a wider sense, sometime distant from the academic meaning but closer to human and social concerns.

Figure 1.1: World Trade Centre twin towers collapse

1.2 Thesis organization

Therefore, *Robustness* and *Reliability Assessment* represent the keywords of this thesis which has as main goal to merge and join together these two aspects of structural engineering; the starting point consist on the design of robust structure with a semi-probabilistic approach, then a single frame of the whole structure is considered and a progressive collapse due to the removal of the central base column is simulated for 100 random combinations of material properties and applied loads through a probabilistic analysis. An amplification factor is applied to loads in order to simulate dynamic response of structure due to suddenly removal of a structural element. The resulting behaviour of each single random simulation could lead to the definition of a reliability index which could describe probability of failure of the entire structural system.

After this brief introduction, in Chapter 2, the different section of the Italian CNR document about structural robustness [3] (Instruction for the construction robustness assessment), are described in all its sections, starting from the definitions of robustness, describing the actions on the structures and the concept of disproportioned collapse, to finish with suggestions on structural design of robust RC structure.

In chapter 4, the design of a concrete structure in seismic zone is presented; the design procedure is conducted observing the NTC 2018 [4]. Assessment respecting ULS are conducted respecting the resistance hierarchy criterion. After the design procedure and thanks to previous thesis work, the structural system is improved to obtain a robust frame which will constitute the basis of the later work steps.

In chapter 5, ATENA 2D software by Cervenka is introduced. It is the chosen finite element software to perform linear and non-linear static analysis on the multi-storey reinforced concrete plane frame, indeed he high level of detail reachable with this software allows the user to perform very refined structural analysis.

In chapter 6 the practical reliability analysis is introduced defining how random loads and material properties are determined and how the 100 different simulation are built defining the characteristics of the FE models. In this section moreover, the capacity curves coming from the set of probabilistic push-down analysis are detected and analysed to describe the global resistance of the structure against the simulated collapse.

Chapter 7 will deal a particular application of the previously found capacity curves: the determination of the dynamic amplification factor (DAF). Firstly, the theory behind the DAF will be reported, after a simplified framework for the robustness assessment will be presented and, therefore, part of it will be used to define the probabilistic distribution of the DAF.

Finally, the last chapter 8 is reserved to conclusions and suggestions for future works on reliability analysis and structural robustness assessment.

Chapter 2

Structural Robustness

2.1 State of art

The concept of *Structural Robustness* has not yet found a universally accepted meaning in literature, indeed it is possible to find so many definitions, often similar but never exactly coincident; this lack of a robust and common theoretical background is accompanied by an equal absence of shared procedure to be applied in order to satisfy the structural robustness requirements. The increasing influence of exceptional events on structural safety and, needs of well-defined procedure to be followed by the designer, will lead hopefully, in a near future, toward a common approved theory and regulation of the structural robustness matter.

It must be specified that all the contents of this chapter are referred to the Italian CNR document regarding *Structural Robustness* [3].

2.1.1 General definitions

According to several authors and technical specifications, a global definition of *Structural Robustness* can be given as follows: it expresses the capability of a structure to avoid disproportioned collapse to exceptional event, that trigger a local damage of the structure.
The *Disproportioned Collapse* represents a case of structural failure of the structure, characterized by the presence of a level of damage which is disproportionate with respect to the original cause.
Sometime the collapse can be a *Progressive Collapse* when, after a local damage, different members of a structure fail one after the other as they get overloaded, like an unstoppable chain of events: the main consequence in this case is the redistribution of loads and the continuous variations of the equilibrium conditions of the structural system.
The disproportioned collapse can be avoided through some mitigation actions in the design phase: the *Specific Load Resistance* aims to increase the local resistance of some specific structural elements, which eventual failure could generate a disproportioned failure of the structural system. Also, the *Alternative Load Path* procedure results to be very useful in the condition aforementioned: indeed, it allows to redistribute the load that was originally sustained by the collapsed elements, transferring thus its portion of load to the nearest ones.
For a broader picture of the situation some other definitions of Robustness are reported

below:

Robustness is the ability of a structure to withstand events like fire, explosions, impacts or the consequences of human error, without being damaged to an extent disproportionate to the original cause [5].

Robustness is a property of the structure and the extent of the initial damage. If the initial damage is specified as a notional damage, its causes are immaterial, and robustness becomes a purely structural property [6].

Robustness: the ability of a structure subject to accidental or exceptional loading to sustain local damage to some structural components without experiencing a disproportionate degree of overall distress or collapse [7].

2.1.2 Current legislation

Unfortunately, any legislation is not yet well developed in the robustness reserved section. Only brief indications of general meaning are given, without neither a deep description of the various problems linked to the non-robustness of a structural system, neither detailed practical indications to improve it on a building.

Eurocode – Basis of structural design [8], at 2.1 for example, states simply that a structure has to be designed in such a way to not be damaged by events like explosions, impacts, consequences due to human error, in a disproportioned measure with respect to the cause of the original damage. Then a list of global safety measures is presented without any detailed specification. While in Eurocode 1 [5] at 3.2 the notions of alternative load path, key elements and ductility are briefly exposed.

Finally, also the Italian NTC 2018 [4], at 3.6 classifies the extreme actions, the risk scenarios giving some suggestion about design procedure to guarantee the robustness of a structure at 2.2.5.

2.2 Accidental actions

In the classic structural design procedure, the involved actions, such all the gravity or seismic loads, are modelled and applied to the structure through well-defined and widely approved methods that, in the case of the semi-probabilistic approach, give good results in terms of reliability and safety of the structural system.

Although it is easy to imagine a lot of causes for the accidental loads, it is not so easy to model them in such a mathematical way, nor to predict the occurrences of this type of accidental actions, which often are totally casual and cannot be predicted previously, since are determined by human actions, like terroristic attack.

Therefore, the main problem of defining the robustness of a structure is firstly to determine which type of actions it will withstand during its life cycle, with what intensity and their frequency of occurrence. Fortunately, when dealing with accidental actions, nearly always, we are talking about rare events that occur only in extraordinary conditions. The acronym *LPHC* (low-probability, high-consequence) describe, on one hand, exactly what was aforesaid, defining the main characteristics of the treated actions: the low probability of occurrence; on the other hand these actions have as main characteristic the big impact that they may cause on a structural system in terms of caused damages.

2.2.1 Classification

Large efforts were spent during last decades, searching for analytical models that should describe these actions, in order to apply them to the structural models and verify if robustness requisites are satisfied. Moreover, all the accidental actions cannot be represented by a unique model, since different are the origin that cause this accidental loading, natural or anthropic, voluntary or involuntary.

A good classification for accidental actions seems to be that proposed by [3] which divide them in three different categories:

- *Category 1*: actions deriving from natural phenomena or from involuntary human activities: the former can be earthquakes, meteorological phenomena and landslides while the latter concern explosions and non-arson fires;
- *Category 2*: actions intentionally caused by man, such as vandalism and terrorist attacks;
- *Category 3*: actions resulting from errors in the conception, design or execution of the construction.

From the point of view of the interaction between the event and the construction, these actions can act on the structure such as:

- distributed loads of exceptional entity;
- impact loads;
- accelerations due to seismic actions;
- induced strains or deformations.

Actions can also be classified on the basis of their duration, although the exceptional actions are in most cases very short compared to the useful life of the structure; in structural modelling, they can be applied to the structure statically, dynamically, or with an impulsive pattern.

2.2.2 Actions of Category 1

Belong to Category 1 all the natural phenomena or those deriving from involuntary human activity included earthquakes, tsunami, landslides, floods, tornadoes, fires and explosions. These exceptional actions and the type of load that they can generate on the structure are briefly described below.

Earthquake is assessed by technical specifications by means of non-epicentral seismic actions, which are taken considering laws for attenuation of the accelerometric components. In the case of epicentral actions, the reduced distance between the epicentre and the structure affected by the seismic action, does not allow adequate damping, and this leads to a substantial increase with respect to design actions, which can therefore be insignificant.

Tsunami is a natural phenomenon due to submarine movements that determine the development and propagation of waves in the sea that can have considerable height when they approach the coast, leading to widespread flooding. Based on the topography of the coastal area, it is possible to evaluate the extent of the areas flooded by a tsunami due to a seismic action, as well as the submersion height and water flow velocity. The effects on the constructions, although variable, can essentially be attributable to impact pressures caused by the flow in movement, by concentrated forces due to the debris transported by it, and hydrostatic thrusts.

Landslides are phenomena due to the loss of stability and/or cohesion of a fractured soil/rock mass, usually of natural origin but sometimes also caused by anthropic action; the impact force of a landslide is a function of the speed and type of soil mass affected by the phenomenon.

Floods are natural phenomena due to heavy rainfall or breakage of hydraulic works along the hydrographic network which lead to the raising of surface waters and the subsequent flooding of normally dry areas. The effects of this phenomenon on buildings are manifold: static and dynamic pressures exerted by the water in quiet or in motion, impacts of objects carried by the current, saturation of underground soils, localized erosion.

Tornadoes are violent vortices of air which form at the base of the clouds reaching the ground; these meteorological phenomena are generated by a low-pressure center around which the air masses rotate producing strong winds and copious rainfall. The strong winds, that are generated during this type of meteorological phenomena, can seriously damage buildings, break down plants and power lines, move cars from the roadway, etc. Therefore, during meteorological phenomena of this magnitude and power, it is good to consider two distinct actions on buildings: the pressure of the wind on the surfaces and the punctual impact forces of the objects moved.

Fires can cause the combustion of structural and non-structural elements; the method of calculating the action, the response of the structures to the fire and prevention are detailed in many regulatory documents to which it is possible to refer.

In *Explosions*, the pressure wave forms a shock surface that moves at a very high speed and carries a significant amount of energy; the arrival of the shock wave on a surface, placed at a certain distance from the explosion point, results in an almost instantaneous increase in pressure. The amount of pressure on the surfaces of a building is different in cases of confined and non-confined environments.

Impacts on structures can be assessed by means of an equivalent static analysis or through a dynamic analysis. The forces that the impacting body transmits to the impacted structure depend both on the type of impact and on the stiffness and deformability of each of the two bodies.

2.2.3 Actions of Category 2

The evaluation of actions due to vandalism and terrorist acts is much more complex than the previously indicated for the actions of Category 1, as it is first of all necessary to analyse the intentions and motivations that push individuals, or the group, to provoke a harm on society.

The objectives of vandalism are usually chosen on the basis of the degree of difficulty in being able to generate damage, on the basis of the degree of protection and surveillance of the structures/infrastructures, on the basis of the number of people necessary to complete the terrorist act.

The theory emphasizes the fact that, when the primary objectives are too protected or difficult to attack, the focus shifts to secondary, simpler objectives. In general, terrorists use similar attack modalities, based on previous attempts that have proven effective, until a good attack modality emerges which turns out to be particularly effective.

2.2.4 Actions of Category 3

Although they cannot be considered as traditional actions acting on a structure, the errors that can be committed in all the design and construction phases of a structure are possible scenarios in which robustness has to be assessed.

These errors lead to the creation of a structure not able to bear the design actions, varying the structural behaviour with respect to what is indicated by the designer. This kind of danger is strictly connected to the quality of the process and to the used control procedures.

Structural conception errors are those concerning the overall behaviour of the whole structure subject to the design actions. The design errors instead concern the final result of the project, including the construction details to be carried out on site or in the factory. Finally, the execution errors are those that concern the construction of the structure, including the connections between the elements, by the workers.

2.3 Disproportioned Collapse

Not always the consequences due to the application of a load on a specific structural element or in a portion of the structure, involves only that element or that section of the building; especially when dealing with extreme actions, which entity is so much higher than the design resistance of each single element or connection, what happen is that also the surrounding structural elements result to be involved in a partial or total failure. When the part of the structure affected by the collapse results to be not proportioned with respect to the action that caused it, then it is possible to talk about *disproportioned collapse*. In the particular case in which a disproportioned collapse is the result of a chain of event triggered by the failure of a single element we can talk about *progressive collapse*; therefore the progressive collapse is only a particular type, a procedure that lead to the disproportioned one, which refers in more global meaning to the entity of the final consequences of the collapse.

The entity of the collapse is, of course, strictly related to the type of structure; in turn the structural typology depends on a lot of factors, the resistance of each single element, the structural redundancy, the ductility of the structural system, the type of connection and others. A typical robust structure has an high ductility reserve and an high structural redundancy, which means that in the case of an eventual failure of some element, the structural system will activate an alternative load path that, together with the structural ductile reserves, will guarantee that the building will not collapse at all, but only in the interested area. On the contrary, structure with no redundancy and rigid connections like a precast structure, are more subjected to disproportioned collapse. In the latter case often, *fuse elements* are adopted, to adsorb the stress increment due to the application of an accidental load.

2.4 Risk Analysis

2.4.1 Risk definition

The term "risk" has a statistical meaning which indicates the probability of the occurrence of a dangerous event capable of triggering a disproportionate event and causing considerable damages to people or things.

In the *Robustness* field, all the structures potentially may collapse, since each building can register during its life cycle the presence of an extraordinary event which causes an exceptional action. Therefore, sensibility and attention must be paid when dealing with the design of each type of structure. Fortunately, the events that can trigger the disproportionate collapse, are characterized by very low probability of occurrence.

In general terms, the risk is determined by the combination of three factors, the hazard (P), the vulnerability (V), and the exposure (E):

$$R = P \cdot V \cdot E \tag{2.1}$$

Risk objective evaluation, result to be very difficult since its conception, is strongly dependent by the point of view of who is evaluating it. For example, common people tend to underestimate the risk evaluating what can happen on average instead of evaluating the probability of the single event, on the contrary, large companies prefer to invest a certain annual sum and take out private insurance to cover the risk of incurring a strongly adverse event. On the other hand, from a community point of view, sensitivity towards accidental events is far superior to events of lesser importance but which over time involve a greater number of people and which statistically speaking are riskier; like in the case of air disaster against cars accident. Therefore, the acceptable risk threshold turns out to be strongly subjective, and regulation by sector authority are needed to overcome this problem. Generally, there is a threshold defined as *de minimis* and it takes a value of $10^{-7}/year$ which represents the limit under which an event in no more considered dangerous by the society.

2.4.2 Probabilistic Risk Analysis (PRA model)

The main goal of a probabilistic risk analysis is to determine the probability of collapse $P[C]$ of a structure, which in turn define if a structure is robust or not. The mathematic model used by [3] to define it, is the *Probability Risk Analysis* (PRA) method, based on the concept of correlated probability. Therefore, considering H (Hazard) that represents a dangerous event with a low occurrence probability but with serious consequences, and considering as well SL as the local failure, the mathematical expression writes as follows 2.2:

$$P[C] = P[C|SL] \cdot P[SL|H] \cdot P[H] \tag{2.2}$$

where:

- $P[C]$ represents the annual probability of structural collapse C due to event H, related to the "resistance to collapse" of the system;
- $P[C|SL]$ which represents, given the local damage SL, the conditional probability of disproportionate collapse;

- $P[SL|H]$ which represents, given H, the conditional probability of local damage;
- $P[H]$ is the probability of occurrence of event H, assumed equal to the average annual occurrence rate.

First, is it important to limit the probability of an exceptional event $P[H]$, by adopting prevention measures that affect the occurrence of the event as well as the average annual rate of occurrence. In this way is possible to work on the mitigation of the dangerousness of the phenomenon.

An alternative choice is work on the probability of local damage given the harmful event $P[SL|H]$; in this way the mitigation of local vulnerability becomes important, which allows you to preserve the structure from a disproportionate event despite the occurrence of the Hazard. The disadvantage of this procedure is that it is uneconomic, moreover it can lead to un underestimation of some action acting on the structure.

Finally, the most interesting strategy for the purpose of this thesis, is work on the third factor that defines the equation of the PRA method, analysing the probability of structural collapse given the local damage $P[C|SL]$ and working on the structure for mitigating global vulnerability, for example by choosing to compartmentalize the structure or foresee the possibility that alternative load paths may develop. $P[C|SL]$ indeed, can be seen as the structural robustness itself of a structural system, therefore, it defines the strength of the structure and is the only term on which a structural civil engineer can efficiently act, in order to reduce it; its assessment in probabilistic terms can be complex, requiring, the use of advanced analysis methods, such as nonlinear dynamic analysis, performed on detailed and realistic numerical models.

In the case in which the designer doesn't act on the term $P[SL|H]$, thus neglecting the local resistance of each single vulnerable element, the 2.2 takes the new form expressed by 2.3 where the term $P[SL|H]$ assume a value equal to 1:

$$P[C] \approx P[C|SL] \cdot P[H] \tag{2.3}$$

In this case the concept of *Alternative Load Path* has to be considered, since it express the capability of a structure to find an alternative for the equilibrium of the whole structural system, reorganizing the internal distribution of the tensional state among the elements surrounding the collapsed one. The attention is therefore focused on the global structural resistance of the structure, and not on the local one. From this point of view, it is possible to take action with constructive provisions aimed to increase greater redundancy and structural ductility, considering resistant mechanisms not usually taken into account in ordinary design; these generally are the second order effects such as the high deformation capability of beams and pillars given by the arc behaviour or by the catenary effect.

2.5 Design approaches classification

In the design phase, the first choice that must be taken, is on the type of approach that has to be followed; it strictly depends on the complexity of the problem and on the level of structural robustness assessment that the designer wants to reach, and therefore the safety level he intends to obtain.

In particular the different approaches can be classified according to [9] as follows:

- general approach used for design: prescriptive design process or performance-based design process;
- structural design method: direct or indirect method;
- risk scenario definition: specific threat or generic threat.

2.5.1 Prescriptive design process and performance-based design process

In most situations, a prescriptive design approach defined by the regulatory bodies is applied, which imposes a performance capability standard on the structure. This type of approach is characterized by standardized threshold that must be checked; these minimum requirements, based on existing structures, results to be sufficient to increase security against a disproportionate collapse, slightly increasing the computational effort of the professional design compared to a traditional one.

The performance-based design approach, on the other hand, has a different nature and does not require following predefined analysis paths, but releases the designer from any regulatory constraint, giving him freedom to experiment with new structures and materials, with the burden of defining the structural verification path himself and to find a valid construction solution. Furthermore, this approach allows a direct evaluation of the structural capabilities allowing the comparison of multiple solutions and making possible a precise cost-benefit analysis.

2.5.2 Direct or indirect approach

The indirect design methods are mainly prescriptive and aim to obtain robustness by guaranteeing a minimum level of connection between the various components of the structure in order to exploit more effectively the redundancy of the system and the ductility of the members. To apply this method, firstly it is necessary to verify that the structure under analysis is comparable to a set of just studied structure with a well-known solution and defined standard. The main purpose of this method is to guarantee a sufficiently robustness requirement paying particular attention to the structural ties like that between beams and columns or between beams of different hierarchy level. These structural ties, Figure 2.1 will affect the structure increasing its ductility and developing secondary phenomena like the catenary effects.

On other hand, the direct method is mainly used in the performance-based approach, aiming to define the structural capabilities that must be achieved to satisfy the design requirements. Unfortunately, it requires more complex analytical models and thus more skills from the designer. In this case, once the risk scenario has been defined, the resistant capacity of the structure is assessed by working to ensure that a disproportionate collapse does not occur.

In this case, two different structural design pathways can be followed:

- *Local resistance method*: key structural elements are strengthened whose local damage under specific exceptional actions could lead to a disproportionate collapse;

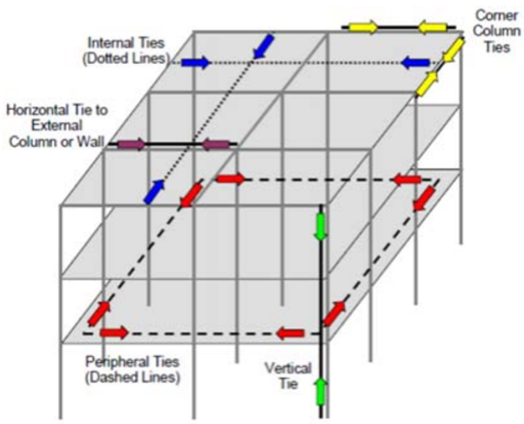

Figure 2.1: Structural connections (DoD, 2016)

- *Alternative load path*: in this case, alternative load paths are designed to prevent the collapse of the structure after the loss of structural element. The analysis is conducted by removing a structural element which is chosen according to the resistance mechanism that the designer wants to test. This simulates the loss of a resistant contribution, for example by removing a column in the case of a building.

2.5.3 Generic or specific threat

Generic threat approach is used when or the exceptional actions or their consequences on the structure are not foreseeable and quantifiable. In the first case nominal actions such equivalent loads are defined and applied to the structure, in the second case an initial local damage is forecasted an its evolution is studied with respect to a possible disproportioned collapse.

While the specific threat design methods foresee the exceptional actions and their consequences on the structure that result to be explicitly defined; an evaluation on how these can lead to a disastrous evolution of the structure is therefore conducted.

2.6 Robustness conceptual design

The collapse risk probability can be efficiently reduced by adopting some design strategies that will improve structure performances during its life cycle, especially when a building has to face with extreme events. These conceptual strategies allow the designer to create a structure that can potentially bear higher loads with respect to another one traditionally designed:

- the *structural redundancy* guarantees an increase of hyper-staticity to the structure being able to exploit an alternative load path;

- the presence of *tri-dimensional ties* results to be very useful in particular when collapse is already started since they allow a good loads redistribution;

- to take good advantage of the redundancy, a good level of *ductility* is required as well, this means that big deformations and rotations must be allowed by the system in the deformed condition after the removal of a structural element;
- *uniform distributions* of structural elements, not only from a geometrical point of view, but intended in a broader sense also as mass, resistance, strength of the single elements, gives a more efficient load redistribution;
- *resistance hierarchy* has to be fully respected guaranteeing that shear or punching failure doesn't precede the membrane one that exploit structural ductility to delay the total collapse of system or sub-system (some floors only);
- capability to support *inversion of the actions*, like in the case of explosions when some structural elements can pass from a tensional state to a compressive one or vice-versa.

Below, three different design methods that use the just explained design strategies in them, will be explained.

2.6.1 Local resistance method (key elements design)

Local resistance method has as main goal that of prevent a disproportioned collapse due to the failure of a single structural element. In other words, if the first element doesn't fail, no chain of event that lead to the total failure of the structure is triggered. With this method therefore, the resistance of each single key element must be correctly calibrated to allow a correct response of the global system. This means, for example, that the failure of beam-column node for bending, must precede the shear or the punching one, this to allow the exploiting of second order effect linked to the bending behaviour of beams and slabs.

Generally, structures for which this approach is suggested, are building with a small structural redundancy and with no possibility to developpe an alternative load path; also structures with critical resistance sections like a transfer floor Figure 2.2 which represent a structural weakness for the whole system, are a perfect field of application of the local resistance method.

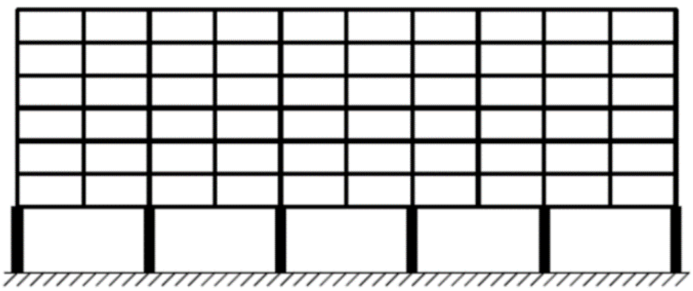

Figure 2.2: Building with a transfer floor (Kokot e Solomos, 2012)

Key elements can be designed in different ways: if the action to which the structural element has to withstand is well defined by the designer, a direct method can be used, evaluating the needed design resistance that the element must have in order to behave as requested exploiting the ductile reservoirs of the system working in bending; while, on the other hand, an indirect method of prescriptive nature is suggested when well already existing elements can be implemented to satisfy the circumstantial requirements.

2.6.2 Alternative load path method

Also in this case, the main objective of the design procedure is to avoid non controlled behaviour of the structure in a critical circumstance like the presence of an exceptional action. What change with respect to the previous case is that for this method, the designer has not to take care about the failure of a single structural elements, but has to face with the global behaviour of the structural system as consequence of the loss of a key element. This means that the structure must be designed taking into account the future possible loss of some bearing section. For this purpose, in the design procedure the loss of a structural element is simulated and the building response in term of loads redistribution is analysed. Also in this case the main goal is to ensure that the structural elements failure will respect the resistance hierarchy principle, triggering second order effects like the catenary one, that in a condition like the removal of a base column, like that reported in Figure 2.3, results to be of paramount importance to avoid the total collapse of the structure.

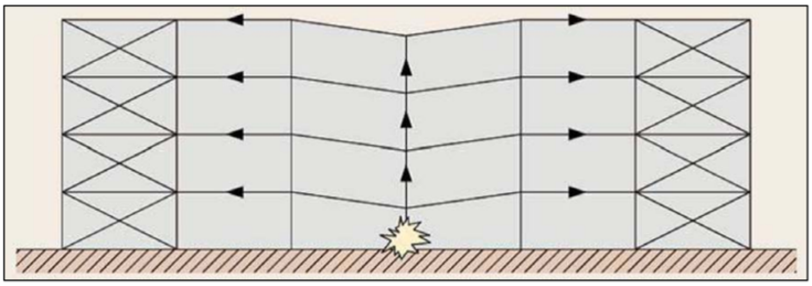

Figure 2.3: Example of alternative load path (SCI, 2011)

2.6.3 Compartmentation

This method is used as well, to prevent the evolution of a local collapse in a global one. It is mainly used in reinforced concrete precast structures that often, are already divided on sub-section depending on their structural scheme. What basically is done is to create strong structural elements at the edges of these sub-structure using fuse-like elements to connect them which weakness allows, in case of collapse of one of these sections, to stop the collapse, preserving the adjacent autonomous structural section. Both prescriptive or performance-based approach can be used in this case.

2.7 Robustness practical design

The study of structural robustness, for a design sensitive to minimizing the risk of disproportionate collapse related to an exceptional event, requires considering a large number of variables for the definition of the model, the materials but also the analysis procedure. Therefore, is important a careful evaluation of expert designers, capable of calibrating the analysis to obtain consistent results.

2.7.1 Structural models

Regarding material properties, the correct choices made by the designer are fundamental to obtain consistent results with respect to the expected ones. Each choice has to be made depending on the level of detail the author wants to reach, and the level of reliability fixed. Different type of structural model can be exploited.

- *constitutive linear-elastic models*: these are the simplest type of models, looking at both the input choice phase and at the output interpretation. They allow to build up simple model allowing the structural system to behave in the elastic filed and, for this reason, they don't admit large displacements and rotations. For this reason, these models result to be very useful in preliminary analysis phase when global structural behaviour have to be studied. But on the other side they are not so good in describing complex phenomena like a disproportioned collapse;

- *constitutive non-linear models*: these models are valid for the study of disproportionate collapse, as they are able to describe the behaviour of the materials due to high deformations in the inelastic field where plasticization, covers an important dissipative role, that cannot be overlooked in case of a realistic analysis. Furthermore, in this type of law it is possible to consider the resistance increases due to the instantaneous application of force (as in the case of explosion, vehicle or aircraft impacts), making the constitutive law dependent on the speed of application of the load which is important to take into account for the definition of robustness;

- *global and local models*: an efficient structural analysis must be conducted on different level of detail, since not all the parts of a building play the same role and have the same structural criticism. Therefore, global models are used to define the general behaviour of the structure, for example in terms of maximum displacement or force reaction distribution, while the local models are exploited for more accurate level of detail and are thus reserved for example for a beam-column connection analysis or a bolt connection of a steel frame structure.

2.7.2 Types of analysis

Robustness analysis involves a large set of simulated events that a structure has to face with, like the removal of a column or the suddenly collapse of a beam; these causes lead the structure to behave in a dynamic way; changes in the static equilibrium conditions indeed, means to force the structure to find a new one, if possible, otherwise collapse happens. These latter phenomena are thus totally dynamic, therefore dynamic analysis have to be considered. Moreover, the critical conditions imposed, trigger plasticization of sections and nonlinear behaviour for which coherent analysis are required. The type of analysis among which is possible to choose in the design phase are the following.

- *static linear analysis*: used for its simplicity of application but it provides approximate results; therefore, it is applied only for very simple structures, using less complex programs. They can be used by increasing the effects by means of a suitable dynamic amplification coefficient; obviously the linear analysis do not allow to capture important effects such as the redistribution of stresses, the geometric and mechanical non-linearities and therefore the catenary effect;

- *non-linear static analysis*: also in this case the dynamic effects are taken into account by means of amplification coefficients but unlike the previous approach the geometric and material non-linearities are considered; in this way, through the definition of realistic constitutive laws, it is possible to study the membrane effect and evaluate the real materials behaviour in the inelastic field;

- *dynamic linear analysis*: allow to take into account the dynamic effects connected to local damage/collapse, however it does not allow to study the effects related to the non-linearity of the problem;

- *dynamic non-linear analysis*: they are the most complete and suitable type of analysis to simulate especially for problems with a high level of complexity. The calculation is generally performed using three-dimensional, non-linear models, in conditions of large deformations. However, not all calculation programs are able to carry out this type of study. Due to the complexity and the large number of parameters involved, this type of analysis can only be carried out by expert designers. The computational efforts that these models entail, especially in the case of large structures, must also be taken into account.

2.8 Reinforced concrete structure cast in-situ

2.8.1 General behaviour of an RC structure

Reinforced concrete structures cast in-situ, present several favourable characteristics towards exceptional actions. Indeed, structural continuity, and thus structural redundancy as well, guarantee generally, a good load redistribution triggering easily an alternative load path such as in the case of a column removal. If the structure is well conceived, the ductility reservoirs can be well exploited and the flexural behaviour, together with the second order bending effects, allow a good behaviour of the structural system also after that plasticization stage starts; of course this characteristics are exploitable only if the structure is designed respecting the resistance hierarchy, avoiding the onset of fragile mechanism especially at nodes. Moreover, reinforced concrete columns result to be not very susceptible to instability phenomena thanks to their dimensions. Finally, although the heavy mass of an RC building ensures a good response to explosion consequences, on the other hand it can be a problem since an eventual redistribution of forces would involve heavy loads to be redistributed to other elements.

2.8.2 Membrane effects on RC beams

Membrane effects on RC beams, as well as in RC slabs, guarantee a useful reservoir of resistance against exceptional vertical forces due to the loss of a column or a suddenly increasing of the design load for which the horizontal system was not designed Figure 2.4. In a few words, it consists on horizontal stresses triggered along the whole beam section which improve the flexural behaviour of the beam itself.

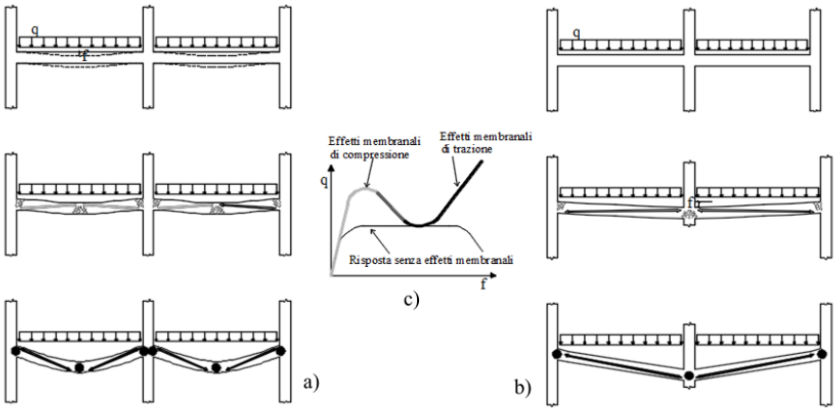

Figure 2.4: Membrane effects on beams (CNR, 2018)

In particular Figure 2.4 (a) represents the case of a distributed vertical overload q on the beams; while Figure 2.4 (b) describe a column removing process in a continuous slab system. In the first case, plastic hinges are formed at the edges and at the mid-spans of the overloaded beams, while in the case of the column removal they starts to form at the nodes were column continue to exist and in the node above the lost column.

The Figure 2.4 (c) finally, defines the behaviour of the load q applied on the slab as function of the inflection generated; it is easy to understand from this last figure as the membrane effect, substantially increases the flexural resistance of the beams, both in compression (in the first stage after cracks starts opening) and in tension (when plasticization occurs).

2.8.3 Behaviour towards column removal

The structural behaviour of reinforced concrete framed buildings subject to a scenario of a vertical load-bearing element removal consists of various phases, depending on the vertical displacement at the section where the column is removed.

The various phases are described with respect to the experimental test shown in Figure 2.5, of a two-dimensional reinforced concrete frame subject to the removal of a non-edge column. The prototype is subject to an imposed displacement at point $P1$, to simulate the relative loss of the column.

The experimental behaviour is represented in Figure 2.6 and Figure 2.7, in terms of force applied at point $P1$, Figure 2.6 and horizontal displacement of point $P2$ Figure 2.7 as a function of the vertical displacement imposed at point $P1$.

The experimental analysis allows to distinguish three different phases:

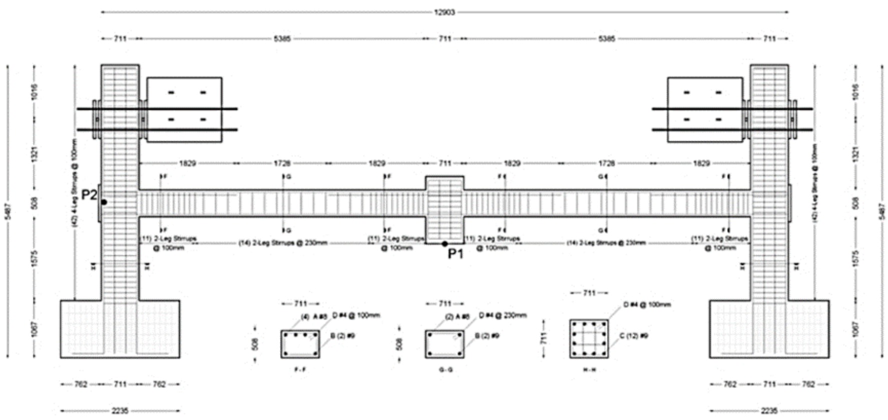

Figure 2.5: Element subjected to experimental tests (Lew et al., 2011)

- Stage OA: related to flexural behaviour of the beam and ends with the formation of plastic hinges at the beam-column connections; point $P2$ is subject to a negative horizontal displacement (outwards) due to the cracking of the beam which leads to an increase in length; If this increase in length is limited by the stiffness of the column, the beam is compressed triggering a compressive arch behaviour.

- Stage AB: softening with decrease of the force applied as the vertical displacement of point P1 increases; the horizontal displacement of point $P2$ begins to change towards cancelling out at point B. In this phase the compression effort in the beam decreases until it is zeroed.

- Stage BC: increase in force applied as the vertical displacement of point $P1$ increases; the horizontal displacement of point $P2$ becomes positive (inwards) and consequently the beam is stretched. In this phase the load is carried by the beam with a combination of flexural effect and a catenary effect from the continuous reinforcement present in the beam. The catenary effect becomes gradually larger as the vertical displacement of point $P1$ increases.

In order for the catenary effect to be established, a continuous reinforcement must be present between the columns on the sides of the one removed by the exceptional and/or extreme event; otherwise the maximum load that can be supported by the structure will be that corresponding only to the flexural behaviour (point A).

2.8.4 Design towards column removal

Using simplifying hypotheses, it is possible to estimate the bearing capacity of a framed system in the case of accidental removal of a bearing column.

The maximum load for purely flexural behaviour (point A of Figure 2.6) can be calculated with the theory of plasticity and with the principle of virtual works with the following formula:

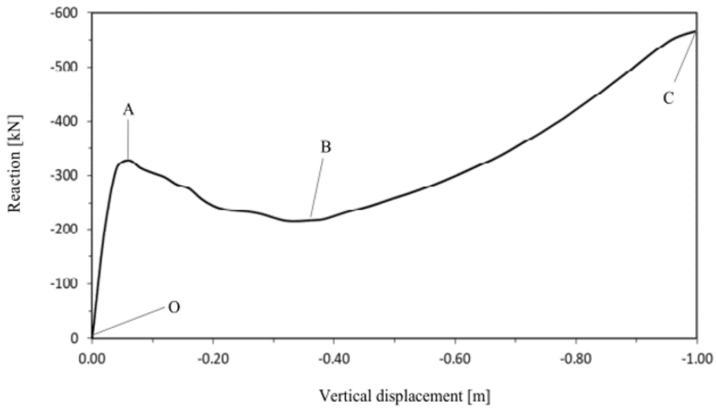

Figure 2.6: Imposed displacement-reaction behaviour with catenary effect

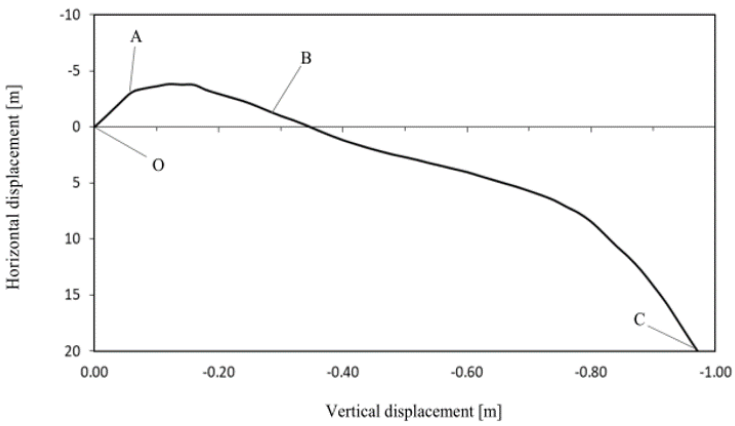

Figure 2.7: Imposed displacement-lateral displacement diagram with catenary effect

$$P_{\mathrm{MAX,FL}} = \frac{2(M^{+}_{\mathrm{PL}} + M^{-}_{\mathrm{PL}})}{L} \tag{2.4}$$

where M^{+}_{PL} and M^{-}_{PL} are the plastic moments of the beam at node for positive and negative moment respectively.

By neglecting the reinforcement in the compressed region in favour of safety, the plastic moments can be calculated in a simplified way as follows:

$$M^{+}_{\mathrm{PL}} = 0.9\,A^{+}_{\mathrm{S}}\,f_y\,d \tag{2.5}$$

$$M^{-}_{\mathrm{PL}} = 0.9\,A^{-}_{\mathrm{S}}\,f_y\,d \tag{2.6}$$

where A^{+}_{S} and A^{-}_{S} are the bar reinforcements of the beam at the connection with the column, respectively for positive and negative moment, d is the useful height of the beam,

f_y is the design yield stress of the reinforcement obtained by applying the relevant safety coefficients for accidental verification.

As regards the catenary behaviour (point B of Figure 2.6), the maximum bearable load can be evaluated as:

$$P_{\mathrm{MAX,CAT}} = 2\,\frac{\delta}{L}\,A_{\mathrm{S,cont}}\,f_t \tag{2.7}$$

where δ is the displacement capacity of the point where the column was removed, $A_{\mathrm{S,cont}}$ is the continuous reinforcement on beam length $2L$ and f_t is ultimate stress of the reinforcement obtained by applying the safety coefficients related to the accidental verification.

For the evaluation of the rotation capacity and the consequent value of δ, reference should be made to experimental values.

In order to establish the catenary behaviour, the designer must ensure that the resulting tensile stress is compatible with the portion of the structure outside the damaged area.

Finally, the catenary behaviour will represent an effective increase in resistance compared to the flexural behaviour, only in the case in which $P_{\mathrm{MAX,CAT}} \geq P_{\mathrm{MAX,FL}}$.

2.9 Probabilistic robustness assessment

Evolution in construction techniques and the mutating social, economic and politic situation have led structural engineers to consider new exceptional actions in the design process; actions that before where marginally taken into account, now need to be considered especially when dealing with structure of high social importance, for which an increasing safety degree is required.

However, is not always possible in the design phase consider all the actions that can intervene during the building life cycle, since it will be uneconomical and technically almost impossible. Moreover, dangerous events can have different impacts depending on the related level of hazard, but also depending on the return period considered for each action as well as the perception that people have of a specific potential risk.

Therefore, only refined comparation, between various potential actions can led the stakeholders to make correct decisions depending on the resulting probability of collapse linked to each of them.

For a correct assessment of disproportionate collapse risk, it may be necessary to consider the presence of multiple harmful events and initial states of damage. In this case, equation 2.2 can be generalized as illustrated in the following equation (valid for independent events):

$$P[C] = \sum_{H} \sum_{\mathrm{SL}} P[C|SL] \cdot P[SL|H] \cdot \lambda_H \tag{2.8}$$

where λ_H can substitute $P[H]$ if occurrence probability is less that $10^{-2}/year$. Values of λ_H are reported in Table 2.1.

If λ_H is lower than the *de minimis* risk threshold, the probability of damage or collapse given that the event H has occurred, will contribute negligibly to the probability of collapse $P[C]$.

Event	λ_H
Gas explosions	$2 \cdot 10^{-5}$ / *apartment*
Bomb explosions	$2 \cdot 10^{-6}$ / *building*
Vehicle impacts	$6 \cdot 10^{-4}$ / *building*
Fires	$5 \cdot 10^{-8}$ / *building*

Table 2.1: Occurrance probability for different exceptional actions

Equation 2.8 can also be extended to define the concept of expected loss, using different metrics for risk assessment: risk of death, probability of collapse and cost-benefit assessment. The annual probability of loss can, in this sense, be calculated according to the equation 2.9:

$$P[L] = \sum_{H} \sum_{\mathrm{SL}} \sum_{C} \sum_{L} P[L|C] \cdot P[C|SL] \cdot P[SL|H] \cdot \lambda_H \tag{2.9}$$

where L represents the appropriate metric to use and contemplates economic losses, serious damage to things and people, loss of human lives and direct costs of the damage.

Conditioned probabilities presented in equation 2.9 can be obtained by a probabilistic risk analysis (PRA), in which it is possible to model uncertainties, study their propagation and the effects on the required performance of the system. In the case of structural systems, this approach is called structural reliability analysis and failure (collapse in the case in question), is considered achieved when demand S (i.e. the effects generated by the actions) exceeds capacity R. The probability of failure is equal to:

$$p_f = \int F_R(x) \cdot f_S(x) \cdot dx \tag{2.10}$$

where $F_R(x)$ *CDF* (cumulative distribution function) of R and $f_S(x)$ is the *PDF* (probability density function) of S.

The probability of disproportionate collapse can be defined in an equivalent manner according to the equation 2.11:

$$p_f = P[S \geq R] \quad or \quad p_f = \Phi(-\beta) \tag{2.11}$$

where β is the reliability index and $\Phi(\cdot)$ is a normal standard distribution function.

If a performance-based design approach is adopted, an acceptable value of risk tolerance has to be defined; in the case of a disproportioned collapse, which main consequence is the loss of human life, decision-makers can assume that the performance objective of safeguarding human life is achieved if the following relationship is verified 2.12:

$$P[C] < p_{\mathrm{th}} \tag{2.12}$$

where p_{th} in the risk threshold dined as *de minimis* which assumes values ranging from $10^{-5}/year$ and $10^{-7}/year$.

Moreover, in the particular case in which the alternative load path method is used in the design phase, the collapse probability becomes $P[C|SL]$, which in turn has to respect the following condition (2.13)

$$P[C|SL] < \frac{p_{\mathrm{th}}}{\lambda_H} \tag{2.13}$$

Therefore, assuming λ_H equal to $10^{-6}/year$ - $10^{-5}/year$, the performance target established by condition 2.13 requires that the conditional probability of collapse be in the order of $10^{-2}/year$ - $10^{-1}/year$.

Consequently, the reference reliability index β_0 for the limit collapse state of conditioned by the occurrence of the damage will be in the order of 1.5, that is significantly lower than that assumed for the ultimate limit state of new buildings for residential use in the case of ordinary actions (i.e. $\beta_0 = 3.8$, which corresponds to a reference probability for the collapse of the order of 10^{-4}).

The theory regarding *structural reliability analysis* until now only marginally treated, will be deepened with more mathematical detailing in the next chapter.

Chapter 3

Basic of reliability method

3.1 Introduction

Generally, in structural engineering, all the parameters involved, such as material properties and design actions, are totally random variables, represented by chosen characteristic values, to facilitate the analysis in a deterministic or more commonly semi-probabilistic approach. This means that each single material used in the construction process, as well as the actions, can never be exactly predicted, therefore the behaviour of the building itself during its life cycle cannot be forecasted with absolute certainty. The term *reliability* is globally used to express the safety level of a structure, a reliable structure means that with high probability it will not fail, but it must be specified that this has not to be considered as an absolute true, since a certain degree of uncertainty will always be present also for the most safe designed structure. People should accept that to build a structure that will never collapse with an absolute certainty, is practically impossible; what engineers can do, is to design following rules based on considerations of social, financial and political nature that define acceptable risk threshold.

3.2 Limit states design, basic principles and uncertainties

The basic principles of structural reliability are reported by the international codes as *ISO 2394*, *EN 1990* and *fib Model Code 2010*.

Reliability and *economy* are the two main concepts on which structural design is based according to these codes. It means that a structure should respect both conditions satisfying *reliability* limits and thus safety requirements but has also to be designed respecting the principle of economic sustainability. The *structural reliability* can be defined as the ability of the structure to comply with given requirements under specific loading conditions during its service life. Quantitatively, the term *reliability* may be considered as the complement to one of the probability of structural failure. The *service life* is intended as the interval for which the structure should accomplish its functionality. The main performance requirements for structural design are represented by *safety*, *serviceability*, *durability* and *robustness* [10].

In order to satisfy the aforementioned requirements, limit states are defined. According to [7] they are defined as "*the condition beyond which the structure, or a part of it, does no longer satisfy one of its performance requirements*". Different limit states exist:

- *Ultimate limit states* (ULS): that define the limit after which the structure or part of it fails. In many sections the ultimate resistance properties of material are reached and deformations a so high to not guarantee the safety of the structure anymore. Reached this stage, several phenomena like instability, large deformations, cracks, loss of equilibrium and others appear.
- *Serviceability limit state* (SLS): describe a state in which some requirements like functionality visual aspect or comfort of the building are no more respected. A significant example can be a high deflection of a slab with consequent practical problems in use that space. The SLS can be reversible or irreversible.

These *limit states* should be addressed for different structures according to different levels of reliability depending from the intended service life.

3.2.1 Uncertainties and their classification

The analysis aimed to define the reliability of a structure have to face with several uncertainties of different nature:

- *randomness*: representing the natural and unavoidable variation of intrinsic material characteristics or loads actions;
- *model uncertainties*: related to the mathematical model used, and to the different choices made when a model is created;
- *statistical uncertainties*: consequences of the limited number of samples involved in the statistic analysis;
- *measurement errors*: performed observing and measuring the data;
- *human errors*: linked to human actions in all the different stages of the design and construction procedure.

All the different sources of uncertainty affect, at different levels, the reliability analysis of a structural system.

Another distinction among the different types of uncertainties lead to the definition of two macro-families, the *aleatory uncertainties* and the *epistemic uncertainties*.

3.2.2 Aleatory uncertainties and their evaluation

Aleatory uncertainties are that related to the intrinsic characteristic of the variable and cannot be modified being strictly linked with the randomness of the variable itself. Material properties are a perfect example of aleatory uncertainties, as well as geometrical parameters and environmental actions. A lot of probabilistic models are present in literature, in particular for construction material in *EN 1990* and *JCSS Probabilistic Model Code, 2010* interesting models can be exploited.

Probabilistic model for concrete properties In general, according to *JCSS Probabilistic Model Code 2001*, *EN 1990* and *fib Model Code 2010* the cylinder concrete compressive strength random variable f_c may be represented by a *lognormal* distribution having:

- *expected value* equal to the *mean value* f_{cm} obtained by testing results or by codes prescription (e.g. *EN 1992-1-1*, *fib Model Code 2010*);
- *coefficient of variation* V_c equal to 0.15; this result shows to be very conservative, in particular, in presence of growing magnitude of the concrete compressive strength (*JCSS Probabilistic Model Code 2001*). However, it can be considered as a safe assumption if experimental or inspection results are not available.

The other parameters as concrete tensile strength f_{ct}, Young modulus E_c, fracture energy G_f, peak strain at concrete compressive strength and ultimate deformation may be evaluated depending from cylinder concrete compressive strength according to expressions reported by *EN 1992-1-1* and *fib Model Code 2010* or probabilistically modelled according to *JCSS Probabilistic Model Code, 2001.*

Probabilistic model for reinforcement properties According to *JCSS Probabilistic Model Code 2001*, *EN 1990* and *fib Model Code 2010* the probabilistic model for the yielding strength of ordinary reinforcements may be defined adopting a lognormal distribution with the following parameters:

- *expected value* equal to the mean value f_{ym} obtained by testing results or by codes prescription (e.g. *EN 1992-1-1*; *fib Model Code 2010*);
- *coefficient of variation* V_y equal to 0.05 in absence of test results (*JCSS Probabilistic Model Code 2001*; *fib Model Code 2010*).

In particular, the elastic modulus E_s can be modelled as a *lognormal* distribution having mean value equal to 210000 MPa and coefficient of variation equal to 0.03.

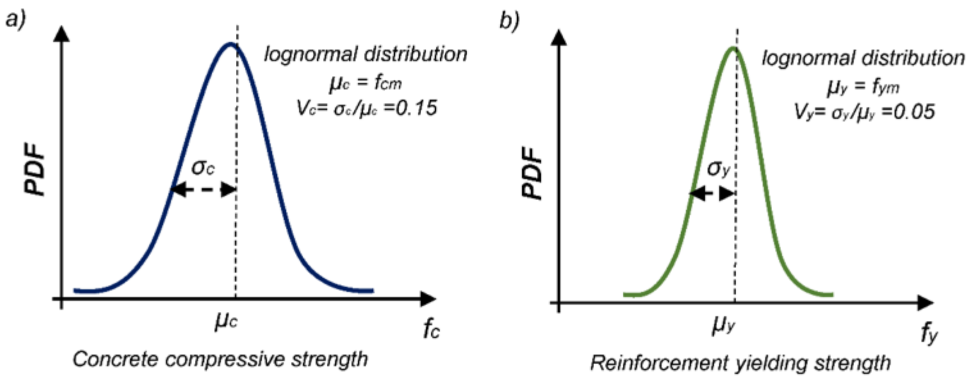

Figure 3.1: Probabilistic modelling of concrete compressive strength (a) and reinforcement yielding strength (b) (Gino, 2019)

3.2.3 Epistemic uncertainties and their evaluation

Epistemic uncertainties concern the lack of information related to the structural model that sometimes are substituted by theoretical assumptions to build up complex model like that used for non-linear analysis. Problems can eventually occur, when wrong assumption are made, generating complex but unrealistic models; in these cases, results better to substitute them with a simpler but also more reliable model.

Detailed resistance model for example, can be affected by lack of information in terms of considered parameters or unknown material behaviour under particular conditions that can lead the designer to make simplified assumptions. A methodology useful to quantify model uncertainties related to resistance models is proposed by *JCSS Probabilistic Model Code, 2001.*

The following aspects have to be considered in order to quantify resistance model uncertainty:

- the *database* of experimental observations should provide all the parameters for the reproduction of the tests and the calculation of the resistance using the model under consideration;
- the *range* of parameters that composes the set of experimental results defines the limits of applicability of the analysis and, consequently, the limits of the resistance model after model uncertainty incorporation;
- statistical inference for the observed sample of the model uncertainty needs to be carried out in order to define the most likely probabilistic distribution and its parameters.

Defining ϑ as the model uncertainty random variable due to factors affecting test and model results, according to *JCSS Probabilistic Model Code, 2001*, in general, the most appropriate probabilistic distribution able to represents ϑ is the *lognormal* one.

3.2.4 General formulation of the structural reliability problem

In reliability analysis, the structural behaviour can be described by means of a set of N basic random variables X_i:

$$X_i = (X_1, X_2, \dots, X_i, \dots, X_N) \qquad i = 1,2, \dots, N \tag{3.1}$$

where the variable X_i may represent *material properties, actions, geometrical properties* and *model uncertainties.*

As already rapidly described in the previous chapter, *probability of failure P_f* is an appropriate way to measure structural reliability. Otherwise the *reliability index β* can be adopted. Moreover, as just seen, a relation exists between the two reliability index, that from (2.11) can be rewritten as follows:

$$\beta = -\Phi(P_f)^{-1} \tag{3.2}$$

Where, once again, the ϕ represents the cumulative standard normal distribution. The *reliability index β* is used very often by international codes (*ISO 2394*; *EN 1990*; *fib Model*

Code 2010) in order to quantify structural reliability. The bigger is the *reliability index* β, the more reliable is the structure (i.e. lower P_f). Moreover, this relation can also be reported in a simple graph Figure 3.2.

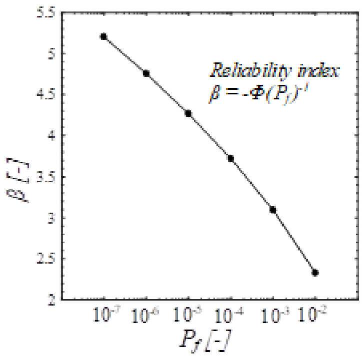

Figure 3.2: Relationship between the probability of failure P_f and reliability index β (Gino, 2019).

Once that a measure of the structural reliability was defined, the limit states to which refer the structural analysis must be outlined. Generally, the previously listed *ULS*, *SLS* are represented by the limit state function Z, which takes the following form as a function of main random variables X_i:

$$Z = g(X_i) = 0 \tag{3.3}$$

The *limit state function* Z is defined, according to Figure 3.3, so that:

$$\begin{cases} Z \geq 0 \rightarrow & \text{safe region} \\ Z < 0 \rightarrow & \text{failure region} \end{cases} \tag{3.4}$$

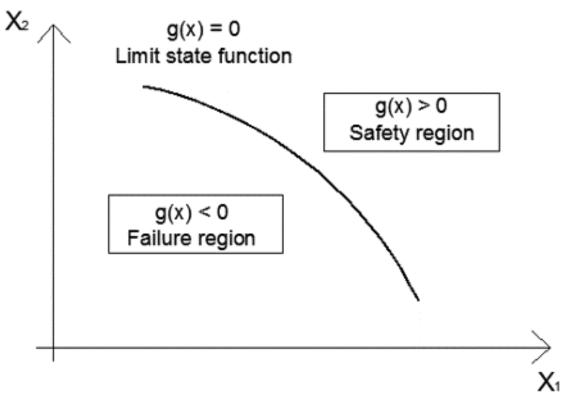

Figure 3.3: General representation of the limit state domain with 2 random variables X_1 and X_2 (Gino, 2019).

Therefore, a positive or zero value of the function Z, define a safe region where collapse doesn't occur while a negative value of the limit state function defines a critical situation for integrity of the structural system. Based to this definition, the *probability of failure* P_f can be calculated as:

$$P_f = P[Z < 0] \tag{3.5}$$

Furthermore, defining as $f_{X_i}(x_i)$ the N-dimensional probability density function of the N basic variables X_i, the *probability of failure* P_f can be expressed in the following integral form:

$$P_f = \int_{Z<0} f_{X_i}(x_i) dx_i \qquad i = 1,2,\ldots,N \tag{3.6}$$

Conversely, the *probability of survival* (i.e. *structural reliability*) P_S can be valuated as:

$$P_S = 1 - P_f \tag{3.7}$$

The *probability of failure* P_f has to be estimated considering a specific reference period t_{ref} that commonly, but not necessarily, corresponds to the design or residual service life.

3.3 Reliability methods and theory background

Structural reliability estimation can be conducted bot with refined or simplified approaches. In general, *the reliability methods* can be classified in four different levels:

- *level III method* (probabilistic);
- *level II method* (probabilistic);
- *level I method* (semi-probabilistic);
- *level 0 method* (deterministic).

Proceeding from the *level III* toward *level 0* the degree of difficulty and the computational efforts requested for the analysis decrease substantially.

3.3.1 Level III method

The choice to use a level III method, implies the resolution of the integral of equation (3.6; unfortunately to solve this integral is possible only when variables involved are represented by simply integrable functions. In the other cases, other strategies like the *Monte Carlo method* must be used.

Integral resolution example: two independent random variables and linear limit state function In the simple case of two independent random variables, R (representing resistances) and S (representing actions) with a linear limit state function expressed by (3.8):

$$Z = g(R, E) = R - E \tag{3.8}$$

the probability of failure P_f is defined as:

$$P_f = \int_{Z<0} f_{R,E}(r, e) dr de = \int_{Z<0} f_R(r) f_E(e) dr de \tag{3.9}$$

The analytical solution may be found easily if both the random variable R and E are *normally* or *lognormally* distributed.

In fact, if R and E are normally distributed with mean values μ_R,μ_E and variance σ_R^2, σ_E^2, respectively, the variable Z of (3.8) is normally distributed too and it has a mean value $\mu_Z = \mu_R - \mu_E$ and variance $\sigma_Z^2 = \sigma_R^2 + \sigma_E^2$.

Then, the *probability of failure* P_f can be expressed according to:

$$P_f = P[Z < 0] = \phi[-\frac{\mu_Z}{\sigma_Z}] = \phi[-\beta] \tag{3.10}$$

where ϕ is the cumulative standard normal distribution and β is the *reliability index.* In case R and E are lognormally distributed the solution is similar, having care to take into account that the variables $R' = \ln(R)$ and $E' = \ln(E)$ are normally distributed.

The Monte Carlo's method and sampling techniques When integral solution cannot be found easily Monte Carlo method results to be a valid alternative to define the failure probability P_f. This probability can be written as:

$$P_f = \int_{g(X_i)<0} f_{X_i}(x_i) dx_i = \int_{-\infty}^{+\infty} I[g(X_i)] f_{X_i}(x_i) dx_i \qquad i = 1{,}2, \ldots, N \tag{3.11}$$

Where $I[g(X_i)]$ is the indicator function and is defined as:

$$I[g(X_i)] = \begin{cases} 0 & \text{if} \quad g(X_i) \geq 0 \\ 1 & \text{if} \quad g(X_i) < 0 \end{cases} \qquad i = 1{,}2, \ldots, N \tag{3.12}$$

Through Monte Carlo method, a large number of samples of the random variable X_i are generated together with the definition of the limit state function; then is possible to check if each realization belongs to the safe region, to the unsafe one or to the limit state boundary. The sum of the realizations belonging to the unsafe region divided for the number of samples gives the failure probability. More specifically:

$$P_f \approx P_f^n = \frac{1}{n} \sum_{j=1}^{n} I[g(X_i)] \quad i = 1{,}2, \ldots, N \quad j = 1{,}2, \ldots, n \tag{3.13}$$

where n is the total number of simulations.

The number of samples to be used for the simulations, is proportional to the inverse of the target probability of failure to be estimated. Consequently, the number of simulations required for the *reliability analysis* is extremely high (commonly around $10^5 - 10^6$ simulations). A method developed to reduce the computational effort for a Monte Carlo simulation is the *Latin hypercube simulation* (LHS).

Latin hypercube simulation The Latin hypercube simulation (LHS) [11] allows the user to reduce computational time in performing structural analysis, using this method each variable is sampled by its probabilistic distribution and, successively, randomly combined with the others. The sampling algorithm ensures that each distribution function is sampled uniformly between the interval of probabilities (0,1). The Figure 3.4 reports the difference between theoretical cumulative distribution for the generic variable X_i and the stratified sampling of a lognormal distribution.

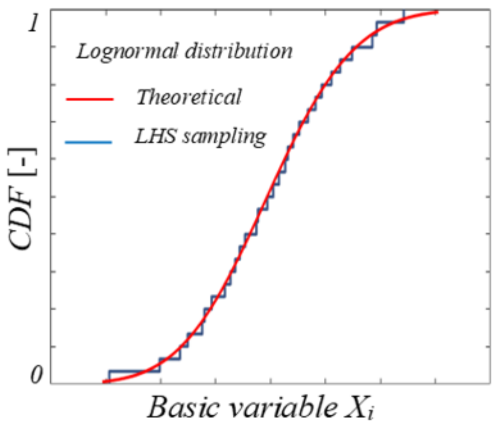

Figure 3.4: Stratified sampling according to LHS: example of LHS sampling from basic variable (Gino, 2019)

The sampling from the probabilistic distribution of basic variables Xi can be performed according to the following steps:

- for each variable X_i the probability interval (0,1) is subdivided in n non-overlapping equiprobable sub-intervals $(h_{\text{inf}}, h_{\text{sup}})$;
- in each one of the n sub-intervals, one value between $(h_{\text{inf}}, h_{\text{sup}})$ is sampled randomly from a uniform distribution and the corresponding value of the basic variable X_i is evaluated;
- a random permutation between the n values sampled for each variable X_i is performed in order to randomly combine the outcomes. In this way, the n input sets of basic variables to perform the simulations is defined.

The *LHS* method can be very efficient in case *reliability analysis* is performed by means of non-linear finite element method; thus, can be adopted efficiently in order to characterize probabilistic distribution of structural resistance by means of a reduced number of samples.

3.3.2 Level II method

Structural reliability analysis using level II method are conducted by using moments of basic variables. In particular, two different methods exist, they are the "First Order Second Moment - FOSM" and "First Order Reliability Methods - FORM" depending on which moment is involved in the analysis.

Within Level II methods, the measure of structural reliability is performed by means the *reliability index* β that, according to [12] can be defined as:

$$\beta = \frac{\mu_Z}{\sigma_Z} \tag{3.14}$$

Then, considering in this case a linearized limit state function $Z = g(X_i)$, the *reliability index* β is defined as the distance between the mean value μ_Z from the failure condition (i.e. $Z = 0$) expressed in number of standard deviation of the limit state function σ_Z Figure 3.5.

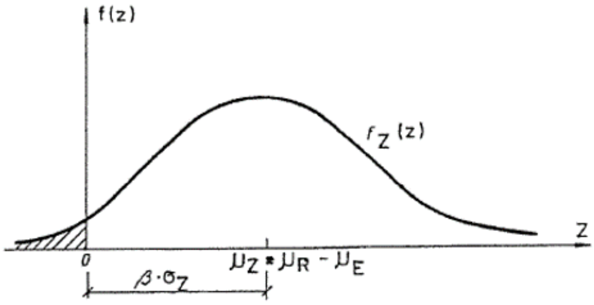

Figure 3.5: Definition of reliability index β according to (Cornell, 1969).

According to [13] a more geometrical definition of β can be given: *reliability index* β is defined as the closest distance between the mean value of the joint probabilistic distribution of basic variables in the standard normal space and the multidimensional limit state surface. The explanation is reported in Figure 3.6 in the case of two random variable R and E with *linear limit state function*.

Where the structural critical condition is defined by the particular limit condition of $Z = R - E = 0$.

However, a more valid alternative presented by [14] for the II level method, is based on the definition of a new limit state function linearized in the so called design point which is that one having the highest probability density. In other words, is the point having coordinates (R_d, E_d) closest to the mean point of coordinates (μ_R,μ_E). The coordinates of the design point may be written in function of the *reliability index* β as:

$$R_D = \mu_R - \alpha_R \beta \sigma_R \tag{3.15}$$

$$E_D = \mu_E - \alpha_E \beta \sigma_E \tag{3.16}$$

where α_R and α_E denotes the First Order Reliability Method - FORM - sensitivity factors of the random variables R and E, evaluated as the direction cosines of the design

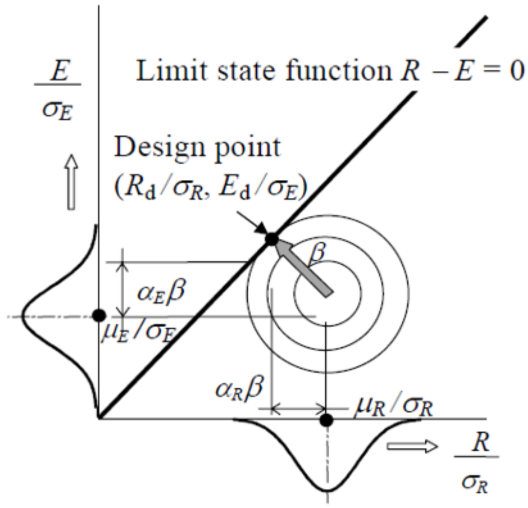

Figure 3.6: Definition of design point and reliability index (Hasofer and Lindt, 1974).

point. According to [8] and [7] suggested values of the sensitivity factors can be adopted; specifically, the value of α_R is set equal to 0.8 and the value of α_S is set equal to -0.7. The mentioned above values for α_R and α_S are defined for dominant random variables. In case of accompanying or non-dominant random variables, the value of FORM sensitivity factors ca be pre-multiplied for 0.4.

3.3.3 Level I method

The level I method is based on a semi-probabilistic approach. Therefore, although probabilistic distributions of both resistances and actions are considered, characteristic values are practically used in the design. These values are taken considering specific percentiles of the aforementioned distributions. In general, the characteristic value is considered as be the 5% quantile of the probabilistic distribution of the resistances, the 50% quantile of the probabilistic distribution of permanent actions and the 95-98% quantile in case of variable actions. *Partial safety factors* for materials γ_m and for actions γ_f are hence introduced and applied to the *characteristic values*, in order to obtain the *design values*.

$$\gamma_m = \frac{R_k}{R_d} \tag{3.17}$$

$$\gamma_f = \frac{E_d}{E_k} \tag{3.18}$$

According to [8] one has to verify whether the design resistance Rd is at least equal to the design value of the load effect $E : d$:

$$R_d \geq E_d \tag{3.19}$$

with E_d and R_d defined as follows:

$$E_d = E(F_{d1}, F_{d2}, \ldots, a_{d1}, a_{d2}, \ldots, \vartheta_{d1}, \vartheta_{d2}) \tag{3.20}$$

$$R_d = R(X_{d1}, X_{d2}, \dots, a_{d1}, a_{d2}, \dots, \vartheta_{d1}, \vartheta_{d2}) \tag{3.21}$$

Where F represents an external actions; X represents a material properties; a is a geometrical property; ϑ is the model uncertainty.

3.3.4 Level 0 method

The level 0 method is a purely deterministic approach that doesn't consider any type of random variability. Therefore, nominal values of both actions and resistances are used, and only a global safety factor is applied. The verification in this case has to respect the following condition:

$$R_{\text{nom}} \geq \gamma \cdot E_{\text{nom}} \tag{3.22}$$

Obviously, reliability analysis based on probabilistic states, cannot be conducted in this case; moreover, the risk to underestimate the safety of a structure become consistent using this obsolete approach

3.3.5 Target reliability and reliability differentiation for new and existing structures

The target reliability is defined considering the consequences due to an eventual structural failure which can cause loss of human and economic resources. An important role is also played by the costs that the safety measures require to reduce collapse probability. Moreover, the reliability index definition, and the acceptable failure probability depend on the considered limit state. Finally, a differentiation has to be made between *new* and *existing* structure, for which different consideration must be taken into account. Indeed, increase the level of reliability of an existing structure often costs much more than design a new one.

In an extremely simplified model, the total costs C_{tot} of a structure during its working life can be expressed as:

$$C_{\text{tot}} = C_i + P_f D \tag{3.23}$$

Where C_i are the initial costs for build the new structure or for up-grade the existing one and $P_f D$ is the expected failure costs related to the working life. The optimum target reliability index can be identified as the one that meet the principle of minimizing the total cost C_{tot} without be lower to the minimum requirements for human safety.

In Table 3.1 the target reliability indexes for *new* and *existing* structures proposed by *fib Model Code 2010* are reported. It must be specified that these values are related to structures for which failure is preceded by a certain level of warning.

3.4 Safety formats for design and assessment of reinforced concrete structures

The *safety format* can be identified as a series of rules and methods defined to perform design or assessment of new and existing structures according to pre-determined reliability

Limit states	Target reliability index β	Reference period
	New Structures (fib Model Code 2010)	
Serviceability (SLE)		
reversible	0.0	service life
irreversible	1.5	50 years
irreversible	3.0	1 year
Ultimate (SLU)		
low consequences of failure	3.1	50 years
	4.1	1 year
medium consequences of failure	3.8	50 years
	4.7	1 year
high consequences of failure	4.3	50 years
	5.1	1 year
	Existing structures (fib Model Code 2010)	
Serviceability (SLE)	1.5	residual service life
Ultimate (SLU)	3.1-3.8*	50 years
	3.4-4.1*	15 years
	4.1-4.7*	1 year
*depending from costs for safety measures and upgrading of the structure; more detailed information can be derived from fib Bulletin 80.		

Table 3.1: Suggested range of target reliability from fib Model Code 2010 for new and existing structures (Gino, 2019)

target. In this Section the basic principles reported by [7], [8] and [15] are described.

3.4.1 The levels of approximation approach

Structural models are only simplifications of reality; therefore, they are affected by different level of approximation depending on the accuracy one wants to reach. A "*level of approximation*" (LoA) is a *design* or *assessment* methodology where the accuracy on the estimate of the response of a structural member or system can be refined by improving the knowledge about the involved physical parameters and the complexity of the mathematical model [10].

Designers can choose different *LoA* depending on the model complexity and on the level of detail they want to obtain from the analysis results. Four different *LoA* exist, a schematic representation is reported in Figure 3.7.

From *level I* to *level IV* the level of detail increases, but on the other hand, the computational efforts and the time spent for the whole evaluation process increase as well.

More in detail, according to *fib Model Code 2010*, for *levels II* and *III* a probabilistic approach implying the determination of the limit states and the failure probability is suggested. While for level I the partial safety factor approach is the most suitable. The latter in particular, involves the use of the coefficients commonly used for the classic design

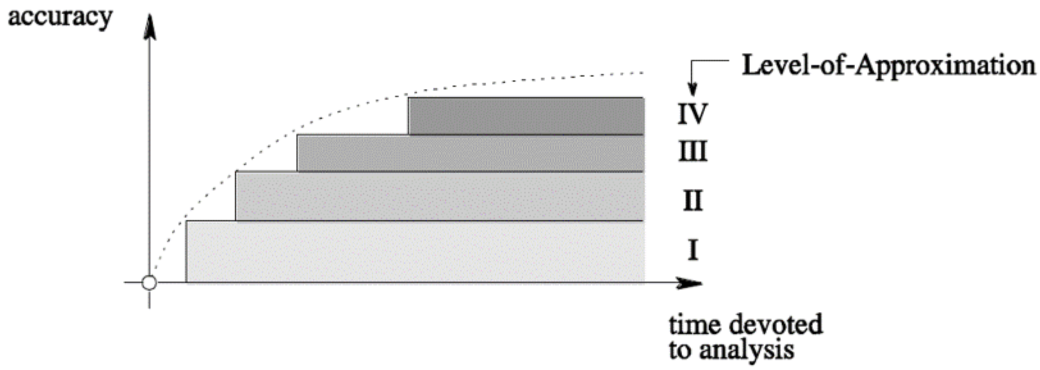

Figure 3.7: Levels of approximation approach as defined by Muttoni and Ruiz, 2012 and fib Model Code 2010.

of new RC building. For the existing structure, *fib Bulletin 80* suggest two assessment methodologies: the "*Design Value Method*" and the "*Adjusted Partial Factor Method*".

3.4.2 Global resistance format

The *global resistance format* (GRF) in mainly used when global structural analysis, often non-linear, are performed. Indeed, this method allows the designer to define a *design global resistance R_d* which takes into account mechanisms of global resistance derived from the secondary order effects on the building, that in a simpler linear elastic analysis are not taken into account. This procedure allows to pass from a local analysis, conducted on the cross sections of the structural elements, to a higher level of detail analysis, that allow the engineer to better understand the behaviour of the whole structural system under critical and exceptional situations like the progressive damaging and eventually the consequent collapse.

Definition of the design global resistance According to the *GRF*, the representative variable for the global resistance is the structural resistance R. The following representative values of resistance can be derived:

- R_m, mean value of global structural resistance;
- R_k, 5% characteristic value of the global structural resistance;
- R_d, design value of the global structural resistance according to specified target reliability index β.

The safety condition is represented by the following equations:

$$F_d \leq R_d\,, \quad R_d = \frac{R_m}{\gamma_R \cdot \gamma_{Rd}} \tag{3.24}$$

where F_d is the design external action defined according to the partial factor format; γ_R is denoted as the *global resistance safety factor*, which account for material aleatory

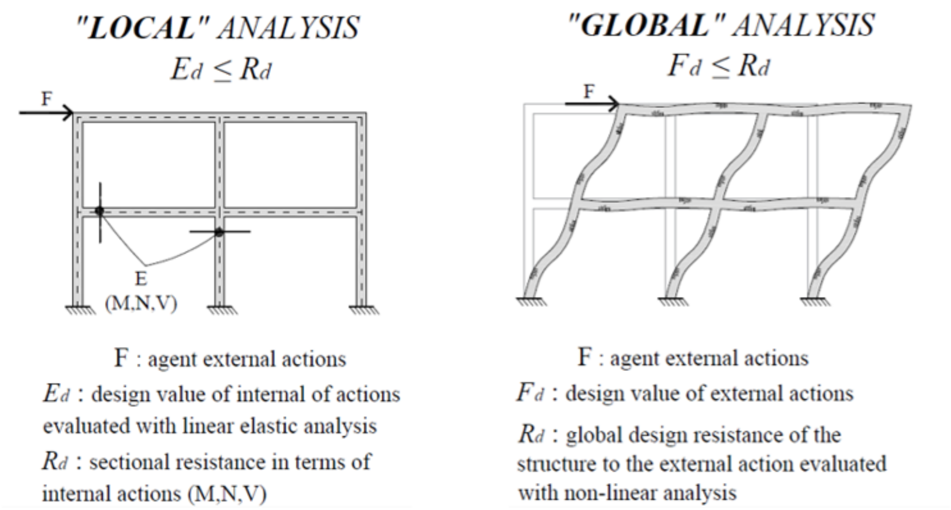

Figure 3.8: Comparison between local structural analysis and global structural analysis

uncertainties; γ_{Rd} represents the *resistance model uncertainty safety factor*, which account for the resistance model uncertainty.

Chapter 4

R.C. multistorey plane frane design in a seismic zone

4.1 General description

Robustness and structural probabilistic analysis were conducted on a R.C. multistorey 2D plane frame which is a section of an R.C. building designed in seismic zone. The building is a residential house situated in L'Aquila at 714 m a.s.l. in a seismic zone of category 2.

Followings codes were taken into account for the design procedure:

- - D.M. January 17 2018: Aggiornamento delle "Norme tecniche per le costruzioni" [4];
- explanatory circular January 21 2019: Istruzioni per l'applicazione dell'Aggiornamento delle "Norme tecniche per le costruzioni" di cui al decreto ministeriale 17 gennaio 2018 [16];
- EN1992 Eurocode 2: "Design of concrete structures" [17];
- UNI EN 206-1: Concrete: Specification, performance, production and conformity [18].

The design concerns the construction of a new structure; the nominal life is intended as the number of years in which the structure, provided it is subject to routine maintenance, must be able to be used for the purpose for which it is intended. In table 2.4.I of [4] here reported as Table 4.1, the standard defines three types of constructions.

In this specific case is assumed a building of category 2, ordinary construction, with a design nominal life of 50 years. The service class of the building is class II, defined in 2.4.2 of [4]: buildings whose use provides for normal crowding, without dangerous contents for the environment and without essential public and social functions. For this class the utilization coefficient C_U is equal to 1 according to table 2.4.I of [4] here reported as Table 4.2.

Therefore, the reference period V_R defined in 2.4.3 of [4] is:

$$V_R = C_U V_N = 50\,\text{years} \tag{4.1}$$

Tipi di costruzioni	Valori minimi di V_N (anni)
Costruzioni temporanee e provvisorie	10
Costruzioni con livelli di prestazioni ordinari	50
Costruzioni con livelli di prestazioni elevati	100

Table 4.1: Minimum values of the design nominal life V_N for the different types of construction [4]

Classe d'uso	I	II	III	IV
Coefficiente C_U	0,7	1	1,5	2,0

Table 4.2: Values of utilization coefficient C_U [4]

In Table 4.3 are reported the concrete properties. The exposure class is XC2, so the minimum concrete cover is 25 mm and, considering a laying tolerance of 10 mm, a concrete cover of 35 mm was chosen. Hot rolled steel in bars with improved adherence is used for the reinforcement; its characteristics are described in Table 4.4.

The building consists of four floors above ground that have an inter-storey height of 3m, it has 4 spans in plan in both directions, as shown in Figure 4.1, and since it respects the requirements of geometric regularity it was possible to carry out the design of a single intermediate plane frame, shown in Figure 4.2.

The ductility class "A" was chosen for the design; finite element modeling and stress calculation were performed with SAP2000 software.

4.2 Actions

In 2.5 of [4], an action is defined as any cause or set of causes capable of inducing limit states in a structure. The loads can be classified according to their intensity variation over time as:

- *permanent loads* G: acting for the entire life-cycle of the structure and over time they can be considered constant;
- *variable loads* Q: that can be of long or short duration;
- *accidental loads* A: due to exceptional events;
- *seismic actions* E: due to earthquakes.

In order to proceed with the verifications according to limit states, combination of actions have to be defined:

- *SLU combination*, fundamental combination of actions for persistent or transient design situations:

$$\gamma_{G1}G_1 + \gamma_{G2}G_2 + \gamma_{Q1}Q_{k1} + \sum_{i=2}^{n} \gamma_{Qi}\Psi_{0i}Q_{ki} \tag{4.2}$$

Resistance class	**C25/30**
Cubic characteristic resistance	$30\,\mathrm{N}/mm^2$
Partial factor for concrete γ_c	1.50
Partial factor for permanent actions α_{cc}	0.85
Design value of concrete compressive strength f_{cd}	$14.17\,\mathrm{N}/mm^2$
Mean value of axial tensile strength of concrete f_{ctm}	$2.56\,\mathrm{N}/mm^2$
Characteristic axial tensile strength of concrete f_{ctk}	$1.8\,\mathrm{N}/mm^2$
Design axial tensile strength of concrete f_{ctd}	$1.20\,\mathrm{N}/mm^2$
Ultimate compressive strain in the concrete ε_{cu}	3.50 ‰
Specific weight	$25\,\mathrm{kN}/m^3$
Secant modulus of elasticity of concrete	$31476\,\mathrm{N}/mm^2$
Poisson coefficient ν	0.20

Table 4.3: Concrete properties

Steel class	**B450C**
Characteristic tensile strength of reinforcement f_{tk}	$540\,\mathrm{N}/mm^2$
Characteristic yield strength of reinforcement f_{yk}	$450\,\mathrm{N}/mm^2$
Partial factor for reinforcing γ_s	1.15
Design yield strength of reinforcement f_{yd}	$391\,\mathrm{N}/mm^2$
Characteristic strain at maximum load ε_{uk}	75‰
Design yielding strain of reinforcement ε_{syd}	1.96‰
Ultimate compressive strain ε_{ud}	$0.9 \cdot \varepsilon_{uk} = 63$‰
Design value of modulus of elasticity	$200000\,\mathrm{N}/mm^2$
Poisson coefficient ν	0.30

Table 4.4: Reinforcement properties

- *irreversible SLS combination*, characteristic rare combination:

$$G_1 + G_2 + Q_{k1} + \sum_{i=2}^{n} \Psi_{0i} Q_{ki} \tag{4.3}$$

- *reversible SLS combination*, frequent combination:

$$G_1 + G_2 + \Psi_{11} Q_{k1} + \sum_{i=2}^{n} \Psi_{2i} Q_{ki} \tag{4.4}$$

- *SLS combination*, quasi-permanent combination for long term effects:

$$G_1 + G_2 + \Psi_{21} Q_{k1} + \sum_{i=2}^{n} \Psi_{2i} Q_{ki} \tag{4.5}$$

- *seismic SLU combination*, for limit states related to seismic actions E:

$$E + G_1 + G_2 + \Psi_{21} Q_{k1} + \sum_{i=2}^{n} \Psi_{2i} Q_{ki} \tag{4.6}$$

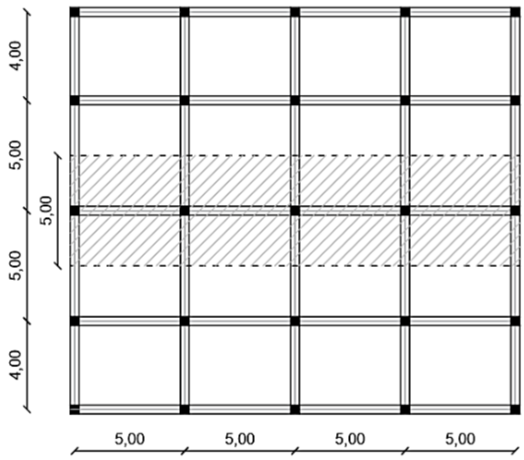

Figure 4.1: Generic floor plane drawing

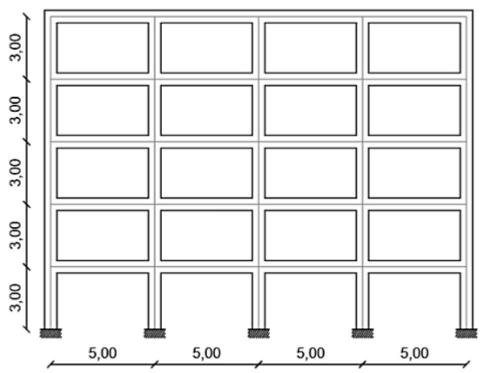

Figure 4.2: Plane frame section

- *accidental SLU combination*, for limit states related to accidental actions A:

$$A + G_1 + G_2 + \Psi_{21} Q_{k1} + \sum_{i=2}^{n} \Psi_{2i} Q_{ki} \tag{4.7}$$

where:

- γ_{G1} is the partial safety factor for permanent live loads;
- γ_{G2} is the partial safety factor for permanent dead loads;
- γ_Q is the partial safety factor for variable loads;
- Ψ_{0i} are the combination factors given by 2.5.I of [4], reported in Table 4.5.

Categoria/Azione variabile	Ψ_{0j}	Ψ_{1j}	Ψ_{2j}
Categoria A - Ambienti ad uso residenziale	0.7	0.5	0.3
Categoria B - Uffici	0.7	0.5	0.3
Categoria C - Ambienti suscettibili di affollamento	0.7	0.7	0.6
Categoria D - Ambienti ad uso commerciale	0.7	0.7	0.6
Categoria E - Aree per immagazzinamento, uso commerciale e uso industriale	1.0	0.9	0.8
Biblioteche, archivi, magazzini e ambienti ad uso industriale			
Categoria F - Rimesse, parcheggi ed aree per il traffico di veicoli (per autoveicoli di peso $\leq$ 30 kN	0.7	0.7	0.6
Categoria G - Rimesse, parcheggi ed aree per il traffico di veicoli (per autoveicoli di peso $>$ 30 kN	0.7	0.5	0.3
Categoria H - Coperture accessibili per sola manutenzione	0.0	0.0	0.0
Categoria I - Coperture praticabili	da valutarsi		
Categoria K - Coperture per usi speciali (impianti, eliporti, \dots)	caso per caso		
Vento	0.6	0.2	0.0
Neve (a quota $\leq$ 1000 m s.l.m.)	0.5	0.2	0.0
Neve (a quota $>$ 1000 m s.l.m.)	0.7	0.5	0.2
Variazioni termiche	0.6	0.5	0.0

Table 4.5: Combination factors Ψ_{0i}

4.2.1 Permanent actions

The permanent structural actions (G_1) are constituted by the own weights of columns and beams, which are taken into account by the calculation software which receives the dimensions and specific weight as input, and the own weight of slab made of R.C. joists and hollow blocks, whose geometry is illustrated in Figure 4.3.

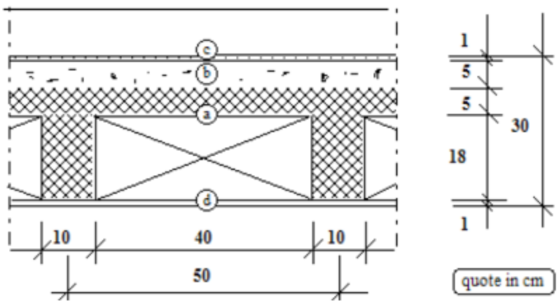

Figure 4.3: Slab scheme

The analysis of the total weight of the composite slab is reported in Table 4.6 with the details of each component.

The permanent non-structural actions (G_2) are given by the non-structural part of the slab and by the internal masonry. The part of the permanent non-structural load of the

Component	**Width** [m]	**Thickness** [m]	**Unitary weight** [kN/m^3]	**Load** [kN/m^2]
slab	1.00	0.05	25.0	1.25
joists	$2 \cdot 0.10$	0.18	25.0	0.90
hollow blocks	$2 \cdot 0.40$	0.18	7.3	1.05
				3.20

Table 4.6: Permanent load of slab

slab is given by the weight of the screed, the paving and the plaster; results are shown in Table 4.7.

Component	**Width** [m]	**Thickness** [m]	**Unitary weight** [kN/m^3]	**Load** [kN/m^2]
screed	1,00	0.05	16.0	0.80
paving	$2 \cdot 0.10$	0.18	25.0	0.90
plaster	$2 \cdot 0.40$	0.18	7.30	1.05
				3.20

Table 4.7: Permanent non-structural loads of slab

For the calculation of the weight of the internal walls, the scheme is illustrated in Figure 4.4.

And therefore, the resulting loads are reported in Table 4.8.

Considering a height of the walls of 2.70 m, the load per unit of length of the masonry will be equal to:

$$G_2 = 2.70 \cdot 0.88 = 2.38\,\mathrm{kN/m} \tag{4.8}$$

that must be compared with the class defined by [4] at 3.1.3 considering that the found linear load, can be taken into account as an equivalent uniformly distributed load g_2 applied on the entire slab. In this case, the value of G_2 equal to 2.38 kN/m lead to a value of g_2 equal to 1.2 kN/m^2. The distributed loads applied on the slabs is appropriately multiplied by the depth of 5 meters of the influence area and modeled as linear loads acting on the beams.

4.2.2 Variable actions

The variable loads due to use, according to table 3.1.II of [4], is equal to 2.0 kN/m^2 for the intermediate floors and 0.5 kN/m^2 for the roof.

The wind action is calculated following the indications of 3.3 of [4]:

$$p = q_b \cdot c_e \cdot c_p \cdot cd \tag{4.9}$$

where:

- q_b is kinetic wind pressure;

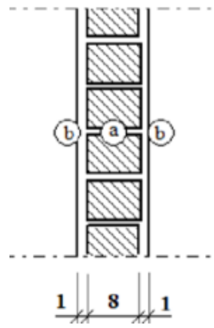

Figure 4.4: Layers scheme of the internal masonry: a) hollow bocks, b) screed

Component	**Thickness** [m]	**Unitary weight** [kN/m^3]	**Load** [kN/m^2]
hollow blocks	0.08	6.0	0.48
screed	0.1	20.0	0.40
			0.88

Table 4.8: Permanent non-structural loads of internal walls

- c_e is the exposure factor;
- c_p is the shape coefficient (or aerodynamic);
- c_d is the dynamic factor.

The reference kinetic pressure q_r is determined with the formula 4.10:

$$q_r = \frac{1}{2}\rho v_r^2 \tag{4.10}$$

Where $\rho = 1.25\,\mathrm{kg/m^3}$ is the air density (assumed constant for simplicity), while the reference wind speed in L'Aquila is 31.3 m/s, thus q_r is equal to $611.3\,\mathrm{N/mm^2}$.

The exposure coefficient c_e depends on the elevation z of the considered point, on the soil topography and on the exposition category of the site in which the building has to be built.

$$c_e(z) = k_r^2 c_t \ln(\frac{z}{z_0})[7 + c_t \ln(\frac{z}{z_0})] \qquad \text{if } z \geq z_{\min} \tag{4.11}$$

$$c_e(z) c_e(z_{\min}) \qquad \text{if } z < z_{\min} \tag{4.12}$$

Moreover, by identifying a roughness class A, a site exposure category V is obtained, for which we have $k_r = 0.23$, $z_0 = 0.7\,\mathrm{m}$ and $z_{\min} = 12.0\,\mathrm{m}$, moreover, c_t assumes a value equal to 1, therefore the following values of c_e must be used at the different levels of the structure.

The pressure coefficient c_p is equal to 0.80 for the upwind facade and -0.40 for the downwind facade, while the dynamic coefficient c_d is equal to 1, so ultimately, taking into

z [m]	c_e [-]
0	1.48
3	1.48
6	1.48
9	1.48
12	1.48
15	1.63

Table 4.9: Values of c_e depending on elevation

account the depth of 5 meters, the wind pressure, inserted as a linear load in the plane model, turns out to be that defined in Table 4.10:

z [m]	p_{up} [kN/m]	p_{down} [kN/m]
0	3.60	-1.80
3	3.60	-1.80
6	3.60	-1.80
9	3.60	-1.80
12	3.60	-1.80
15	4.00	-2.00

Table 4.10: Values of linear loads due to wind pressure

Snow load is applied in all that surfaces where the snow has the possibility to accumulate (roofing, balcony, terrace). It depends on many factors such as the shape and the characteristics of the surface (roughness, inclination, heat capacity) and local weather (wind, precipitation).

Snow load is computed according to 3.4 of [4] through this expression:

$$q_s = \mu_i \cdot q_{sk} \cdot c_e \cdot c_t \tag{4.13}$$

where:

- q_{sk} is the characteristic ground snow load;
- μ_i shape coefficient;
- c_e is the exposure coefficient;
- c_t is the thermal coefficient.

In this case, given an altitude of 714 m a.s.l. $q_{sk} = 2.72\,\mathrm{kN/m^2}$, μ_i is 0.8 and the two coefficients c_e and c_t are unitary, hence q_s is $2.17\,\mathrm{kN/m^2}$.

4.2.3 Seismic actions

The seismic action was determined by following the indications of 3.2 [4]; it is a function of the following parameters:

$$S_e(T) = f(a_g, F_0, T_c^*) \tag{4.14}$$

where:

- a_g is the peak ground acceleration;
- F_{0i} is the maximum amplification factor of the site;
- T_c^* is the starting point of the constant velocity part of the spectrum.

These parameters are computed according to the reference period V_R of the structure defined by 4.1 and equal to 50 years.

For the realization of the response spectra, the Excel spreadsheet made available by the Italian Ministry of Infrastructure and Transport was used. By inserting within the program, the geographical coordinates of the area being studied in phase 1, the nominal life (50 years) and the use coefficient ($C_u = 1$) in phase 2, the soil category (B) and the topographic one (T_3) in phase 3, it is possible to obtain the elastic response spectrum.

A conventional damping $\xi = 5\%$, was chosen to define the structure spectrum, being the structure made of reinforced concrete.

For the inelastic design response spectrum, it is necessary to define a further parameter, the structure factor q. Considering the structural typology, the ductility class, the regularity in elevation and the number of floors, the structure factor is determined according to the following formulation, indicated in 7.3.1 of [4]:

$$q = q_0 K_R \tag{4.15}$$

The parameter K_R, which is a reductive factor that depends on the regularity characteristics of building with elevation, is taken equal to 1 since the structure is regular.

q_0 is the basic value of the structure factor which depends on the expected ductility level, on the structural typology and on the ratio α_u/α_1. By choosing a high ductility class "A", the value of q_0 is obtained from the following relationship:

$$q_0 = 3\frac{\alpha_u}{\alpha_1} = 4.5 \cdot 1.3 = 5.85 \tag{4.16}$$

Where the ratio α_u/α_1 was obtained considering the structure to belong to the category of multistory frame structure with more than one span, 7.5.2.2 of [4].

Therefore, q became:

$$q = q_0 K_R = 5.85 \cdot 1 = 5.85 \tag{4.17}$$

On Figure 4.5 and Figure 4.6 are reported the LLS response spectra for ULS verification and the DLS response spectrum for the SLS assessment of the displacement at floors.

From these spectra, the values of accelerations at T_B, T_C and T_D can be detected.

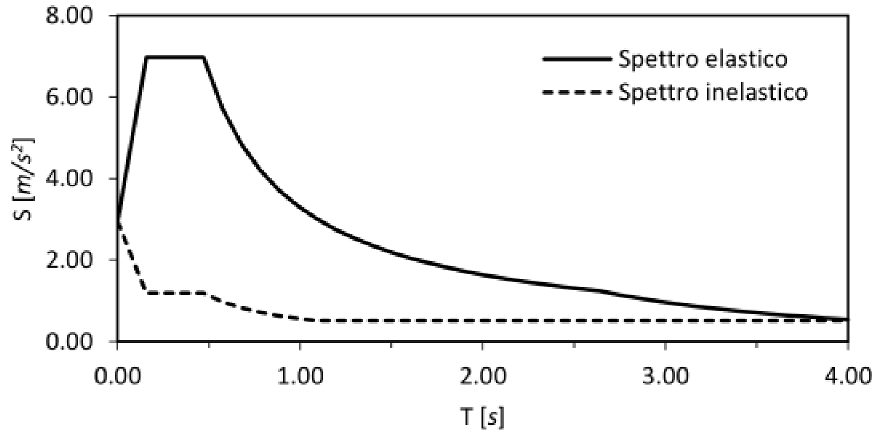

Figure 4.5: LLS life-saving limit state elastic and anelastic response spectra

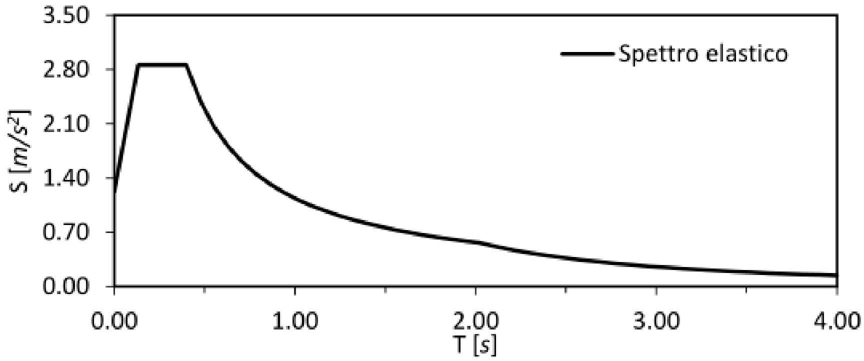

Figure 4.6: DLS damage limit state response spectrum

4.3 Finite element modeling

The modeling was carried out using a flat frame using the SAP2000 finite element software; it was chosen to study a frame with square section columns, with sides of 0.6 m, and rectangular beams 0.5 m high and 0.4 m wide; beams and columns are modeled with beam elements linked through interconnection nodes and have the same dimensions for all floors.

Moreover, it was decided to use perfect fixed constraints at the base of the columns, neglecting the soil-structure interaction.

Figure 4.7 shows the finite element model with the names of the different structural elements.

4.4 Model analysis

Considering the geometrical regularity of the structure, it was decided to proceed with a linear analysis for the assessment of the solicitations determined by an eventual earthquake.

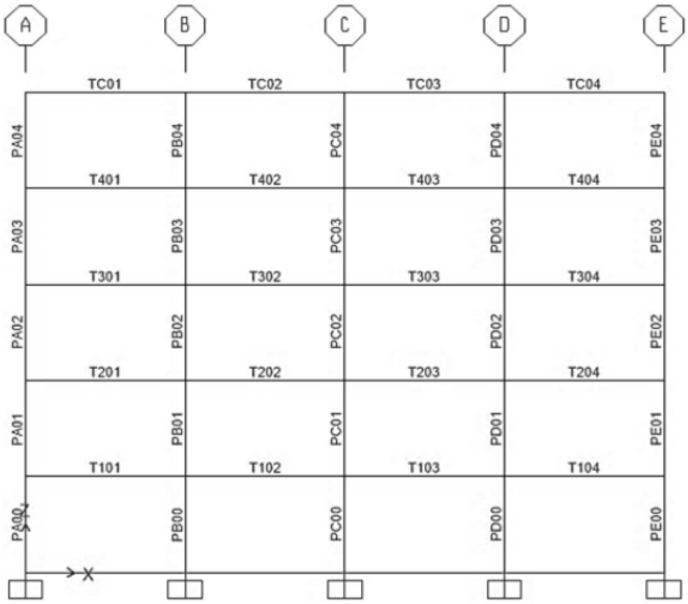

Figure 4.7: DLS damage limit state response spectrum

A modal analysis was hence performed, it represents a conventional procedure for assessing the effects of seismic action and is carried out to determine the vibration modes of the structure considered in the elastic field.

According to [4] it is necessary to take into account all the eigenmodes that contribute significantly to the overall response of the structure. More in detail the code imposes that the sum of the effective modal masses of the considered modes, must represent at least 85% of the total mass of the structure, moreover, that is necessary to consider all the vibration modes characterized by an effective modal mass greater than 5% of the total mass. The seismic mass of the structure that has been taken into account in the calculation of the vibration modes is given by 4.5.

As a result of the performed modal analysis, it is observed that the aforementioned conditions are respected by considering the first 2 eigenmodes; however, considering the model simplicity and the low computational effort required, the first 12 vibration modes were considered in the calculation of the stresses related to seismic actions.

4.5 Design assessment

The stresses analysis was conducted using SAP2000 software, through a linear static analysis for the load combinations of SLU and SLE and through a modal analysis for seismic combinations.

The verifications were carried out according to the resistance hierarchy criterion: it aims to make the formation of global collapse mechanisms highly unlikely, favouring first the formation of ductile local mechanisms.

The beams are ductile elements, which must first be plasticized in bending to dissipate energy in the event of an earthquake; therefore, the bending reinforcement of the beams is defined on the basis of the computed stresses. Everything else, i.e. shear reinforcement in beams, bending and shear reinforcement of the columns, is defined starting from the bending reinforcement of the beams.

The procedures used to verify the structural elements at the ultimate and serviceability limit states are illustrated below.

4.5.1 Beams: bending ULS

To determine the amount of longitudinal reinforcement required for the beam, it is necessary to refer to the envelope values of the calculation moment acting on the beams obtained using SAP2000 software. The Table 4.11 resumes the geometrical characteristics of beams elements.

Element	B [mm]	H [mm]	c [mm]	d [mm]	d' [mm]
Beams	400	500	35	52	448

Table 4.11: Beam geometrical properties

The value of M_{Ed} acting on the beam, must be compared with $M_{Rd,\mathrm{lim}}$ obtained as:

$$M_{Rd,\mathrm{lim}}[\mathrm{kN\,m}] = 0.2961\, B\, d^2\, f_{cd} = 336.8\,\mathrm{kN\,m} \tag{4.18}$$

Although the obtained value results to be always greater than the acting one, and thus should lead to not consider compressive bending reinforcement in the design, a minimum amount of rebars will always be considered according to [4].

Knowing the material properties and the values of β_1 and β_2 (filling coefficients) equal to 0.8095 e 0.4160, it is possible to determine the design value of x_u through the binomial expression which terms are the following:

$$a = \beta_1\, \beta_2\, B\, f_{cd} \tag{4.19}$$

$$b = \beta_1\, B\, f_{cd}\, d \tag{4.20}$$

$$c = M_{Ed} \tag{4.21}$$

And thus, the reinforcement on the tensile zone can be computed by using the expression 4.22:

$$A_{s,\mathrm{min}}\,[\mathrm{mm}^2] = \frac{\beta_1\, B\, f_{cd}\, x_u}{f_{yd}} \tag{4.22}$$

Depending on the minimum reinforcement value required, the number of rebars is chosen using the diameters available on the market.

Moreover for the rebars design, the following suggestions given at 7.4.6.2.1 of [4] have to be considered:

- at least two bars with a diameter of not less than 14mm must be present at the top and bottom for the entire length of the beam;
- at each edge of the beam there must be a compression reinforcement in correspondence with the critical sections not less than half of the tension one ($\rho'_s \geq 0.5\rho_s$), while in the other sections $\rho'_s \geq 0.25\rho_s$, where:

$$\rho_s = \frac{A_S}{B\,H} \qquad \rho'_s = \frac{A'_S}{B\,H} \tag{4.23}$$

- - in each section of the beam, the geometric percentage of longitudinal tension reinforcement at the upper edge and at lower edge must be within the following limits:

$$\frac{1.4}{f_{yk}} \leq \rho \leq \rho' = \frac{3.5}{f_{yk}} \tag{4.24}$$

Once that the amount of reinforcement is defined, the assessment can be carried out; the value of x_u has firstly to be determined:

$$x_u = \frac{f_{yk}(A_S - A'_S)}{\beta_1\,B\,f_{cd}} \tag{4.25}$$

In order for the initial hypothesis of yielding of the reinforcement to be verified (Field 3 with $\varepsilon_{cd} = 0.35\%$ and $\varepsilon_s > 0.196\%$) it may be necessary to use a linear interpolation, for which a value of x_u is obtained such that the system is in equilibrium and the condition (4.26) is verified:

$$C + S' - S = 0 \tag{4.26}$$

where:

$$C = \beta_1\,B\,f_{cd}\,x_u \qquad S = f_{yd}A_S \qquad S' = \varepsilon'_s E_s A_S \tag{4.27}$$

Once x_u is obtained, the following verifications have to be made:

- *Ductility*: $x_u < 0.45d$
- *Resisting moment*: $M_{Ed} < M_{Rd}$ with:

$$M_{Rd} = \beta_1\,B\,f_{cd}\,x_u(d - \beta_2 x_u) + f_{yd}A'_S(d - d') \tag{4.28}$$

For the arrangement of the longitudinal reinforcement of the beams, it was chosen for simplicity to use only bars with a diameter of 18 mm. The checks on the ULS for bending and the construction details made a reinforcement disposition, with the following characteristics:

- 3 continuous rebars in the lower strip for all the beams and for the entire length of the same, suitable for supporting the positive moments in the span;
- 2 rebars in the upper strip for all the beams, which when crossed, form on the supports a reinforcement area equal to that of 4 rebars;
- from 1 to 3 additional rebars in the upper strip at the supports, to obtain a reinforcement area necessary to cover the peaks of negative moment.

4.5.2 Beams: shear ULS

For the design of the main beams [4] require to ensure a certain amount of shear reinforcement.

The stirrups are arranged with a variable spacing s_w along the beam in order to meet the relevant regulatory requirements in terms of strength and minimum quantity of transverse reinforcement. Following the criterion from the hierarchy of the resistances, the design shear is determined starting from the resistant moments at the ends of the beams at the time of the formation of the plastic hinges, also taking into account the contribution due to the gravitational loads, as follows:

$$V_{Ed} = \gamma_{Rd} \frac{M_{Rb,1} + M_{Rb,2}}{l_c} + \frac{1}{2}(G + \psi_2 Q) l_c \tag{4.29}$$

where

- l_c is the simply supported beam length;
- $M_{Rb,1}$ is the resisting bending moment at the first edge;
- $M_{Rb,2}$ is the resisting bending moment at the second edge;
- γ_{Rd} is the amplification factor equal to 1.2 for A ductility class, and 1.0 for the B class;
- $G + \psi_2 Q$ is the gravitational load related to the seismic design.

Knowing the acting shear, it is possible to proceed with the shear reinforcement design according to 4.1.2.3.5.2 of [4].

The calculation model is based on the Ritter-Morsch truss, an ideal isostatic grid that is formed due to the combined effect of bending and shear, consisting of an upper strip of compressed concrete, a lower strip tensioned represented by the longitudinal reinforcement, concrete struts inclined of θ with respect to the longitudinal direction and ties with inclination α with respect to the longitudinal direction represented by stirrups, in this case vertical, therefore $\beta = 90°$. Limitations have to respected for θ:

$$1 \leq \cot\theta \leq 2.5 \qquad \cot\theta = 1 \text{if class } A \tag{4.30}$$

Assuming this behaviour, with reference to core concrete, the design resistance to "compression shear" is calculated with:

$$V_{Rcd} = 0.9\, d\, v\, b_w\, \alpha_c\, f_{cd}\, \frac{\cot\alpha + \cot\theta}{1 + \cot^2\theta} \tag{4.31}$$

With reference to the transversal reinforcement, the design resistance to "traction shear" is calculated with:

$$V_{RSd} = 0.9\, d \frac{A_{sw}}{s}\, f_{yd}(\cot\alpha + \cot\theta)\sin\alpha \tag{4.32}$$

where

- d is the effective beam height;
- b_w is the cross-section width;
- α_c equal to 1 in this case, considers the tension in the compression zone;
- $v\, f_{cd}$ is the reduced compressive strenght of core concrete with $v = 0.5$;
- A_{sw} is the transversal reinforcement area;
- s is the transversal spacing.

The shear assessment for ULS are the following:

- $V'_{Ed} < V_{Rcd}$ with V'_{Ed} equal to the shear at the exact edge of the beam;
- $V''_{Ed} < V_{Rcd}$ with V''_{Ed} equal to the shear at distance d from the column.

Moreover, for ductility requirements, V_{RSd} has to be lower than V_{Rcd}.

For the definition of the construction details, the dissipative zone is distinguished from the non-dissipative one. The dissipative zone, with a length equal to 1.5 and 1.0 times the height of the beam, respectively for class "A" and "B", is the area at the end of the beam, where the formation of plastic hinges is expected.

Limitation are illustrated in 4.1.6.1.1 e 7.4.6.2.1 of [4]:

- In the dissipative zone, the stirrups must be arranged with a spacing no greater than the smaller of the following sizes:
  - a quarter of the effective height of the cross-section;
  - 175 mm and 225 mm respectively for class A and B;
  - 6 times and 8 times the minimum diameter of the longitudinal rebars considered for the assessment, respectively for class A and B;
  - 24 times the diameter of the transversal rebars.
- In the non-dissipative zone, which is that in between the two dissipative zones, the stirrups must be arranged following the limitations below:
  - Total section not lower than $A_{st} = 1.5b\,\mathrm{mm}^2/\mathrm{m}$ with b core thickness in mm;
  - 3 stirrups each meter;
  - Spacing not higher than 0.8 times the effective section height.

In order to comply with the aforementioned checks and limitations, it was chosen to use a transversal reinforcement arrangement that is the same for all the beams of the frame, which includes two-arm stirrups $\phi 8$, with a spacing equal to 7.5 cm in dissipative zones and 15 cm in the non-dissipative ones.

4.5.3 Beams: SLS

Limitations on tensions [17] prescribes that the maximum stresses in concrete and steel are lower than the following limit values:

- $\sigma_c < 0.6 f_{ck}$ for rare-characteristic combination;
- $\sigma_c < 0.45 f_{ck}$ for quasi-permanent combination;
- $\sigma_c < 0.45 f_{yk}$ for rare-characteristic combination.

Where tensions are computed with Navier expressions:

$$\sigma_c = \frac{M}{I_{om,x}} y \tag{4.33}$$

$$\sigma_s = n \frac{M}{I_{om,x}} y \tag{4.34}$$

having found the position of the neutral x axis by canceling the static moment of the section, in order to calculate the moment of inertia of the homogenized section; n indicates the homogenization coefficient.

The y value indicates the distance from the neutral axis of the fiber considered; the values of the distance of the tension reinforcement from the neutral axis will be used for the calculation of the stresses in the steel, and for concrete those of the distance of the outermost fiber, being subjected to greater deformation and therefore to higher tensions.

By calculating the stresses in the most stressed sections, i.e. at the ends and in the center of the beams, all the checks were satisfied.

Cracking The cracks width must be limited to not compromise the functionality, durability and aesthetics of the structure.

[17] allows to use limit values for the cracks width w_{max}, indicated in table 7.1N of the same standard, depending on the load combination and the environmental exposure class; the verification can be carried out through the analytical calculation of the cracks width:

$$w_{\max} = s_{r,\max}(\varepsilon_{sm} - \varepsilon_{cm}) \tag{4.35}$$

where:

- $s_{r,max} = k_3 c + k_1 k_2 k_4 \Phi / \rho_{\text{eff}}$ is the maximum cracks distance;
- c is the concrete cover;
- k_1 is the coefficient that takes into account the adhesion properties of the reinforcement (0.8 for bars with improved adherence; 1.6 for smooth bars);
- k_2 is the coefficient that takes into account the distribution of deformations (0.5 for bending; 1.0 for pure traction);
- $k_3 = 0.4$;

- $k_4 = 0.425$;
- ε_{sm} is the average reinforcement strain, taking into account the imposed strain and the effect of "tension stiffening";
- ε_{cm} is the average concrete stain among cracks.

The difference between the two average strains is computed as follows:

$$\varepsilon_{sm} - \varepsilon_{cm} = \frac{\sigma_{s,\max} - \frac{k_t f_{ctm}}{\rho}(1 + \alpha_e \rho_{\text{eff}})}{E_s} \tag{4.36}$$

where:

- k_t is the load-dependent factor (0.6 for short-term loads; 0.4 for long-term loads);
- $\alpha_e = E_s/E_c$;
- $\rho_{\text{eff}} = A_s/Bh_{c,\text{eff}}$;

Known $\varepsilon_{sm} - \varepsilon_{cm}$, w_k is calculated, which is compared with $w_{\max}$; it was found that the crack openings were always less than the maximum indicated in the standard, equal to 0.3 mm.

Deformation The functionality of the structure must be guaranteed by establishing adequate deformation limit values. In general, we have that:

- - The appearance and functionality of the structure can be compromised if the deflection of a beam, plate or cantilever subjected to quasi-permanent loads is greater than 1/250 of the span;
- For the secondary elements, such as partitions, walls, fixtures, windows, the deflection must not exceed 1/500 of the span.

According to [4], for beams and slabs with spans not exceeding 10 m it is possible to ignore the verification of the deflections considering it implicitly satisfied if the slenderness ratio $\lambda = l/h$ between span and height respects the limitation C4.1.4 of the aforementioned standard:

$$\lambda \leq K(11 + \frac{0.0015 f_{ck}}{\rho + \rho'})(\frac{500 A_{s.\text{eff}}}{f_{yk} A_{s,\text{calc}}}) \tag{4.37}$$

where f_{ck} is the characteristic compressive strength of concrete, ρ and ρ' are the tense and compressed reinforcement ratios respectively, $A_{s,\text{eff}}$ and $A_{s,\text{calc}}$ are, respectively, the tension reinforcement present in the most stressed zone and the calculation reinforcement in the same section, f_{yk} is the yield strength characteristic of the reinforcement (in MPa) and K is a corrective coefficient, which depends on the structural scheme. The verification was satisfied for all beams.

4.5.4 Colums: bucklings ULS

For the column buckling assessment, it is correct to start from the limitations on the longitudinal reinforcement, following what [4] suggests in 4.1.6.1.2 and 7.4.6.2.2:

- the rebars parallel to the column axis must have a diameter greater than or equal to 12 mm and a spacing smaller than 300 mm;
- reinforcement area must be greater than $0.10\, N_{Ed}/f_{yd}$ and in any case not lower than $0.003A_c$;
- reinforcement area must respect the following limits:

$$1\% \leq \rho \leq 4\% \tag{4.38}$$

where ρ is given by the ratio between the total longitudinal reinforcement area and the area of the gross concrete section. In the case in question, there are square columns with a side of 600 mm, therefore the minimum reinforcement is equal to 3600 mm^2, for which a reinforcement consisting of 12 rebars with a diameter of 20 mm is chosen for all the columns, of which 4 are of corner and 8 additional intermediates, which form a total area of 3770 mm^2.

This choice translates into a single moment-normal resistance domain, Figure 4.8, since this depends only on the geometry of the section.

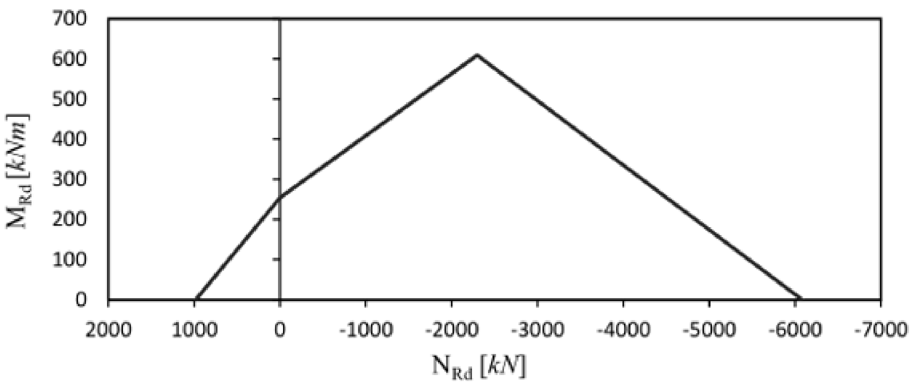

Figure 4.8: M-N resistance domain of columns

Following the resistance hierarchy, for each direction and each orientation of seismic actions application, the columns must be protected from premature plasticization by adopting appropriate design bending moments: this condition is reached if, for each beam-column node and for each direction and towards the seismic action, the overall resistance of the columns is greater than the overall resistance of the beams amplified by a coefficient γ_{Rd}, in accordance with 7.4.4.2.1 of [4].

Thus, equation (4.39) follows:

$$\sum M_{c,Rd} \geq \gamma_{Rd} \sum M_{b,Rd} \tag{4.39}$$

where:

- γ_{Rd} is the over resistance factor equal to 1.3 for ductility class A and B;
- $M_{c,Rd}$ is the resistance moment of the generic column at node, calculated for the normal action present in the seismic combinations of actions;
- $M_{b,Rd}$ is the generic resistance moment of the beam at node;

For the base section of the column of the ground floor, is used as design moment the largest between the moment resulting from the analysis and the moment $M_{c,Rd}$ of the top section of the column. The criterion of hierarchy of the resistances does not apply to the top sections of the columns of the top floor, because this would determine very large sections them, therefore for these sections it is better to proceed with the classic assessment procedure, which includes the inclusion of the point N_{Ed},M_{Ed} within the resistance domain.

With the reinforcement consisting of 12 rebars with a diameter of 20 mm, the ULS assessment and the construction limitations were satisfied.

4.5.5 Colums: shear ULS

In order to exclude the formation of inelastic mechanisms due to the shear solicitations, the criterion of the resistance hierarchy provides that the shear stresses to be used for the checks and for the reinforcement design are obtained from the equilibrium condition of the column, subject to the action of the resistant moments in the upper end sections $M^s_{c,Rd}$ and lower $M^i_{c,Rd}$, according to the expression provided in 7.4.4.2.1:

$$V_{Ed} = \gamma_{Rd} \frac{M^s_{c,Rd} + M^i_{c,Rd}}{l_p} \tag{4.40}$$

where l_p is the column length.

Knowing the acting shear is thus possible to proceed with the shear design as suggested in 4.1.2.3.5.2 of [4].

As described for the beams, the calculation model is based on the Ritter-Morsch truss. Assuming this behaviour, with reference to core concrete, the design resistance to "compression shear" is calculated with (4.31) and (4.32).

For ductility requirements it must be also verified that $V_{Rsd} > V_{Rcd}$.

According to 7.4.6.1.2, in the absence of more accurate analyses, it can be assumed that the length of the dissipative zone is the greater than:

- Section height;
- 1/6 of the column free length;
- 45 cm;
- The column free length, if it is smaller than 3 times the section height.

Moreover, according to 7.4.6.2.2, in the dissipative zones, the following requirements must be taken into account:

- the corners rebars must be contained by the stirrups;

- at least one rebar every two, of those arranged on the sides, must be held by internal stirrups or by links;
- the not fixed rebars must be at less than 20 cm from a fixed rebar for ductility class B and at less than 15 cm for class A.

The diameter of the containment stirrups and links must be not less than 6 mm and their spacing must be no greater than the smaller of the following quantities:

- 1/3 or 1/2 of the smaller side of the transversal section respectively for class A and B;
- 175 mm or 125 mm respectively for class A and B;
- 6 or 8 times the diameter of the longitudinal rebars respectively for class A and B.

The mechanical ratio of the transversal confinement reinforcement ω_{wd} within the dissipative zone must be not less than 0.12 in class a and 0.8 in class B where:

$$\omega_{wd} = \frac{\text{confinement stirrups volume}}{\text{concrete core volume}} \frac{f_{yd}}{f_{cd}} \tag{4.41}$$

In all the columns, and for the entire length of the same, 2 stirrups with 2 arms were used, for a total of 4 arms, in both directions with a diameter of 8 mm, with spacing of 10 cm and this meant that they came comply with the resistance checks and regulatory limitations.

4.5.6 Nodes

A node is defined as the area of the column that crosses with the beams competing with it. The resistance of the node must be such as to ensure that it does not reach failure before the areas of the beam and column adjacent to it; it is also necessary to avoid, as far as possible, the presence of eccentricity between the axis of the beam and the axis of the column competing in the same node.

The nodes assessment is aimed at checking that the maximum diagonal compression and the maximum diagonal tension in the node do not exceed the resistance values of the concrete.

In 7.4.4.3.1, [4] provides that the horizontal shear acting in a beam-column node, for each direction of the seismic action, can be determined through simplified expressions :

- for internal nodes:
$$V_{jbd} = \gamma_{Rd}(A_{s1} + A_{s2})f_{yd} - V_c \tag{4.42}$$
- for external nodes:
$$V_{jbd} = \gamma_{Rd}A_{s1}f_{yd} - V_c \tag{4.43}$$

where:

- A_{s1} is the reinforcement of upper strip;

- A_{s2} is the reinforcement of lower strip;
- V_c is the shear force in the pillar above the node, in the seismic condition;

The diagonal compression induced in the node by the truss mechanism must not be greater than the compressive strength of the concrete; in the absence of a more accurate model, this prescription can be verified by the use of the following rule:

$$V_{jbd} \leq \eta f_{cd} b_j h_{jc} \sqrt{1 - \frac{v_d}{\eta}} \tag{4.44}$$

where:

- $\eta = \alpha_j (1 - f_{ck}/250)$ with
- α_j equal to 0.48 for inner nodes and 0.60 for external nodes;
- $v_d = N_{Ed}/(A_c f_{cd})$ normalized axial force above the column;
- h_{jc} distance between the farthest rebars of the column;
- b_j effective node width assumed as the smaller between:
  - the greater of the widths of the column and beam section;
  - the smaller of the widths of the column and of the beam section, both increased by half the height of the column section.

To avoid that the maximum diagonal traction of the concrete exceeds f_{ctd}, adequate confinement must be provided which, in the absence of more accurate models, is given by horizontal stirrups with a diameter of not less than 6mm such that:

$$\frac{A_{sh} f_{ywd}}{b_j h_{jw}} \geq \frac{(\frac{V_{jhd}}{b_j h_{jc}})^2}{f_{ctd} + v_d f_{cd}} - f_{ctd} \tag{4.45}$$

where:

- A_{sh} is the total area of the horizontal stirrups;
- h_{jw} is the distance between the upper and lower rebars of the beam.

Alternatively, the integrity of the node due to the diagonal cracking can be fully guaranteed by the horizontal stirrups if:

- for internal nodes:

$$A_{sh} f_{ywd} \geq \gamma_{Rd} (A_{s1} + A_{s2}) f_{yd} - (1 - 0.8 v_d) \tag{4.46}$$

- for external nodes:

$$A_{sh} f_{ywd} \geq \gamma_{Rd} A_{s2} f_{yd} - (1 - 0.8 v_d) \tag{4.47}$$

In all nodes 2 stirrups with 2 arms were used, for a total of 4 arms, in both directions with a diameter of 8 mm, with a spacing of 5 mm and this meant that the aforementioned checks were respected.

4.5.7 Inter-storey displacements

According to 7.3.6.1 of [4], the required condition in terms of structural stiffness is considered satisfied if the structural elements deformation does not cause damage on the non-structural elements such as to make the construction temporarily unusable. In the case of civil and industrial buildings, if the temporary inaccessibility is due to excessive inter-storey displacements, this condition can be considered satisfied when the inter-storey displacements obtained by the analysis in the presence of the design seismic action corresponding to the limit state and utilization class considered are lower than the limits indicated below:

$$qd_r \leq 0.01h \tag{4.48}$$

where d_r is the inter-storey displacement, (i.e. the difference between the displacements of the upper and lower floors), calculated, in the case of an earthquake with DLS elastic spectrum and h is the height of the floor, equal to 3 m.

The verification is satisfied for all floors of the frame.

4.6 Summary of the design choices

The main characteristics of the frame designed according to the ultimate limit state method are summarized below, in compliance with the hierarchy of resistances and the constructive limitations of the standard:

- columns cross-section: 60x60 cm;
- beams cross-section: 40x50 cm;
- longitudinal columns rebars: 12ϕ20;
- longitudinal beams rebars: 3ϕ18 in the upper zone and $2-5\,\phi$18 in the lower one;
- 4 arms stirrups(ϕ8) spacing, in columns: 10 cm;
- 2 arms stirrups (ϕ8) spacing, in dissipative zone of beams: 7.5 cm;
- 2 arms stirrups(ϕ8) spacing, in non-dissipative zone of beams: 15 cm;
- 4 arms stirrups(ϕ8) spacing, in nodes: 5 cm;

Attached are the tables concerning the geometry and the arrangement of the reinforcement bars in the structural elements.

4.7 Robustness adjustments

The design choices described in the latter paragraph of this chapter, are the result of a traditional design procedure, following a semi-probabilistic approach in accordance with the specification suggested in [4] and [17]. The R.C. frame obtained is hence designed to withstand permanent, accidental and seismic actions; extreme events, which entity and impact on the structure cannot be exactly defined, have not yet been taken into account.

Thus, a robustness analysis which consider such exceptional action, in order to prevent a disproportioned collapse, still has to be conducted; moreover, aim of this thesis is to proceed with a probabilistic approach that was not yet exploited until this design stage.

For this purpose a preliminary robustness analysis is described below, recalling some work steps and some results obtained in previous Master's thesis works [19] and [20].

Therefore, this brief discussion constitutes the logical conjunction point between the traditional design just described, and the probabilistic robustness analysis of the next chapters, that will lead to obtain the final probabilistic capacity curves of the structure.

4.7.1 Preliminary analysis

In order to analyse the behaviour of the structure under particular situation, specific analysis have been conducted; more specifically, *pushdown* analysis have been carried out to simulate the loss of the central column at the ground floor of the structure to study the frame behaviour under this extreme event, reproducing the effect of a possible impact or explosion near that element during the service life of the structure.

The pushdown analysis has been conducted removing the ideally lost column and imposing a controlled displacement et the top of the previously existent element.

Firstly, preliminary analysis conducted by [19] and [20] started considering the exceptional combination of actions that writes as follows:

$$G_1 + G2\Psi_{21}Q_{k1} + \Psi_{22}Q_{k2} + \dots \tag{4.49}$$

where G_1 and G_2 are the permanent structural and non-structural loads respectively, Q_{kj} are the variable actions and Ψ_{ij} are the coefficients of combinations relating to the j-th variable action, equal to 0.3 for the overload due to the use in intermediate floors and equal to 0 for wind, snow and overload on the roof.

The analysis conducted with this exceptional combination allows to compute a value of the reaction at the base of the central column equal to 1032 kN.

Once the reaction was founded, a dynamic amplification factor $\lambda = 1.5$ was applied to loads, carrying out another analysis that lead to a new value of reaction equal to 1548 kN.

This application of the dynamic amplification factor is generally used in structural analysis to simulate the suddenly and accidental removal of a structural element. Indeed, when a structural element like a column collapses, what happen is that the static equilibrium is perturbated, thus the structure responses in a dynamic way trying to find a new equilibrium condition represented by a balance between displacement and internal solicitations.

Deeper argumentations on this theme of paramount importance for this thesis, will be deeply discussed in the next chapters.

Once the amplified reaction is calculated it can be applied to the structure during the pushdown analysis and interesting results can be found. In particular, what [19] and [20] want to stress in their works, is that the results of the capacity curves describe a structural situation according to which the frame is not able to bear the amplification of lads; indeed from the capacity curve obtained it was found a value of maximum flexural resistance moment equal to 1035 kN, which is so much lower that the value of the previously mentioned reaction equal to 1548 kN that the structure has ideally to bear. Moreover, also the value of the maximum membrane resistance moment equal to 942 kN, is even smaller.

This made the authors to deepen the reinforcement design of the beams obtaining interesting results.

4.7.2 Reinforcement adjustments

In [19] and [20], different reinforcement modifications have been exploited; all the treated aspects started from the analysis of the global behaviour of the frame, read as consequence of local failure process like formation of plastic hinges in some specific points. This analysis brought authors to apply the following progressive modifications to the longitudinal rebars of the beams:

- *rebars continuity*: the application of continuous rebars along the entire length of the beams improves the homogeneity of tension redistribution, leading to an increase of resistance reserves, in terms of maximum appliable displacement.
- *rebars symmetry*: the use of symmetric rebars, lead to an increment of both flexural an membrane maximum resistance moment, indeed have more rebars in the lower strip of the beam allow to trigger higher positive resistance moment that are needed when column is removed and the beam, at the central node, undergoes a change in sign of the acting moment from negative to positive.
- *rebars homogeneity in floors*: finally, the application of homogeneous rebars at all the beams of each floor, lead to a global improvement of the structural behaviour; in particular catenary effects can be detected from capacity curve analysis, as well as an increment of the membrane maximum resistance moment that exceeds the flexural peak.

These improving steps have brought to a final design model in which all the beams have a longitudinal reinforcement constituted by $5\phi18$ both in upper and lower strip. This constitute the model on which analysis will be carried out in the next chapters.

Chapter 5

Modeling with Atena 2D

5.1 Software overview

Probabilistic capacity curves determination was possible through detailed structural analysis carried out with a dedicated non-linear analysis software: ATENA 2D.

ATENA 2D belongs to a bigger family of software produced by *Cervenka Consulting* software house, specialized in the production of structural analysis software. In general, ATENA software allow users to make static or dynamic non-linear analysis both in 2D or 3D environment, considering several complex behaviour of construction materials like concrete, steel, but also masonry, soil and rocks. Indeed, detailed materials constitutive laws are exploitable, testing construction material behaviours in different inelastic situations as plastic stages, softening or cracks opening. Moreover, specific conditions like influence of viscosity, thermal effects, or humidity and their consequences on the materials can be studied with a high level of detail.

Very accurate solutions can be obtained thanks to the multiple choices of finite element among which the user can choose (several 2D isoparametric elements or 3D solid elements) and tanks also to the various exploitable FEM solutions.

5.1.1 Software organization

Using ATENA 2D for structural analysis, three distinct utilization steps can be detected when a common user have to face with the software:

- *Pre-processing*: in this first phase, materials, geometry, supports and actions can be defined, in this stage moreover, the analysis conditions have to be chosen, in terms of loading history and solution parameters. Monitoring points can be also placed, and the mesh is generated.
- *FE non-linear analysis*: this is the phase during which the software runs, applying the loads to the previously constructed model and analysing the various results. The graphical interface allows users to follow in real time the evolution of the events.
- *Post-processing*: when analysis ends, all the found results are accessible tanks both to interactive interface in a graphical way, or in a list format choosing firstly which

type of information one wants to read an eventually export for further analysis.

Finally it must be specified that the *Pre-processing* stage can be conducted not only by using the graphical interface of the software; indeed it is possible to write a *code* in a ".cct" format containing all the information described for this stage,. The file can be directly imported in the software making often the pre-processing stage more rapid and efficient, especially when the user has to deal with several similar models.

Conducted analysis overview

ATENA 2D in particular, allows to perform non-linear static analysis in a 2D environment; this choice results to be sufficient for the purposes of this work. More specifically one particular type of model was created starting from the 2D R.C. multistorey plane frame designed in the previous chapter: the type of analysis was a displacement controlled Push-down analysis conducted on a model where the central column of the ground floor was removed to simulate an exceptional event; the probabilistic analyses were required for the final determination of the capacity curves which data have been then used to determine the dynamic amplification factors, simulating the column removal dynamic effect on each of the aleatory model. Results are so interpreted, trying to understand finally, if each of them will withstand or not the consequences of a sudden column removal, without a disproportioned collapse.

5.2 Pre-processing

As just said, the pre-processing stage is the first phase of the structural analysis during which material properties, structural geometry, constraints and loads are defined in detail.

All these model properties can be defined through the menu on left side of the graphic interface of the software.

5.2.1 Materials

In the section Materials, ATENA 2D gives the possibility to choose among several types of construction materials: *Plane Stress Elastic Isotropic; Plane Strain Elastic Isotropic; 3D Non Linear Cementitious; SBeta Material; Microplane 4 Material; 3D Bilinear Steel Von Mises; 2D Interface; Reinforcement; Spring; Bond for Reinforcement; 3D Drugker-Prager Plasticity; Material with Random Field.*

The materials used for the modeling of a reinforced concrete building are concrete, defined with *SBeta Material* and steel of the reinforcement bars, defined with *Reinforcement.*

SBeta Material The name *SBeta* derives from the software in which this material model was used for the first time and represents the German abbreviation of *StahlBETonAnalyse*, which means "analysis of reinforced concrete". SBeta material includes the following effects of concrete behavior:

- nonlinear behaviour in compression, including both the hardening and softening phases;

- cracking of tensioned concrete according to non-linear laws of fracture mechanics;
- criterion of resistance in a state of biaxial tension;
- tension stiffening effect;
- fixed or variable reduction of shear stiffness after cracking;
- two models of cracking: fixed and rotated direction of the crack.

All these aspects of concrete behaviour can be managed thanks to five different graphic windows: *Basic, Tensile, Compressive, Shear and Miscellaneous.*

Basic In this stage are defined the tangent elastic modulus E, the Poisson coefficient μ, the tensile strength f_t and the and the compressive one f_c. Figure 5.1.

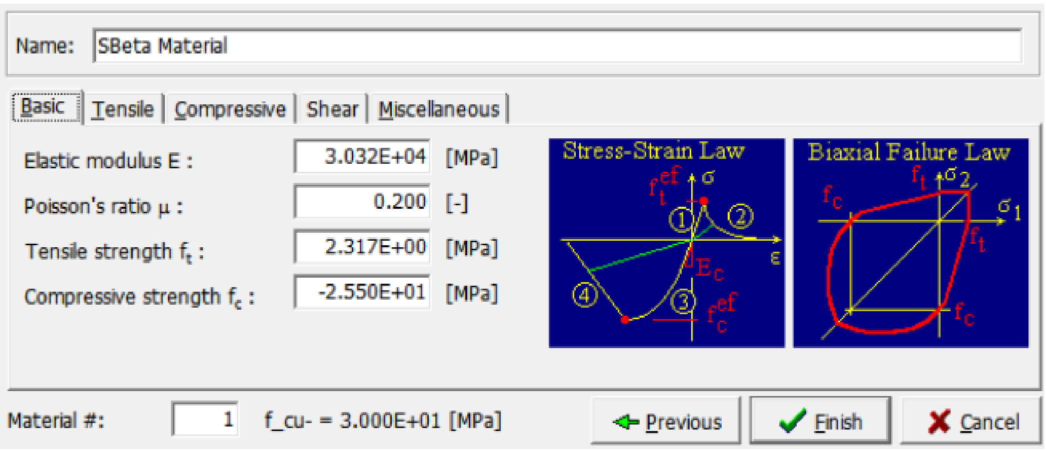

Figure 5.1: SBeta Basic Window

Tensile Here it is possible to choose the concrete traction law among exponential, linear and local deformation; it is also possible to define the softening parameter c_3 and the crack model, which can be fixed or rotated. Figure 5.2.

Compressive The compressive deformation value at the compressive resistance in the uniaxial test, the reduction coefficient of the compression resistance due to cracking, the softening law, and the softening parameter c_d are requested. Figure 5.3.

Shear It is necessary to choose a reduction law of the fixed or variable shear modulus, and the type of compression tension interaction, which can be linear or described by two different hyperbolic laws. Figure 5.4.

Miscellaneous The specific weight of the material ρ and the thermal expansion coefficient α are requested. Figure 5.5

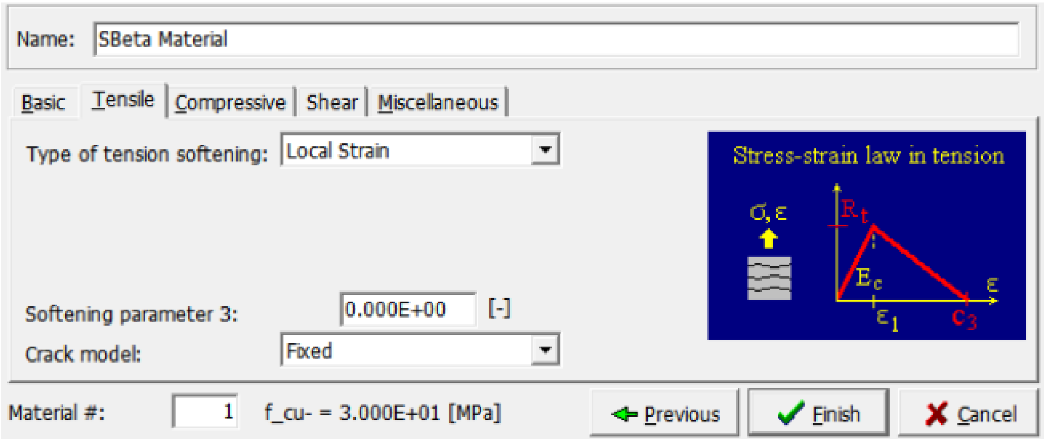

Figure 5.2: SBeta Tensile Window

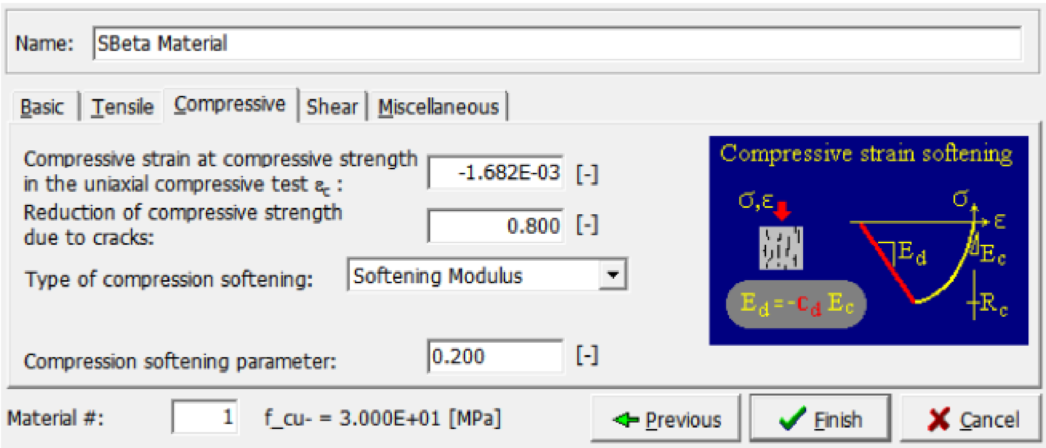

Figure 5.3: SBeta Compressive Window

Reinforcement The material type *Reinforcement* can be defined in two distinct ways, i.e. discreetly or widely. Discrete reinforcement is in the form of reinforcement rebars and is modeled linearly by entering the start and end points; diffuse reinforcement is considered as a component of the composite material to which it belongs.

In both cases, the constitutive law relating to the monoaxial test used in all steel types is considered, which can be modeled in the program as linear, bilinear, multilinear or bilinear with hardening. For the definition of the latter, in the *Basic* section four parameters are required, which are the elastic modulus E, the yield stress σ_y, the ultimate stress σ_t and the ultimate strain ε_{lim}. While in the Miscellaneous window the specific weight of the material ρ and the thermal expansion coefficient α are requested.

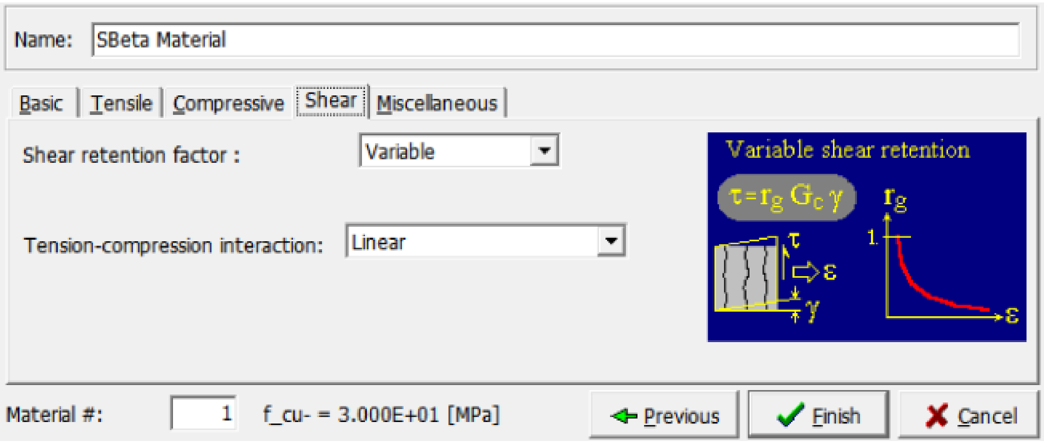

Figure 5.4: SBeta Shear Window

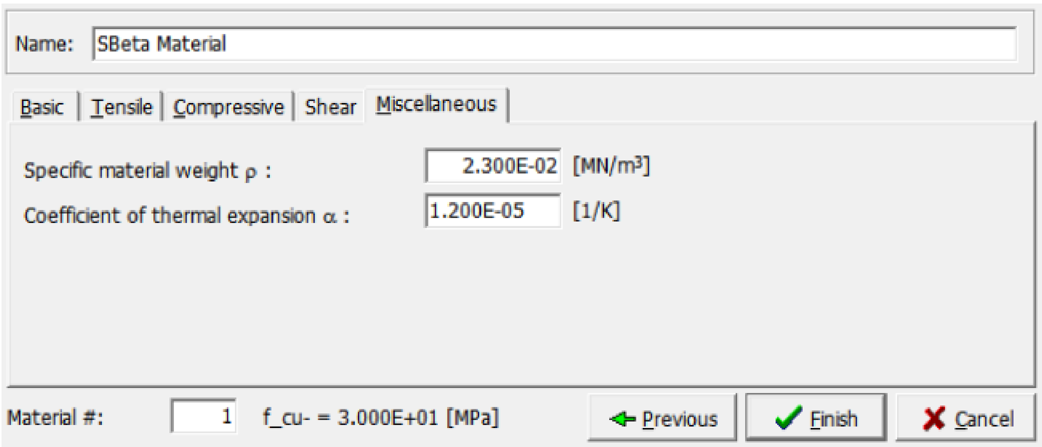

Figure 5.5: SBeta Miscellaneous Window

5.2.2 Geometry

The elements geometry in reinforced ATENA 2D is defined in the *Topology* section by means of *nodes*, *lines* that connect the various nodes and *macro-elements* that are enclosed within multiple lines.

The *points* are defined in the *Joints* subsection, where the values of the X coordinate and the Y coordinate are requested, as shown in Figure 5.8; there is also the possibility of inserting springs in each defined point.

The lines are defined in the Line subsection, where the markers of the start and end points are inserted Figure 5.9; also, for the lines it is possible to create springs that act on the entire length of the lines themselves.

In the *Macro-elements* subsection macro-elements are created: a Boundary list is requested, which is the list of markers of the lines that enclose the element, the type of mesh, which can be triangular, quadrilateral or mixed, the size of the mesh , the material and

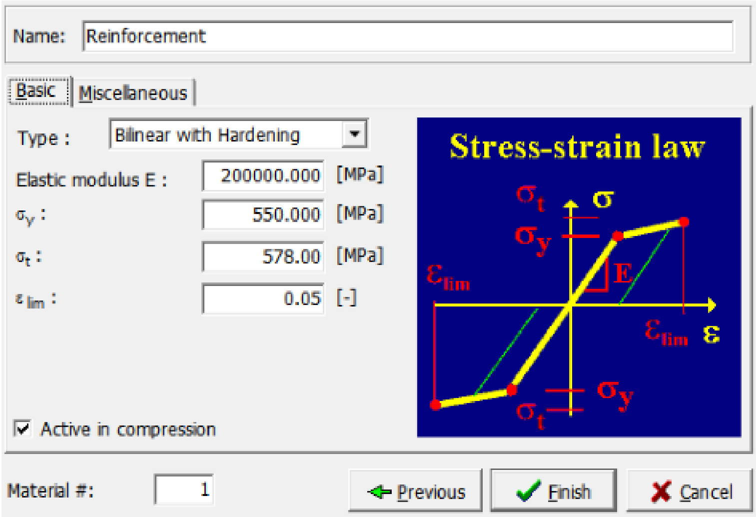

Figure 5.6: Reinforcement Basic Window

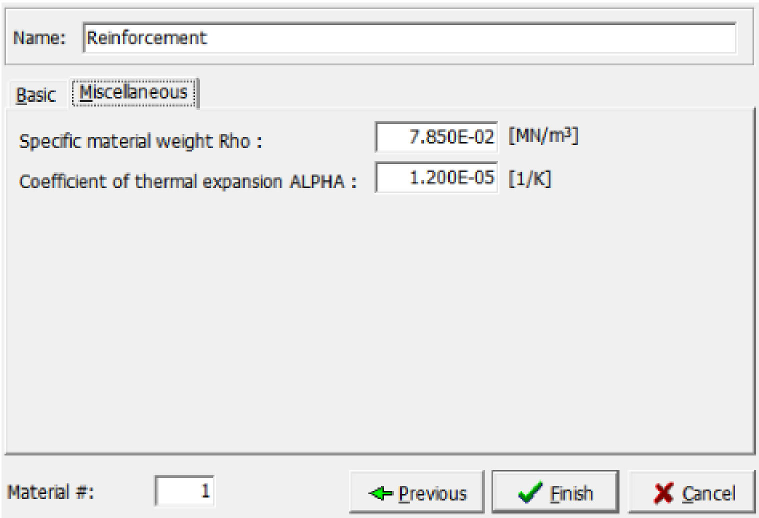

Figure 5.7: Reinforcement Miscellaneous Window

the thickness, as shown in Figure 5.10. The diffused reinforcements can be defined in this phase by means of the Layers of *smeared reinforcement* sub-window.

While the discrete reinforcing bars are defined in the *Reinforcement* subsection by means of the material, the coordinates of the start and end points Figure 5.11, the area of the bar section and the interaction between steel and concrete, which can be considered to be perfect adherence, or it can be modeled through a specific bond Figure 5.12.

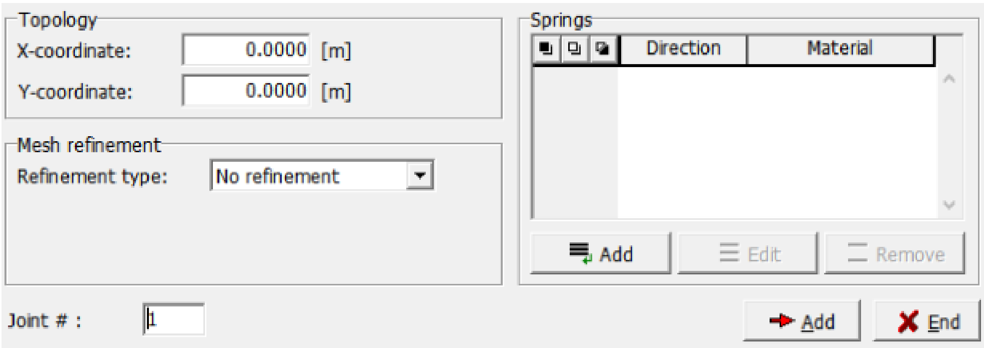

Figure 5.8: Nodes definition

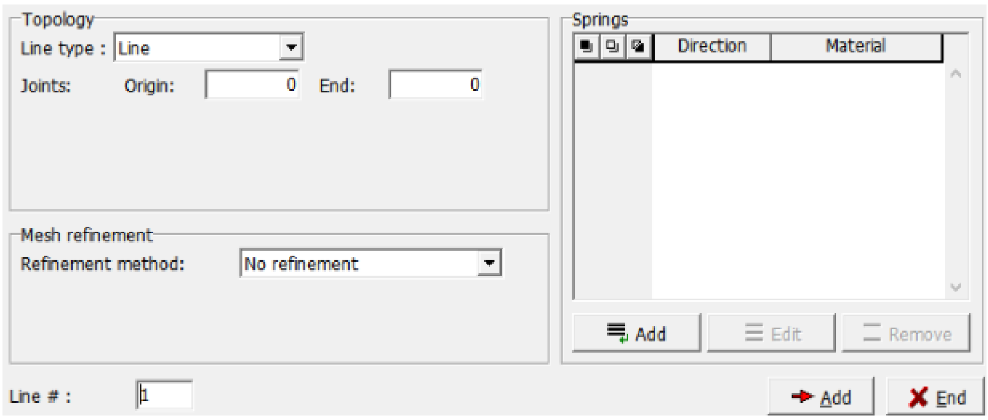

Figure 5.9: Lines definition

5.2.3 Mesh generation

Once the geometry of the model is fully defined, it is possible to automatically generate the *Mesh* trough the executing button. Depending on the geometry of the *Macro-elements* previously created, the software creates a Finite Element mesh that will represents the nest which nodes will be the representing points of the structural elements, and in that point the analysed solutions will be found. The dimension and the refining of the mesh around specific edges of the elements, are choices of paramount importance for the quality of the final results; therefore knowing a-priori the most interesting structural zones, it possible to refine there the mesh and also save computation time.

It is important to underline that similar mesh density have to be used for adjacent element with different characteristic to allow the software to fit the elements belonging to the two different sections.

5.2.4 Support and Loads

In the *Loads* and *Supports* section, it is possible to define the constraints of the structure, the applied loads, the imposed displacements, the effects of thermal variation, shrinkage

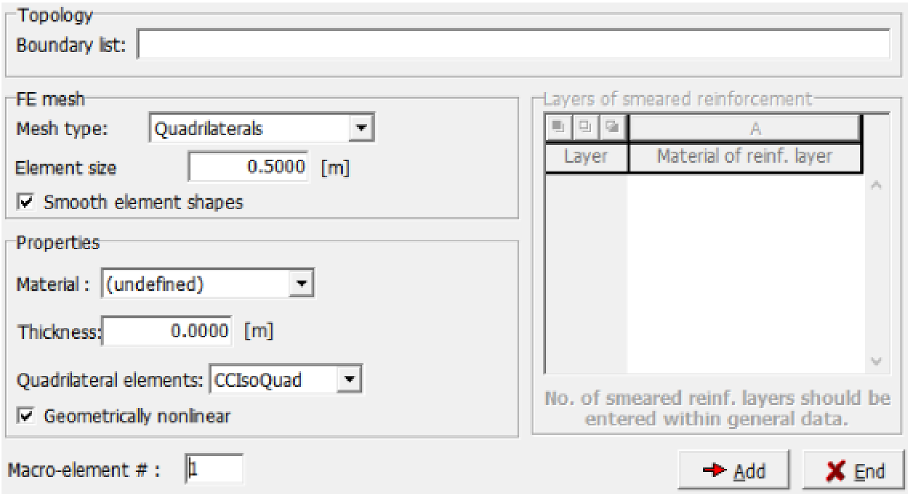

Figure 5.10: Macro-elements definition

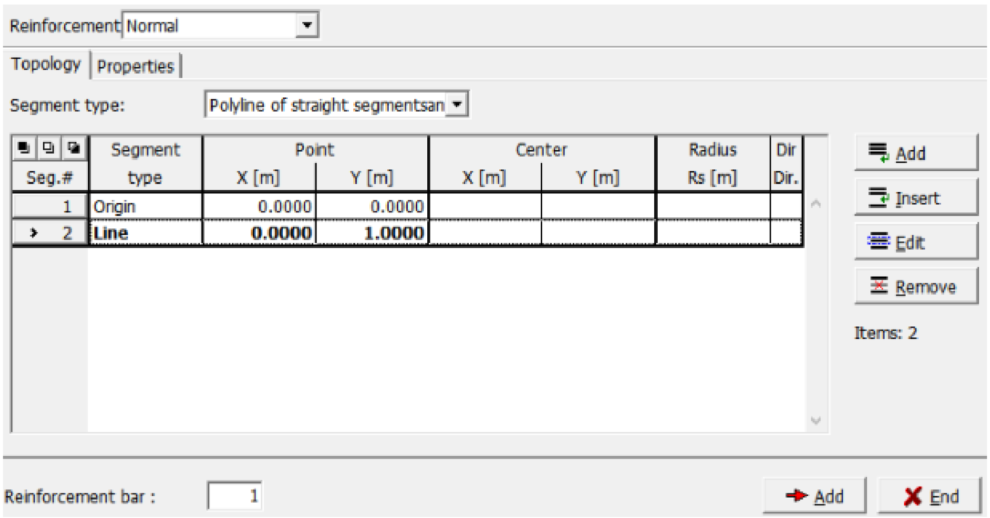

Figure 5.11: Reinforcement Topology definition

and prestressing, as shown in Figure 5.13.

Once the various Load cases have been created, the second step is to apply them on the model; to do this, it is necessary first activate one element by clicking on Set active in the bottom window, and then select the reference points, lines or macro-elements in the model. Then click on the *Joint*, *Line* or *Macro-element* subsections in the *Loads and supports* section, and enter the required parameters, which are shown in Figure 5.14, Figure 5.15 and Figure 5.16 respectively for the definition of imposed constraints, forces and displacements:

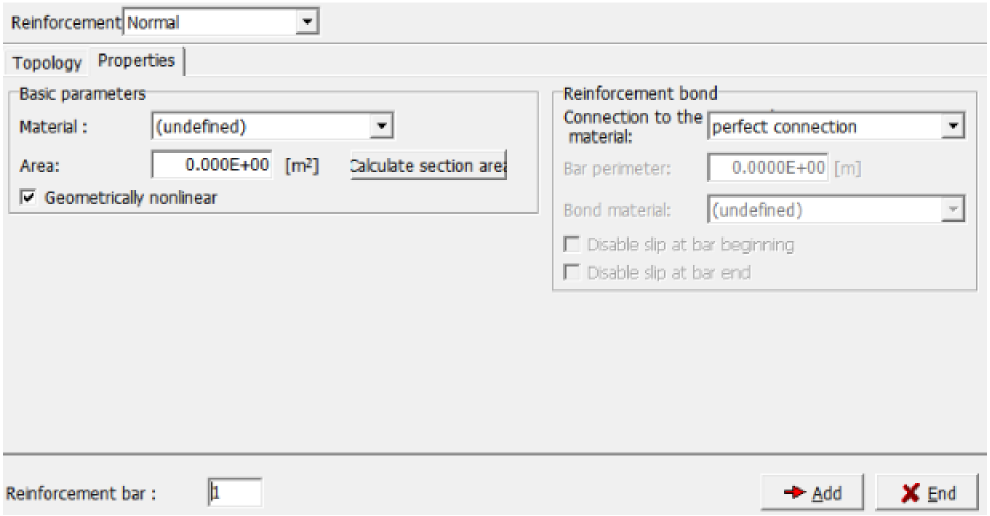

Figure 5.12: Reinforcement Properties definition

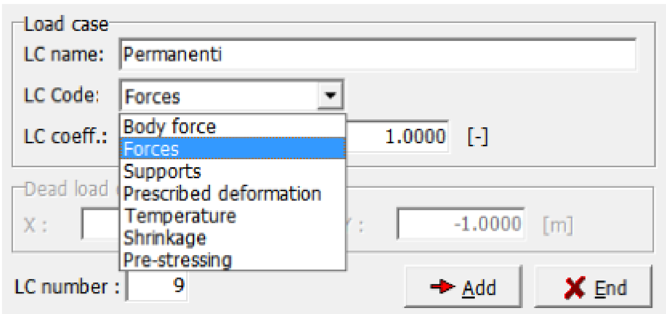

Figure 5.13: Reinforcement Properties definition

5.2.5 Analysis parameters

The analysis settings are defined in the *Run* section; in particular, the main subsections are represented by the *Analysis steps* and by the *Monitoring points*.

The individual analysis steps are created by clicking on *Add* in the *Analysis steps* subsection; here the list of *Load cases* to be considered in the analysis is requested and the type of non-linear calculation, which can be *Standard Newton-Raphson* and *Standard arc length*: in Figure 5.17 a possible sequence of analysis steps is illustrated:

The monitoring points are specific points of the model, where user wants to know for example the displacement or the nodal reaction and are created by clicking on *Add* in the *Monitoring points* subsection; the coordinates of the point and the type of monitoring are therefore requested; Figure 5.18 illustrates a possible list of monitoring points.

With the setting of the monitoring points, any curves to be checked in the *post-processing* phase are automatically selected: each component will have a value for each analysis step, which can be related to all the other components in the form of graphs, which can be for example force-displacement curves or displacement-displacement curves.

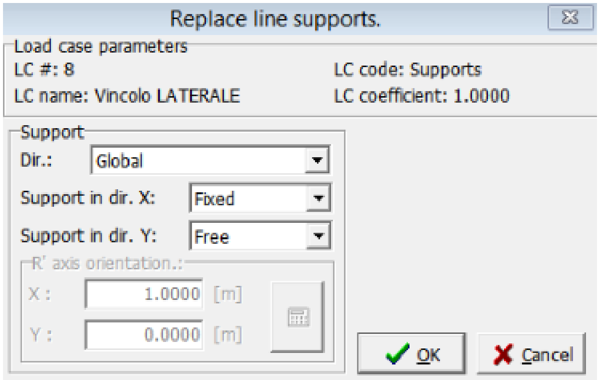

Figure 5.14: Definition of linear constraints

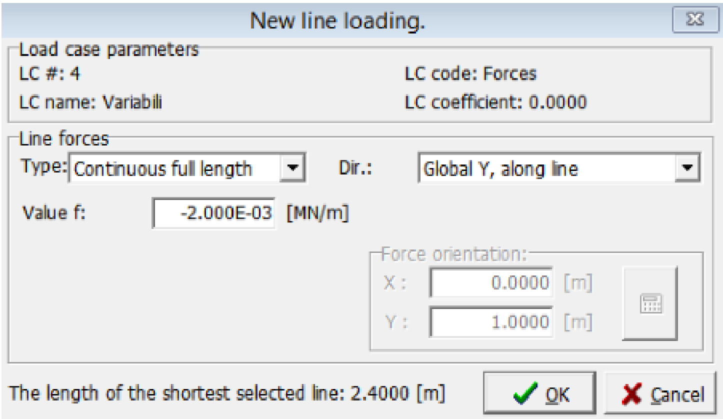

Figure 5.15: Definition of linear distributed load

5.3 FE non-linear analysis

Once that all the *Pre-processing* steps are defined and thus the model is completed and the FE Mesh is generated, it is possible to proceed with the actual analysis.

5.3.1 Starting analysis

By clicking on the *Run* button hence, the analysis can start; an initialization windows opens allowing the user to select which steps he wants to run and if for each step the results must be saved. Moreover, it is possible to choose which type of diagram visualize during the analysis, even if it can be changed also while the software is running Figure 5.19.

Obviously if data for certain load step are not saved, the relative results cannot be analysed during the *Post-processing* stage.

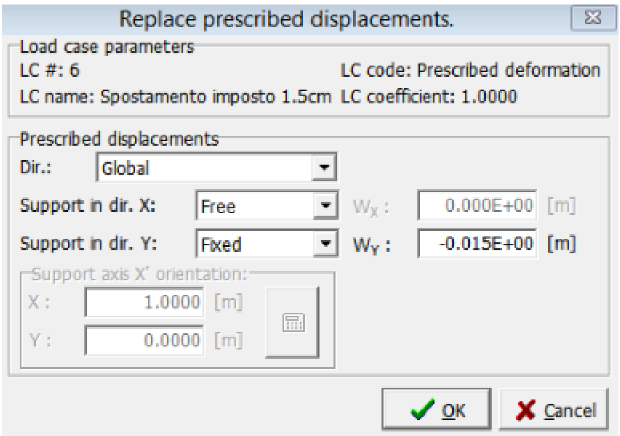

Figure 5.16: Definition of imposed displacement

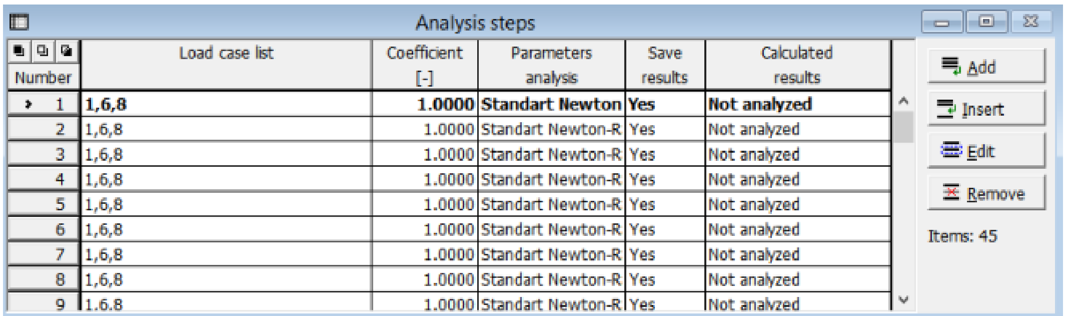

Figure 5.17: Example of Analysis steps

5.3.2 Interactive window

When the *Analyze* button is pressed, analysis starts, and a new graphic interface opens. Managing it, is possible to change the quantities represented in the live 2D graph; therefore, since nonlinear analysis are usually very expensive from a computational point of view and often take a long time, ATENA 2D allows the results to be graphically displayed not only at the end of the analysis, but also in real time, i.e. at the end of each step Figure 5.20. This means that for example is possible to monitor the displacements and cracks evolution in the structure using also a magnification factor that facilitates the visualization of even small opening or movements of the model.

5.4 Post-processing

The *post-processing* phase is that relating to the control of the results; these can be checked graphically using rendering maps that are overlapped to the geometrical model to facilitates an immediate visualization of the global behaviour of the model. Cracks pattern, stress and strain maps, as well as displacement at each integration point can be thus easily seen.

Below, some examples of possible graphical results are reported: Figure 5.21, Figure

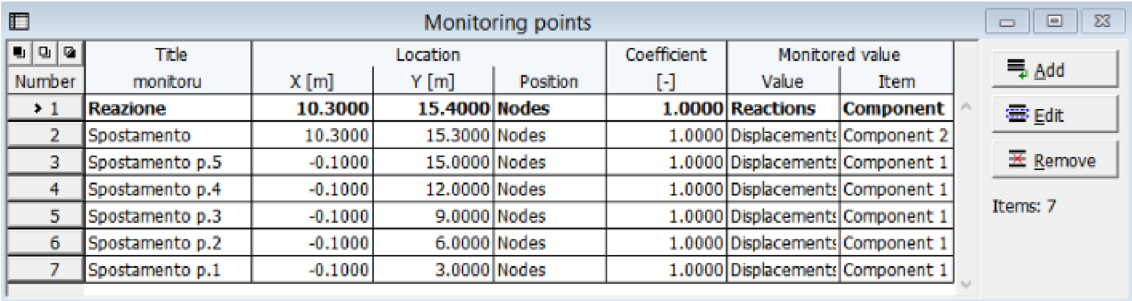

Number	Title monitoru	Location X [m]	Location Y [m]	Location Position	Coefficient [-]	Monitored value Value	Monitored value Item
1	**Reazione**	**10.3000**	**15.4000**	**Nodes**	**1.0000**	**Reactions**	**Component**
2	Spostamento	10.3000	15.3000	Nodes	1.0000	Displacements	Component 2
3	Spostamento p.5	-0.1000	15.0000	Nodes	1.0000	Displacements	Component 1
4	Spostamento p.4	-0.1000	12.0000	Nodes	1.0000	Displacements	Component 1
5	Spostamento p.3	-0.1000	9.0000	Nodes	1.0000	Displacements	Component 1
6	Spostamento p.2	-0.1000	6.0000	Nodes	1.0000	Displacements	Component 1
7	Spostamento p.1	-0.1000	3.0000	Nodes	1.0000	Displacements	Component 1

Figure 5.18: Example of Monitoring Points

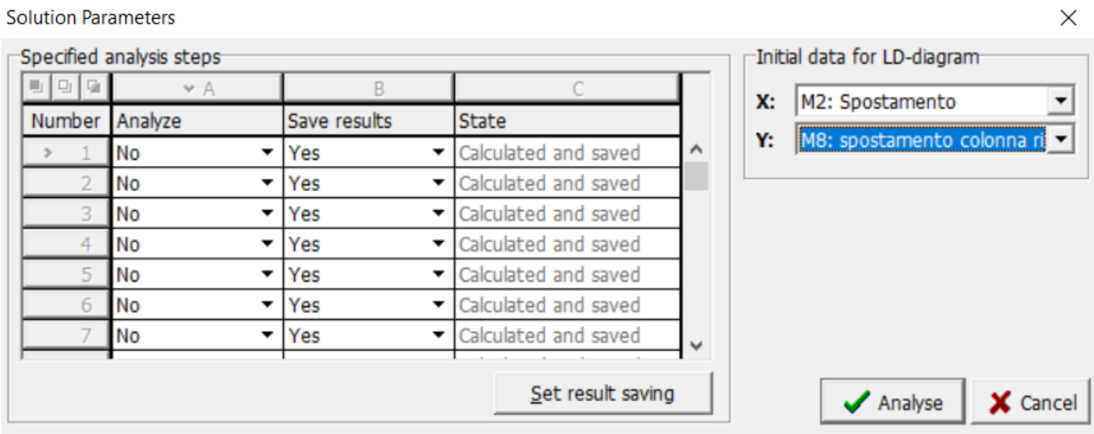

Number	Analyze	Save results	State
1	No	Yes	Calculated and saved
2	No	Yes	Calculated and saved
3	No	Yes	Calculated and saved
4	No	Yes	Calculated and saved
5	No	Yes	Calculated and saved
6	No	Yes	Calculated and saved
7	No	Yes	Calculated and saved

Figure 5.19: The dialog window before the finite element analysis

5.22 and Figure 5.23.

Moreover, the software allows the user to obtain all these sets of results in a text format, so that they can be exported and analysed with other software or simply algorithm. Figure 5.24

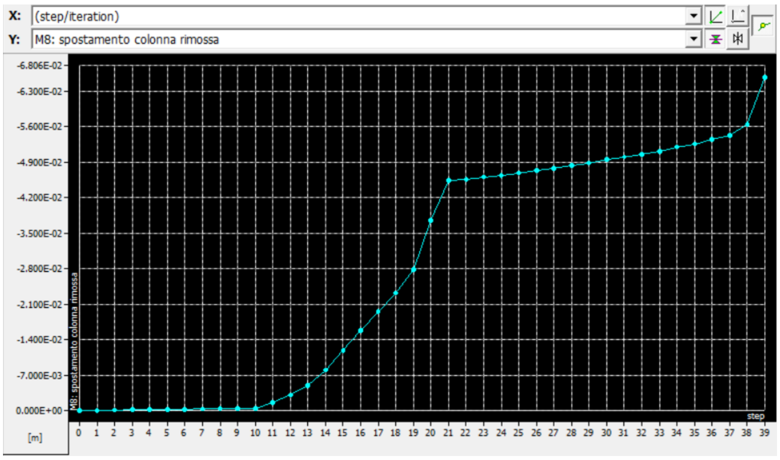

Figure 5.20: Example of 2D interactive graph

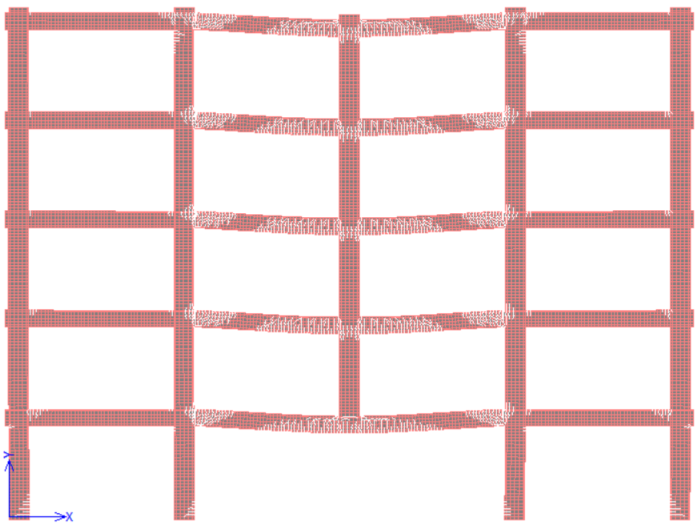

Figure 5.21: Example of displacement and cracks pattern of a plane frame model

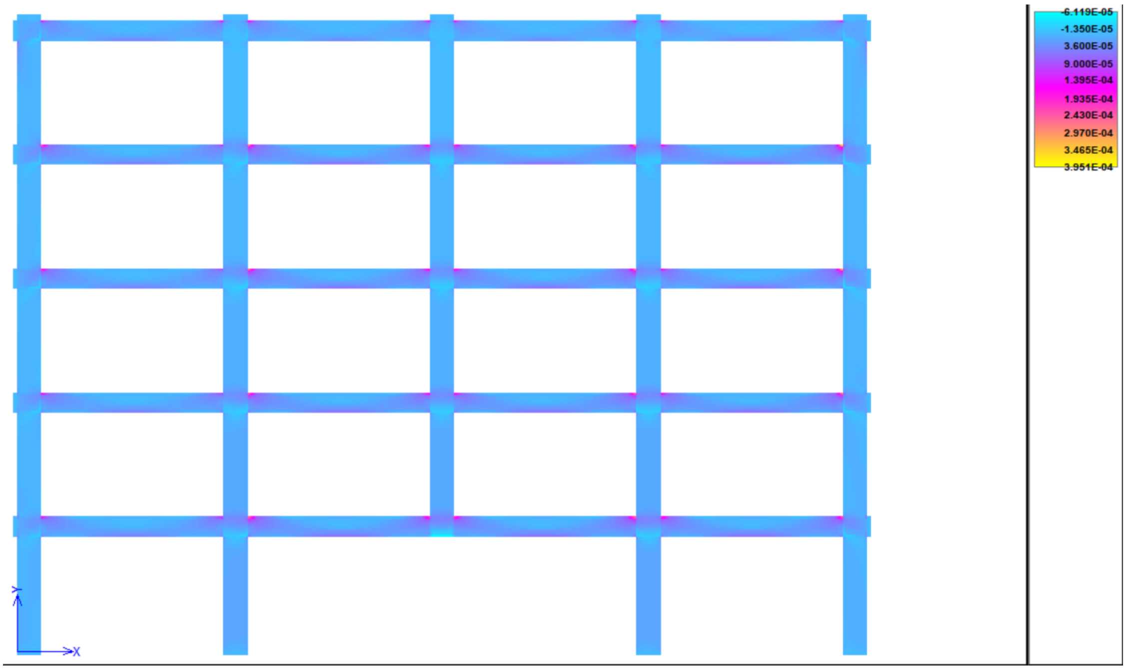

Figure 5.22: Example of Principal Total Strain rendering plot of a plane frame model

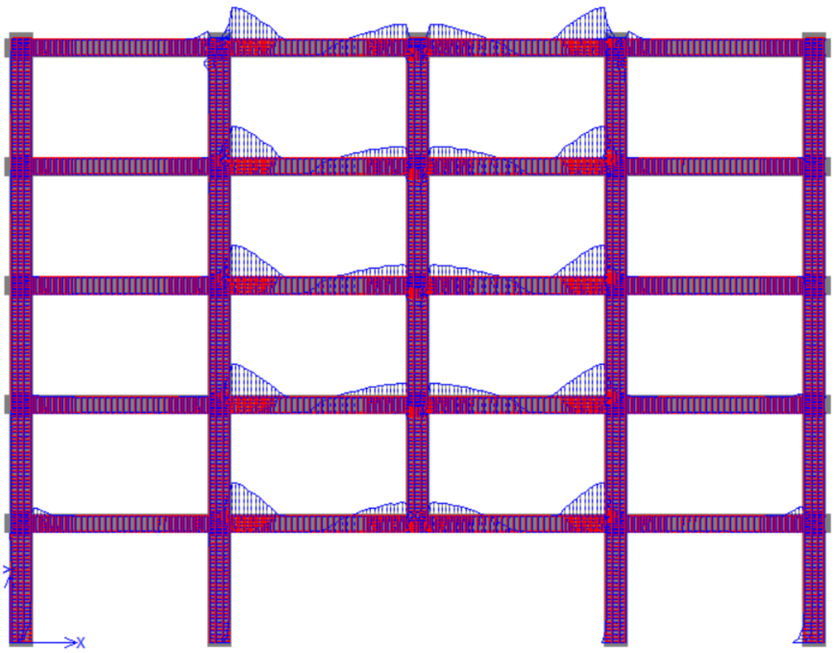

Figure 5.23: Example of reinforcement Principal stress plot of a plane frame model

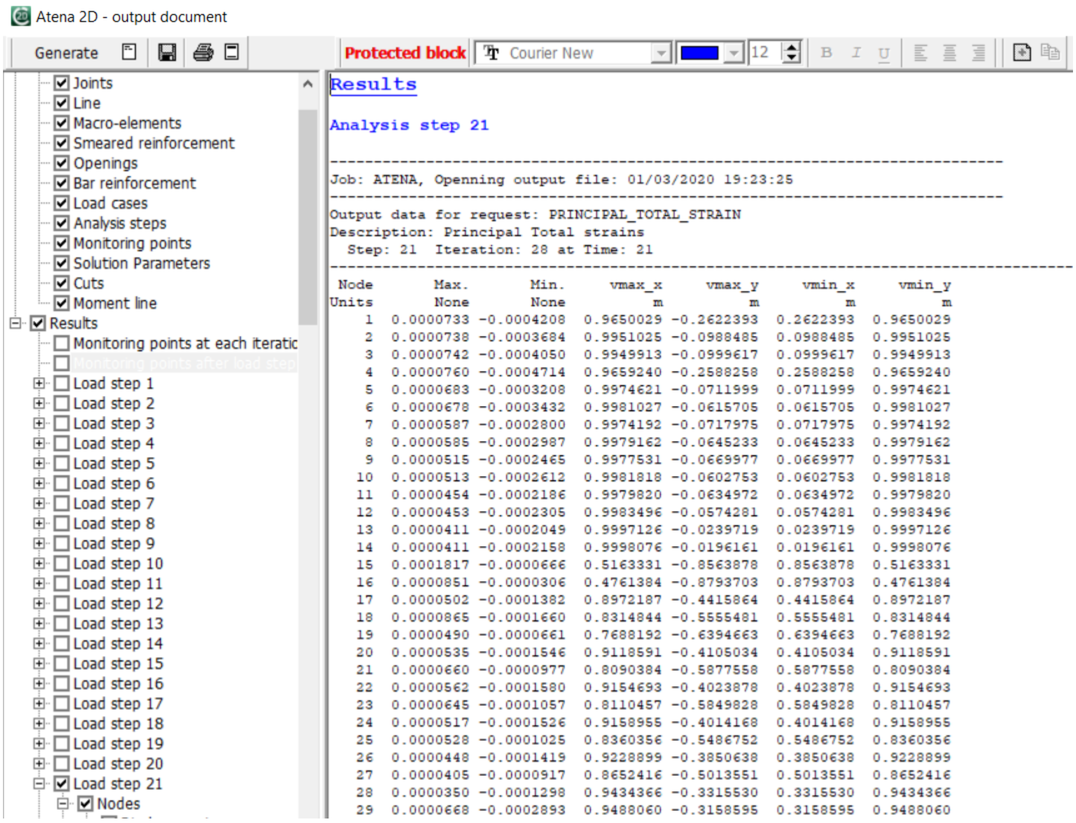

Figure 5.24: Example of results in text format

Chapter 6

Push-down analysis and probabilistic capacity curves

In this chapter the FE model built on ATENA 2D will be described in detail in all its sections: materials and constitutive laws, geometry, applied loads, constraints and mesh.

Later, the push-down analysis will be introduced defining all the parameters involved to perform them; thus, the resulting probabilistic capacity curves will be discussed.

6.1 Introduction

Since the analysis conducted on the 2D plane frame are not simply deterministic, one single model is not sufficient to study the structural robustness from a probabilistic point of view; therefore 100 different FE models have been created to obtain statistically significant results. More in detail, what differentiate each model from the others, are the randomly sampled material properties.

In reality, it will be shown that also the applied loads have been sampled in the same stage of the material properties sampling; indeed, the random data obtained from the application of the used LHS sampling method (3.3.1), strongly depends on the amount of variables to be sampled and on the correlation matrix that links them.

Therefore, for completeness, the entire sampling (material properties and loads) will be described in the next paragraph, even if the sampled loads will be not taken into account for the push-down analysis, since they will be exploited only in the next chapter.

6.2 Probabilistic sampling

Before to start with the definition of all the model characteristics, is hence necessary to describe the probabilistic sampling that have been carried out.

As just said, both materials properties and actions have been sampled trough a particular simulation technique, the *Latin hypercube simulation* (*LHS*). In 3.3.1 it was described as a particular simplified technique, used to reduce the computational efforts required for a traditional Monte Carlo simulation, which in turn is adopted when using III method approach, the integral of P_f cannot be easily computed.

Using this method, each variable is sampled by its probabilistic distribution and, successively, randomly combined with the others. The LHS method can be very efficient in case *reliability analysis* is performed by means of non-linear finite element method; thus, can be adopted efficiently in order to characterize probabilistic distribution of structural resistance by means of a reduced number of samples.

Firstly, the sampled concrete properties will be discussed, then the reinforcement ones and finally the actions on the structure; for each variable the *PDF* distribution, the histogram representation and the scatter plot will be shown. At the end, an overview of the sampling will be given, showing also variables correlation effects on sampling.

6.2.1 Concrete properties

Regarding the concrete properties, two of them have been sorted since the others can be directly detected from them: the *compressive strength of concrete* f_c and the *concrete density* ρ.

Concrete compressive strenght The starting point for the probabilistic evaluation of the concrete compressive strength f_c is the characteristic compressive cubic strength of concrete at 28 days R_{ck} that, for the chosen concrete C25/30, is equal to $30\,\mathrm{N/mm^2}$; thus, the characteristic compressive cylinder strength of concrete f_{ck} can be obtained thanks to the expression (6.1) suggested in 11.2.10.1 of [4]:

$$f_{ck} = 0.83 \cdot R_{ck} \tag{6.1}$$

The mean value of concrete cylinder compressive strength f_{cm} in turns, can be found following the expression coming from of 3.1 of [17]:

$$f_{cm} = f_{ck}^{1.645V_c} \tag{6.2}$$

Where V_c is the coefficient of variance of concrete which suggested value is 0.15 according to [7]. Moreover, the fib Model Code 2010 again, suggests modelling the concrete compressive strength f_c with a lognormal distribution:

$$f_c = LN(f_{cm}, V_c = 0.15) \tag{6.3}$$

The *PDF* distribution assume thus the aspect shown in Figure 6.1a. It is also possible to see from Figure 6.1b, how the lognormal distribution exactly fits the histogram of the sampled variable. Finally, also the scatter plot Figure 6.1c, shows how values are distributed with respect to the maximum the minimum and the mean value (red line).

Concrete density The second concrete property is the density ρ; this variable is simply sampled from a Normal distribution with the following characteristic:

$$\rho = N(\rho_m, V_\rho = 0.05) \tag{6.4}$$

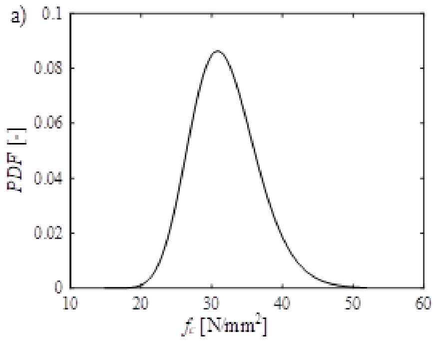

(a) Probability density function of f_c

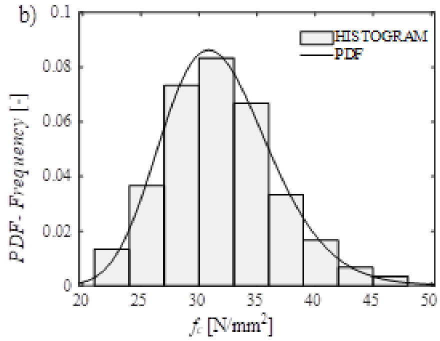

(b) Histogram and probability density function of f_c

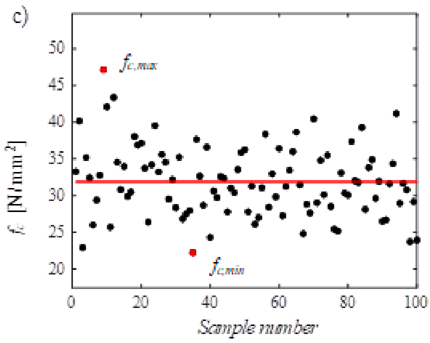

(c) Scatter plot of f_c

Figure 6.1: Plots for f_c

with ρ_m mean value equal to $25\,\mathrm{kN/m^3}$, considering that one of the reinforced concrete since in the model the steel density is set equal to zero. Instead the value of V_ρ is suggested by [7]. Also, for this sampled variable, the three graphs representing the PDF distribution, the fitted histogram and the scatter plot are reported in Figure 6.2.

All the other concrete properties needed to complete the ATENA 2D model will be derived successively from these just discussed.

6.2.2 Reinforcing steel properties

The steel chosen for the rebars of the structure is B450C. The sampled reinforcement properties are the following: *elastic modulus* E_S; *tensile yielding strength* f_y; *tensile ultimate strength* f_u; *tensile ultimate strain* ε_u.

Elastic modulus The elasticity modulus of steel E_S used for reinforcement is modelled as a lognormal distribution with mean E_{Sm} equal to 210000 MPa and a coefficient of variation equal to 0.03 as suggested by [26]. Thus, the distribution can be expressed as:

$$E_S = LN(E_{Sm}, V_E = 0.03) \tag{6.5}$$

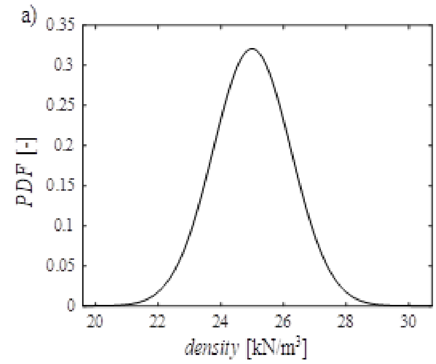

(a) Probability density function of ρ

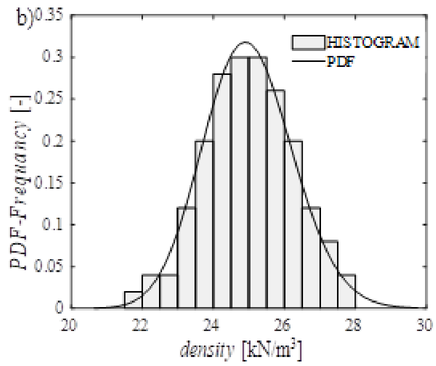

(b) Histogram and probability density function of ρ

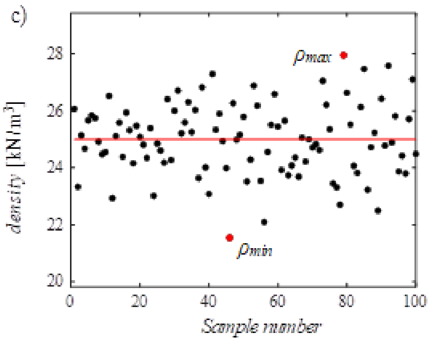

(c) Scatter plot of ρ

Figure 6.2: Plots for ρ

Also for this sampled variable, the three graphs representing the PDF distribution, the fitted histogram and the scatter plot are reported in Figure 6.3.

Tensile yielding strenght The tensile yielding strength f_y is modelled as a lognormal distribution with mean f_{ym} that derive from the characteristic yielding strength of reinforcement f_{yk} equal to 450 N/mm^2, according to the equation:

$$f_{ym} = f_{yk} e^{1.645 V_S} \tag{6.6}$$

Where V_S is the coefficient of variance of steel which suggested value is 0.05, according to [7]. Thus, the distribution can be expressed as:

$$f_y = LN(f_{ym}, V_S = 0.05) \tag{6.7}$$

Also for this sampled variable, the three graphs representing the *PDF* distribution, the fitted histogram and the scatter plot are reported in Figure 6.4.

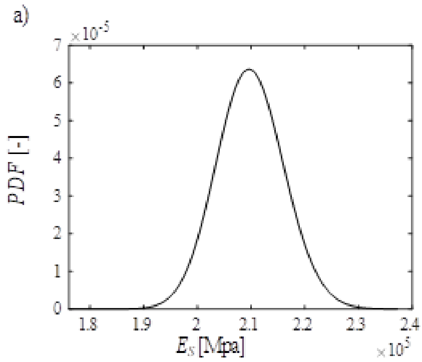

(a) Probability density function of E_S

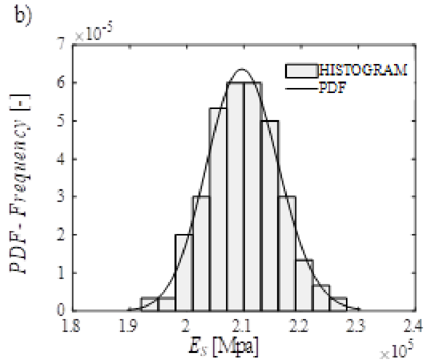

(b) Histogram and probability density function of E_S

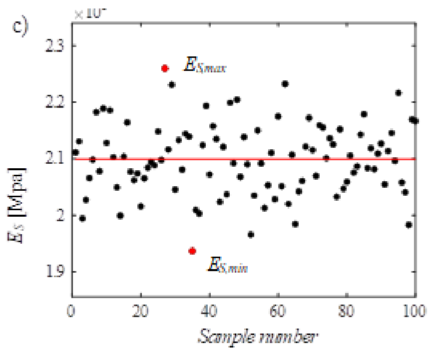

(c) Scatter plot of E_S

Figure 6.3: Plots for E_S

Tensile ultimate strenght The tensile ultimate strength f_u is modelled as a lognormal distribution with mean f_{um} that derive from the tensile yield strength f_y previously sampled, according to the equation:

$$f_{um} = f_{ym} + \alpha f_{ym} \tag{6.8}$$

Where α is a coefficient equal to 0.15 according to [7]. Considering a coefficient of variation equal to 0.05, the distribution can be expressed as:

$$f_u = LN(f_{um}, V_u = 0.05) \tag{6.9}$$

Also for this sampled variable, the three graphs representing the PDF distribution, the fitted histogram and the scatter plot are reported in Figure 6.5.

Tensile ultimate strain The last steel property sampled is the tensile ultimate strain ε_u. In this case the mean value for the used steel B450C is the mean value of that suggested by [21] in table 4 and equal to 14%. For the value of the coefficient of variance V_ε, a deep research had led to use the value of 0.09 as suggested by [22], [23] and [24].

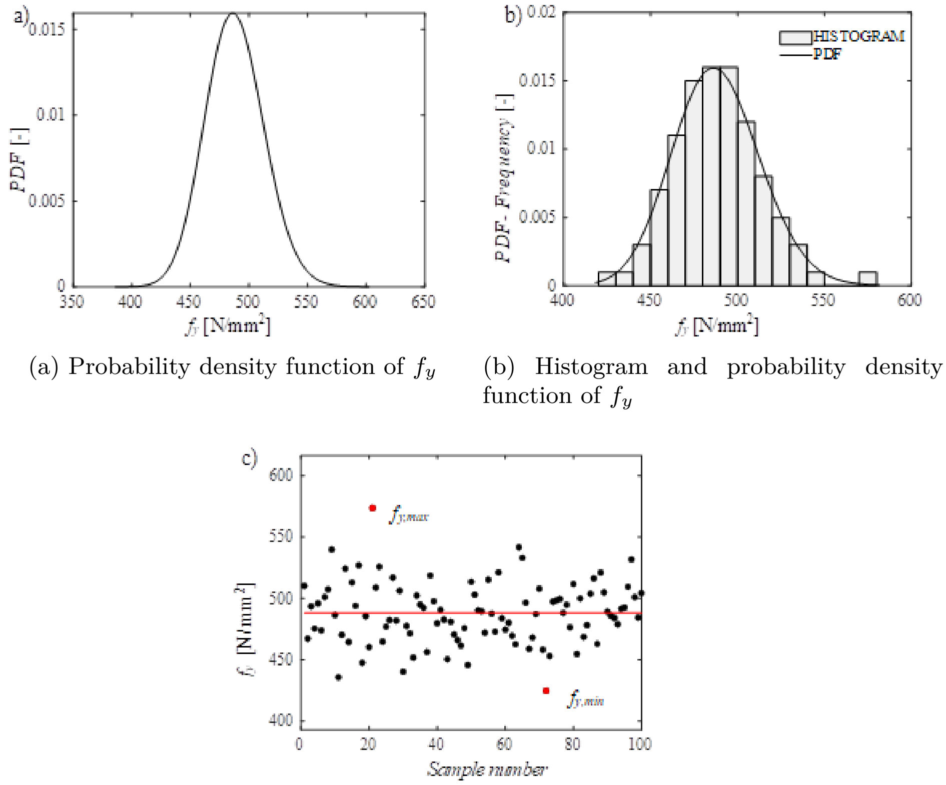

(a) Probability density function of f_y

(b) Histogram and probability density function of f_y

(c) Scatter plot of f_y

Figure 6.4: Plots for f_y

Therefore, the distribution can be expressed as:

$$\varepsilon_u = LN(\varepsilon_{um}, V_\varepsilon = 0.09) \tag{6.10}$$

Also for this sampled variable, the three graphs representing the *PDF* distribution, the fitted histogram and the scatter plot are reported in Figure 6.6.

6.2.3 Loads

The loads acting on the structure are that computed with the expression given in chapter 4; they are applied on the beams as distributed linear loads and their entity come from the analysis of the influence areas. The Table 6.1 below resume their values.

Permanent structural load For this variable, a normal distribution is considered with mean value equal to the design one, 16 kN/m, and a coefficient of variation equal to 0.05 as suggested by [15] and [25].

Therefore, the distribution can be expressed as:

$$G_1 = N(G_{1m}, V_{G1} = 0.05) \tag{6.11}$$

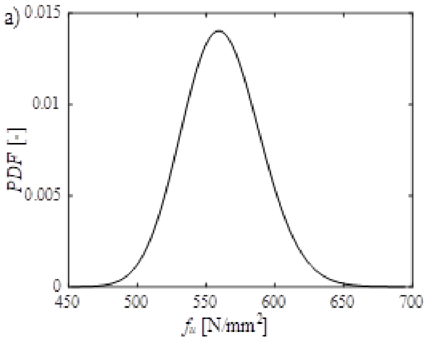

(a) Probability density function of f_u

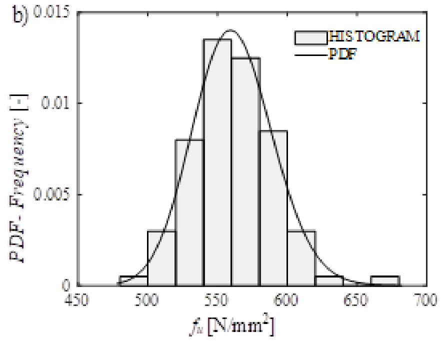

(b) Histogram and probability density function of f_u

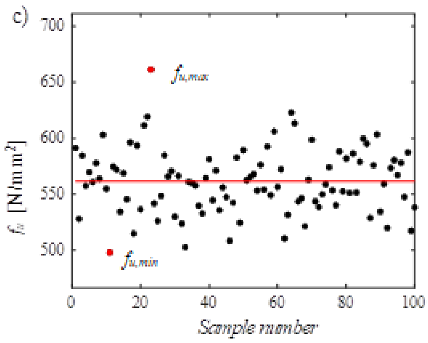

(c) Scatter plot of f_u

Figure 6.5: Plots for f_u

va	**load** [kN/m]	**exceptional combination coefficient**
Permanent structural load	16.00	1.0
Permanent non- structural load	13.00	1.0
Variable at floors	10.00	0.3
Variable at roof	2.50	0.0

Table 6.1: Values of linear distributed loads on the beams

Also for this sampled variable, the three graphs representing the PDF distribution, the fitted histogram and the scatter plot are reported in Figure 6.7.

Permanent non-structural load For this variable, a normal distribution is considered as well with mean value equal to the design one, 13 kN/m, and a coefficient of variation equal to 0.05 as suggested by [15] and [25].

Therefore, the distribution can be expressed as:

$$G_2 = N(G_{2m}, V_{G1} = 0.05) \tag{6.12}$$

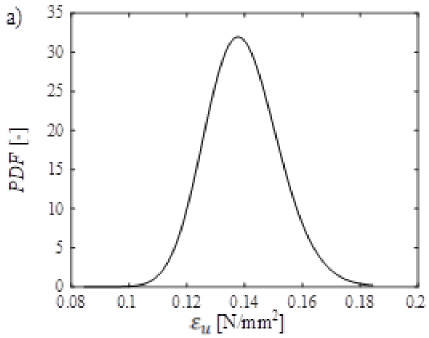

(a) Probability density function of ε_u

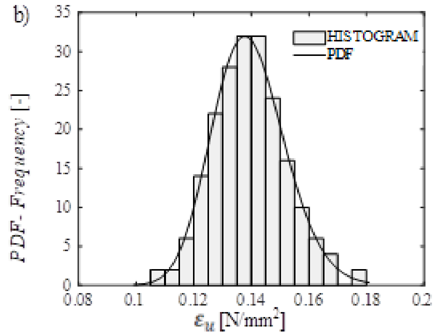

(b) Histogram and probability density function of ε_u

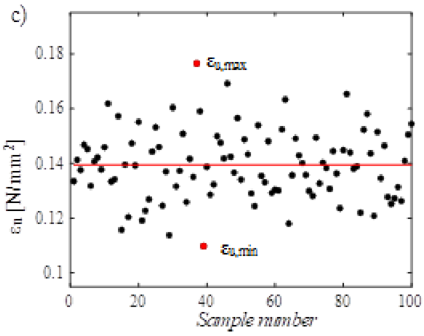

(c) Scatter plot of ε_u

Figure 6.6: Plots for ε_u

Also for this sampled variable, the three graphs representing the *PDF* distribution, the fitted histogram and the scatter plot are reported in Figure 6.8.

Variable loads The variable loads are instead represented by a Gumbel distribution. The mean values of the distributions for the floors action Q_f and for the roof one Q_r, are the 98° percentile at 50 years of normal distributions with an averages equal to 10 kN/m and 2.5 kN/m respectively, thus they are equal to 6.5 kN/m and 1.6 kN/m. The same value of the coefficient of variation is considered according to [25], and is equal to 0.2.

The Gumbel distribution require also, to define the two parameters θ_1 and θ_2 defining the position and the dispersion of data in the distribution plot; these parameters are defined according to the following expressions:

$$\begin{cases} \theta_1 & = \bar{x} + \gamma_E \theta_2 \\ \theta_2 & = \frac{\sqrt{6}}{\pi} s \end{cases} \tag{6.13}$$

where:

- $\bar{x}$ is the mean value of the variable;

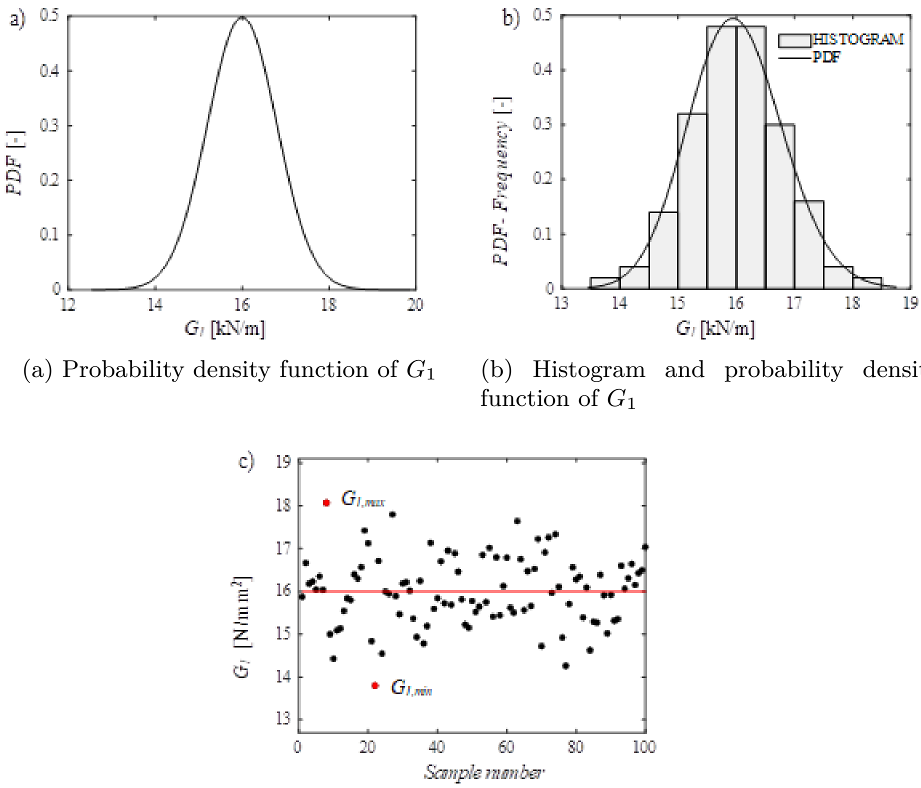

(a) Probability density function of G_1

(b) Histogram and probability density function of G_1

(c) Scatter plot of G_1

Figure 6.7: Plots for G_1

- s is the standard deviation;
- γ_E is a coefficient equal to 0.5772.

Therefore, the distributions can be expressed as:

$$Q_f = \text{Gumbel}(Q_{fm}, \theta_1, \theta_2\, V_{Qf} = 0.2) \tag{6.14}$$

$$Q_r = \text{Gumbel}(Q_{rm}, \theta_1, \theta_2\, V_{Qr} = 0.2) \tag{6.15}$$

Also for this sampled variables, the three graphs representing the *PDF* distributions, the fitted histograms and the scatter plots are reported in Figure 6.9 and Figure 6.10.

6.2.4 Variable correlations

As just said, the sampling has been made in a unique solution to obtain consistent values of each variable, depending the *LHS* technique on the amount of variables and on their correlation. Correlated variables are present in this case since the tensile yielding strength f_y, the tensile ultimate strength f_u and the tensile ultimate strain ε_u of steel, are correlated

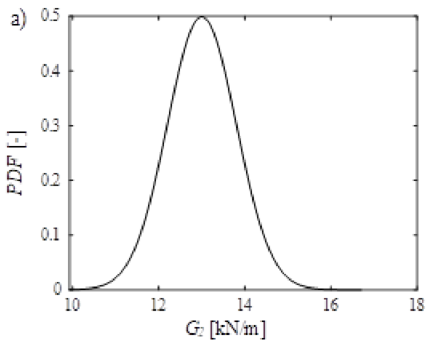

(a) Probability density function of G_2

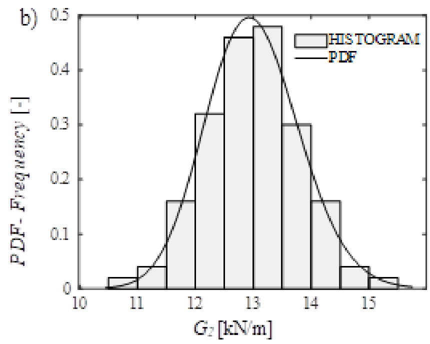

(b) Histogram and probability density function of G_2

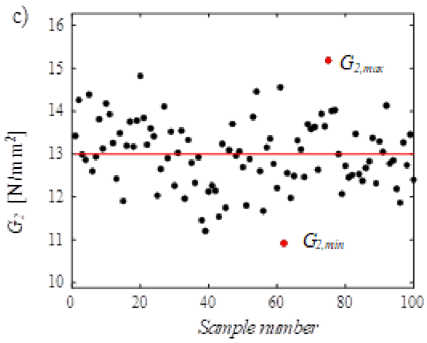

(c) Scatter plot of G_2

Figure 6.8: Plots for G_2

according to table B "correlation matrix" of [26]. In this specific case the whole correlation matrix assumes the form expressed in Table 6.2.

Moreover, since the sampling is totally random, as well as the combination of the various variables to form the 100 different combinations, all of them have to be sampled in the same running process to allow the best random variables sorting according to correlation coefficients.

The correlation between the different variables can also be seen looking at the plots reported in Figure 6.11 In particular from these three images, it is possible to see that when no correlation exists between two random variables (coefficient equal to zero), like in the case of E_s vs. f_y, the points which coordinates in the graph represent the values, that those two variables have in one combination, are sparse Figure 6.11a; while in the case in which a coefficient of correlation different from zero exists, like in the case of Figure 6.11b and Figure 6.11c, then the point are more or less distributed along a line which direction and slope depend respectively on the sign and the value of the coefficient, and with a dispersion from that imaginary line that decreases if the correlation coefficient increases.

In Figure 6.12 the joint-PDF of the three previous cases are reported both in 2D and 3D histograms; for each lognormal distribution 105 samples were generated and their correlation was analysed and plotted.

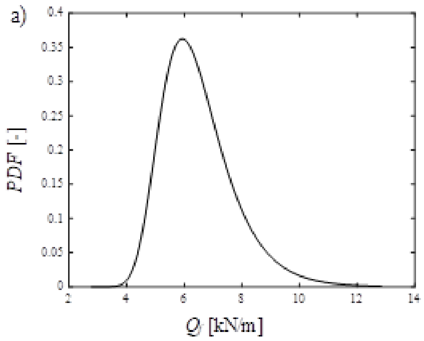

(a) Probability density function of Q_f

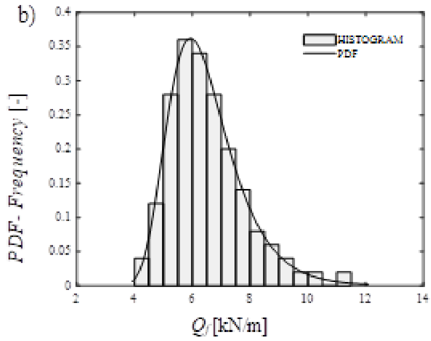

(b) Histogram and probability density function of Q_f

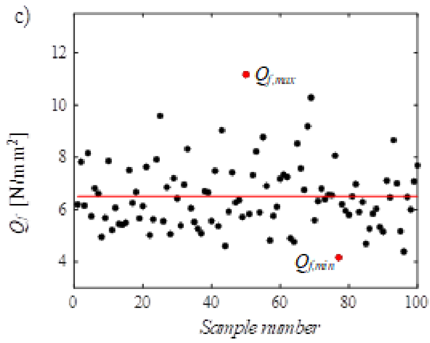

(c) Scatter plot of Q_f

Figure 6.9: Plots for Q_f

	f_c	ρ	E_s	f_y	f_u	ε_u	G_1	G_2	Q_f	Q_r
f_c	1	0	0	0	0	0	0	0	0	0
ρ		1	0	0	0	0	0	0	0	0
E_s			1	0	0	0	0	0	0	0
f_y				1	0.75	-0.45	0	0	0	0
f_u					1	-0.60	0	0	0	0
ε_u						1	0	0	0	0
G_1							1	0	0	0
G_2								1	0	0
Q_f									1	0
Q_r										1

Table 6.2: Correlation matrix

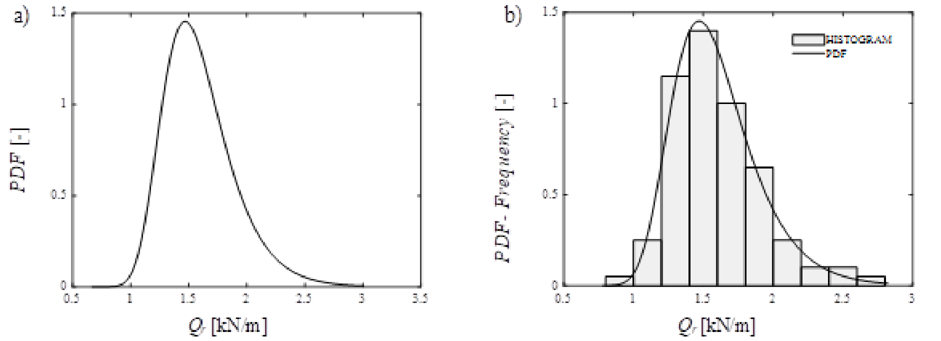

(a) Probability density function of Q_r

(b) Histogram and probability density function of Q_r

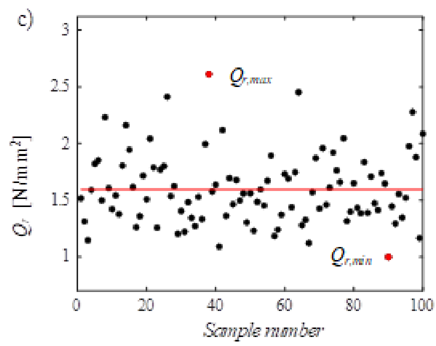

(c) Scatter plot of Q_r

Figure 6.10: Plots for Q_r

6.2.5 Summary of sampled variables

The Table 6.3 resumes all the main information concerning the sampled variables: the type of variable, the chosen distribution, the mean value and the coefficient of variation used for the sampling.

6.3 FE model

Once that the probabilistic variables have been made, the whole FE model can be described in all its parts.

6.3.1 Materials

The two adopted construction material are the concrete modelled in ATENA 2D as *SBeta Material*, and the reinforcing steel for which *Reinforcement* option was chosen. The information needed by the software and the physical explanation have been rapidly discussed in chapter 5, moreover in the same chapter, some of the variables required were just presented discussing about the probabilistic sampling; therefore only a brief resume of those

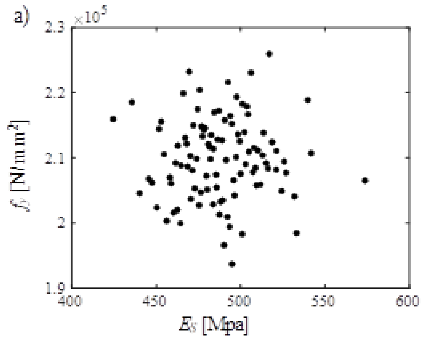

(a) Correlation graph, steel elastic modulus-steel-yielding strenght

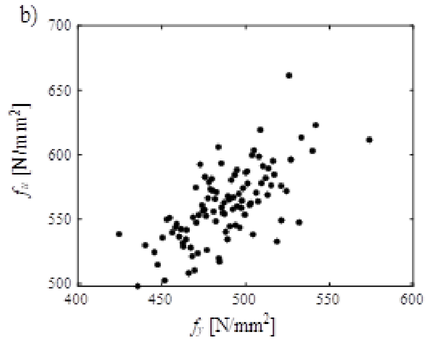

(b) Steel yielding strenght-steel ultimate strenght

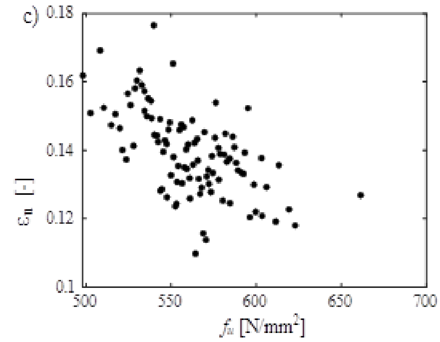

(c) Steel ultimate strenght-steel ultimate strain

Figure 6.11: Correlation between various variables

	Distribution	**Mean value**	**Coefficient of variation**$[-]$
f_c	Lognormal	$31.8685\,\mathrm{N/mm^2}$	0.15
ρ	Normal	$25\,\mathrm{kN/m^3}$	0.05
E_s	Lognormal	$210000\,\mathrm{MPa}$	0.03
f_y	Lognormal	$488.5772\,\mathrm{N/mm^2}$	0.05
f_u	Lognormal	$561.8638\,\mathrm{N/mm^2}$	0.05
ε_u	Lognormal	14%	0.09
G_1	Normal	$16\,\mathrm{kN/m^3}$	0.05
G_2	Normal	$13\,\mathrm{kN/m^3}$	0.05
Q_f	Gumbel	$6.5\,\mathrm{kN/m^3}$	0.20
Q_r	Gumbel	$1.6\,\mathrm{kN/m^3}$	0.20

Table 6.3: Variable sampling summary

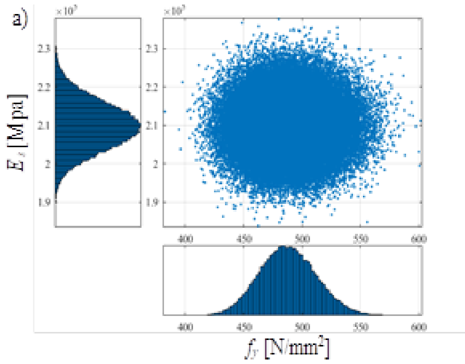

(a) 2D joint-PDF histogram of steel elastic modulus-steel yielding strength

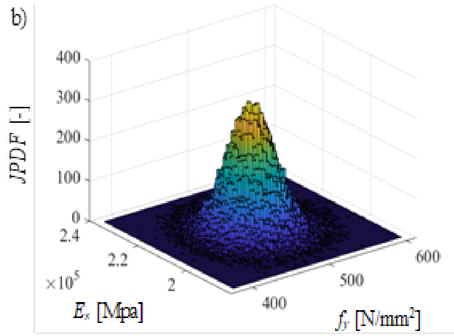

(b) 3D joint-PDF histogram of steel elastic modulus-steel yielding strength

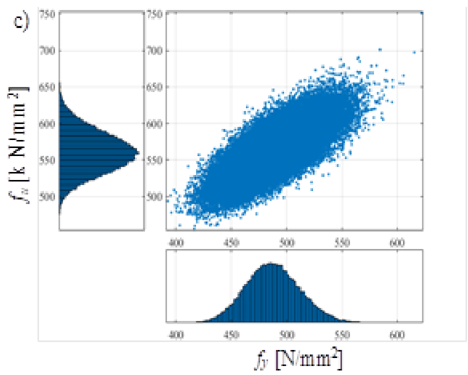

(c) 2D joint-PDF histogram of steel yielding strength-steel ultimate strength

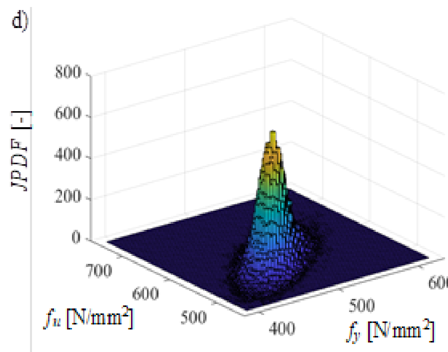

(d) 3D joint-PDF histogram of steel yielding strength-steel ultimate strength

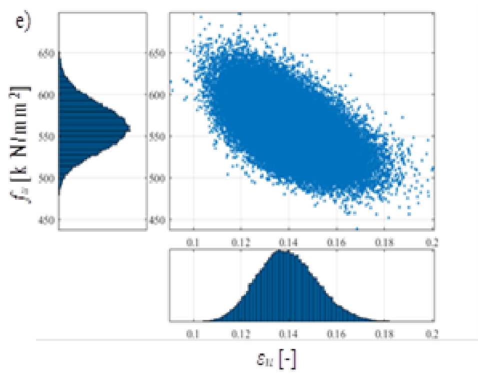

(e) 2D joint-PDF histogram of steel ultimate strength-steel ultimate strain

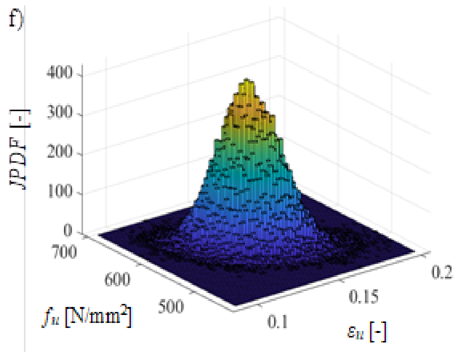

(f) 3D joint-PDF histogram of steel ultimate strength-steel ultimate strain

Figure 6.12: 2D and 3D histograms of various variables

data and the description of those not yet analysed will be given here. The constitutive law of concrete according to Saatcioglu and Razvi (1992) [27] theory will be also described.

Concrete Concrete is a composite material, made up of cement and aggregates and for this reason it has a typically non-linear behaviour, due to the internal micro-cracks that are created due to the stress concentrations at the interface between cement matrix and aggregates.

The $\sigma - \varepsilon$ resistance curve of concrete, depends on various factors, including the lateral confinement, made possible in the beams and columns of reinforced concrete structures by the presence of transverse stirrups.

The non-linear behaviour of confined and non-confined concrete was described in this study with the model of Saatcioglu and Razvi (1992) 6.13, through which it was possible to consider different behaviours with varying confinement.

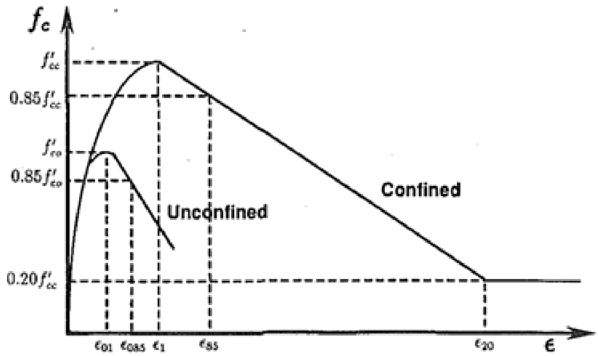

Figure 6.13: Proposed strain-stress relationship [27]

The implementation of the Saatcioglu and Razvi theory, resulted in four resistance curves of the concrete for each single structural model, different with respect to the geometry and the longitudinal and transverse bars and relating to the columns, the nodes, the dissipative zone of the beams and the non-dissipative zone of the beams. While for the concrete cover this model was not applied since there the concrete is not confined and thus classical expression can be adopted.

The application of such constitutive model highlights properly the influence of confinement on the resistance of the concrete, indeed the higher is the number of rebars and thus the confinement level, the higher as well is the resistance of concrete. This can be easily seen studying the resistance curves of the nodes or the columns, which result to be improved with respect to that of the beam where confinement is smaller.

The model was implemented in an Excel spreadsheet, which requires as input the sampled value of concrete compressive strength f_c, the geometry of the section, the concrete cover, the sampled yield stress of the steel f_{ym}, the diameter of the four side bars enclosed from the stirrups, the diameter, the number of arms and the spacing of the stirrups. Some of these data, having been sampled, are different for each of the 100 different models while others, like the concrete cover remain invariant.

The model was implemented in an Excel spreadsheet, which requires as input the sampled value of concrete compressive strength f_c, the geometry of the section, the concrete cover, the sampled yield stress of the steel f_{ym}, the diameter of the four side bars enclosed from the stirrups, the diameter, the number of arms and the spacing of the stirrups. Some

of these data, having been sampled, are different for each of the 100 different models while others, like the concrete cover remain invariant.

Now the concrete properties used as input data for ATENA 2D model, will be listed according to the software organization of the SBeta Material described in 5.2.1 of this thesis (the variables in bolt font characters are that requested by the software):

- *Basic window*: the Elastic modulus $\boldsymbol{E}$ is taken considering the tangent one E_{ctm} obtained from the secant one E_{cm}, which in turns came from the confined compressive strength f'_{cc} computed through the Saatcioglu and Razvi model (see Table 3.1 of 3.1.3 and (2) of 3.1.4(2) of [17]); the Poisson ratio ν is constant and equal to 0.2; the tensile strength $\boldsymbol{f_t}$ is derived from the characteristic compressive strength of concrete f_{ck} and is always equal to the mean value of axial tensile strength of concrete f_{ctm} 2.558 MPa (see Table 3.1 of 3.1.3 of [17]); for the compressive strength $\boldsymbol{f_c}$ the aforementioned f''_{cc} is considered.

- *Tensile window*: the type of tension softening chosen is the local strain one; while for the crack model the fixed one was chosen with a softening parameter $\boldsymbol{c_3}$ depending on the tensile strength f_t and the tangent elastic modulus E_{ctm} aforementioned according to the expression $c_3 = 10 \cdot f_{ctm}/E_{ctm}$.

- *Compressive window*: the compressive strain at compressive strength in the uniaxial compressive test ε_s derive from the Saatcioglu and Razvi model; the reduction of compressive strength due to cracks is taken equal to 0.8 as suggested by the software theoretical manual [28]; the type of compression softening is the *softening modulus*; while the compression softening parameter derives from the Saatcioglu and Razvi model as well.

- *Shear window*: the shear retention factor is assumed variable; while the tension-compression interaction is considered linear.

- *Miscellaneous window*: the specific material weight ρ is that previously sampled; the coefficient of thermal expansion α is constant and equal to $1.2 \cdot 10^{-5}$ 1/K.

Reinforcing steel The modelling of the steel rebars is an important phase of this study; indeed, this significantly affects the predisposition of the beam to the membrane behaviour and therefore to the development of the catenary mechanism.

As shown previously, the steel used is B450C, characterized by a characteristic yield strength $f_{yk} = 450$ MPa and a ductility class C (hot rolled steels).

The windows governing the Reinforcement on ATENA 2D are two:

- *Basic window*: in which the four sampled properties are requested: *elastic modulus* E_S; *tensile yielding strength* f_y; *tensile ultimate strength* f_u; *tensile ultimate strain* ε_u.

- *Miscellaneous window*: the specific material weight ρ is set equal to zero as just said since the influence of the steel on the dead load is just taken in to account in the reinforced concrete density; the coefficient of thermal expansion α is constant and equal to $1.2\,10^{-5}$ 1/K.

6.3.2 Geometry

Following the conceptual scheme described in 5.2.2, the geometry was defined in the ATENA 2D software firstly building the points, then the lines, followed by the macroelements and finally the reinforcement rebars; rigid edge plates were also built in the external nodes with a thickness of 10 cm to control the displacements in that points avoiding stress concentrations in the constraints and in the imposed displacement points.

The scheme adopted provides for a subdivision of beams, pillars and nodes consistent with the various constitutive laws of concrete due to confinement.

The columns have been divided into four vertical bands, two external ones represented by the concrete cover and two internal ones divided by the barycentric axis, while vertically can be detected three different zones representing the two dissipative regions at the edges and the non-dissipative one in the middle.

The beams have been divided vertically into three bands, two external represented by the concrete cover and one internal, for which vertical rows of four points have been inserted for each beam, and three regions in the longitudinal direction representing the two dissipative zones and the non-dissipative one.

It must be reminded that, since this model have been built for a push-down analysis, the central column of the ground floor is missing from the structural model.

In total 1025 points have been defined; their scheme is reported in Figure 6.14

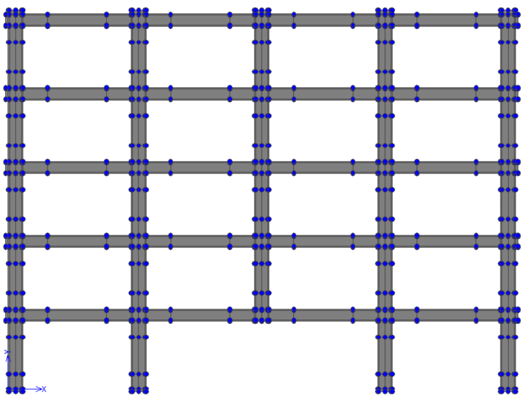

Figure 6.14: Nodes scheme in blue

Once that all the points have been identified, 1890 lines have been drawn to link them. Thus, 850 macroelements have been created to define the surface of the plane frame, each of them results to be enclosed inside four lines constituting a rectangular region Figure 6.15.

The reinforcements have been arranged discreetly both for the longitudinal direction and the transversal one. The stirrups spacing used, obtained from the shear tests, is 5 cm for the nodes, 10 cm for the columns, 10 cm for the dissipative area of the beams and 15 cm for the non-dissipative area of the beams. The longitudinal reinforcement of the columns in the 2D model are represented by four vertical rows given the presence of two bars in the intermediate part, while the longitudinal reinforcement of the beams have been arranged in two rows, which represent the lower reinforcement and the upper reinforcement. Figure 6.16 shows the arrangement of the bars in the model.

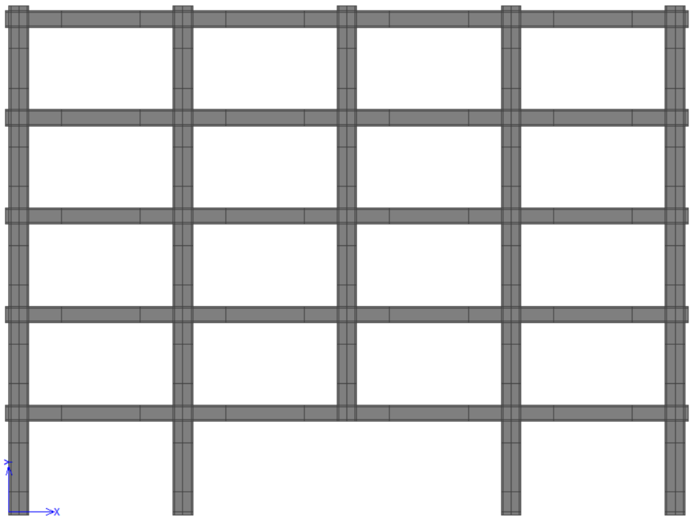

Figure 6.15: Lines arrangement in dark grey and macroelements in light grey

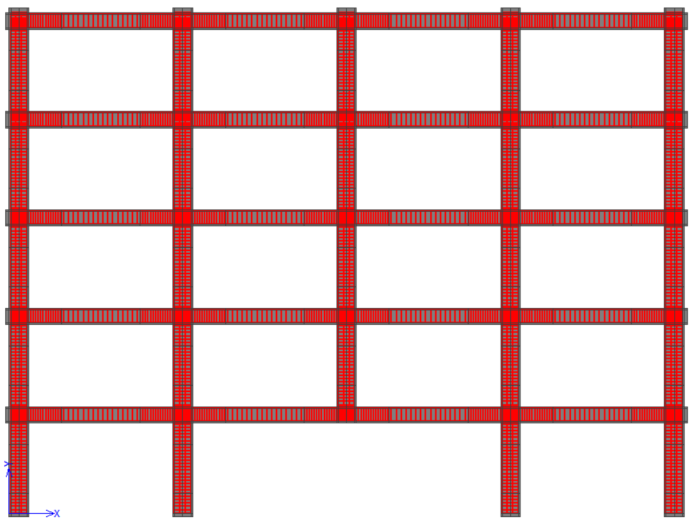

Figure 6.16: Rebars arrangement in red

6.3.3 Loads and constraints

Even if all the permanent and the variable loads have been sampled, in this stage of the analysis, no loads are considered in performing the structural assessment, since the type of analysis conducted is a displacement-controlled push-down that consist on estimate the vertical reaction generated by an imposed displacement. However, the loads sampling will return useful in the next chapter to compute the vertical reaction under the removed column for the calculation of the dynamic amplification factor.

Therefore, the load cases applied in this procedure consists simply on the fixed constraints at the base of the four columns Figure 6.17, and a gradual imposed displacement

δ at the top point of the central column removed, simulating hence the element removal itself.

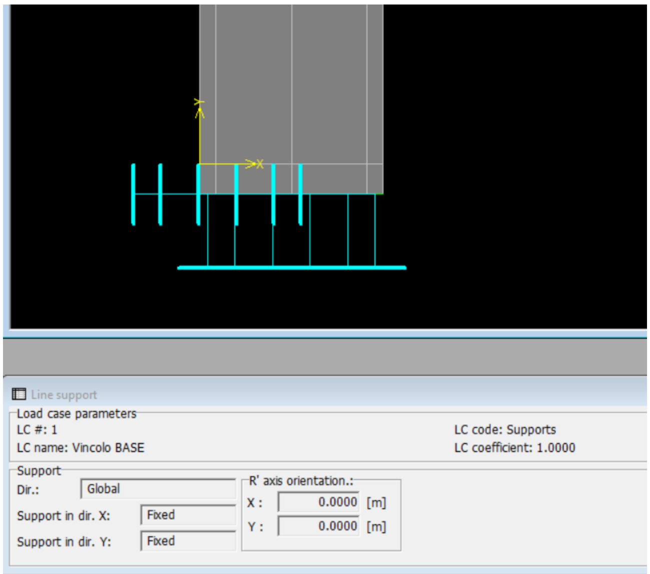

Figure 6.17: Fixed contrain at the base of the column

6.4 Non-linear displacement-controlled push-down analysis

6.4.1 Analysis type choice

The analysed structure is made of reinforced concrete, that as well known, is the results of a successful materials coupling between concrete and steel. In performing usual analysis and traditional assessment, the behaviour of these two materials can be approximatively considered linear elastic; unfortunately this approach, cannot be used when dealing with particular circumstances in which structures have to undergo particular situations that lead the structural system in a condition of large non-linear displacements. When these condition starts, material non-linearity behaviour appears, involving a series of event like plasticization, that cannot be analysed through linear elastic theory.

Therefore, when dealing with particular structural analysis as the investigation on progressive collapse due to a column removal, non-linear analysis allow the designer to perform detailed analysis. As shown by [29] indeed linear elastic analysis produce conservative estimations of the resistance capacity of structure neglecting the non-linearity of construction materials in the inelastic field.

However, it must be specified that also the non-linear analysis represent a simplification of the reality; indeed when a progressive collapse is simulated, the non-linear analysis doesn't allow to consider the dynamic effects triggered by the suddenly changes of internal equilibrium conditions, for example as discovered by [30], performing non-linear analysis doesn't allow to take into account the lateral load spread, that instead assumes a more vertical load path. This of course influence the analysis of the structure sections surrounding that directly interested by the collapse. Moreover, [31] found that static non-linear analysis overestimates the structure capacity when simulating a collapse, respect to the results obtained performing a non-linear dynamic analysis.

Although, only non-linear dynamic analysis seems to be the best solution to obtain consistent and very detailed results, if the purpose of the study consist on finding the capacity curve of the structure, as in this case, non-linear analysis results to be an optimal solution [29].

More in detail, the type of non-liner analysis performed in this specific case is a push-down analysis. The proposed method is inspired by the pushover method commonly used in earthquake engineering [32]. According to many authors [31], [32], [33] indeed this procedure allows to define the structural resistance of a structure when dealing with a progressive collapse simulation. The study of the structural robustness is therefore enabled by the analysis of the resulting capacity curves.

Push-down analysis can be conducted following different procedures; basically, these different procedures belong to two big families: the load-controlled push-down analysis and the displacement-controlled ones. In any case it must be underlined the independency of the results from the initial condition of load, therefore this type of analysis is valid for any potential hazard. In this specific case a displacement-controlled analysis seems to be the best option. According to [31] indeed, this choice allow the designer to see the behaviour of the structure also after the failure of the system, giving the possibility to study the complete collapse process without problems of numerical convergence. Moreover, load-controlled push-down often requires reruns of the analysis to find the best analysis parameter conditions to obtain consistent solutions and in addition, a strong dependency on the load steps and on the chosen error tolerance was found by [33].

In conclusion, non-linear displacement-controlled push-down analysis have been chosen in this particular case, since it seems to be the best solution guaranteeing reliable results in terms of structural robustness.

6.4.2 Analysis setting

To perform the push-down analysis and build the force-displacement curves, the external loads were no activated as just said, but only the fixed constraints and the imposed displacements. The steps were set with the Standard Newton-Raphson nonlinear calculation model, all with step coefficient equal to 1.0 and always with constraints present; finally, it was decided to perform the first 15 steps, which relate to sudden changes in the slope of the curve, with an imposed displacement of 1.5 cm and the remaining, corresponding to more rounded corners of the capacity curve, with an imposed displacement of 3.0 cm, in order to reduce the analysis time. A total displacement of 1.2 m is thus imposed at the end of the 45$^{\text{th}}$ step, even if the structural collapse is always reached before that step for all the 100 probabilistic simulations, ensuring a correct estimation of the capacity curves.

The arrangement of the monitoring points was set in accordance with what is illustrated in Figure 6.18: the displacement δ and reaction of the point at the point of the structure in correspondent with the removed column and the lateral displacements of the various floors were then monitored, evaluated only on one side of the structure given the symmetry of the problem.

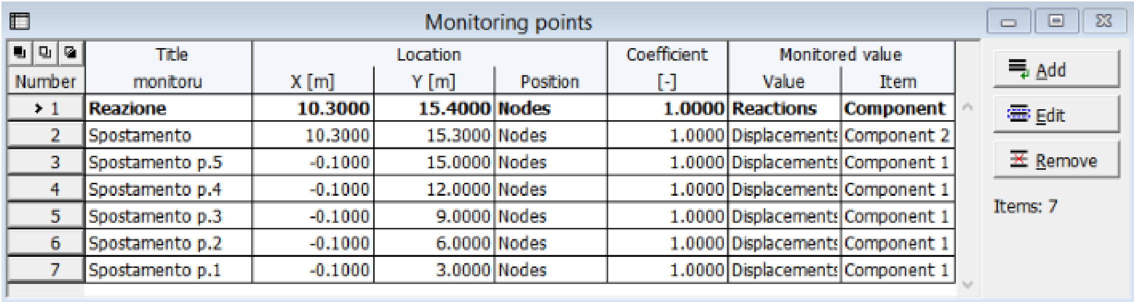

Number	Title monitoru	Location X [m]	Location Y [m]	Location Position	Coefficient [-]	Monitored value Value	Monitored value Item
1	**Reazione**	**10.3000**	**15.4000**	**Nodes**	**1.0000**	**Reactions**	**Component**
2	Spostamento	10.3000	15.3000	Nodes	1.0000	Displacements	Component 2
3	Spostamento p.5	-0.1000	15.0000	Nodes	1.0000	Displacements	Component 1
4	Spostamento p.4	-0.1000	12.0000	Nodes	1.0000	Displacements	Component 1
5	Spostamento p.3	-0.1000	9.0000	Nodes	1.0000	Displacements	Component 1
6	Spostamento p.2	-0.1000	6.0000	Nodes	1.0000	Displacements	Component 1
7	Spostamento p.1	-0.1000	3.0000	Nodes	1.0000	Displacements	Component 1

Figure 6.18: List of monitoring points

The position of the monitoring points on the structure is shown in Figure 6.19.

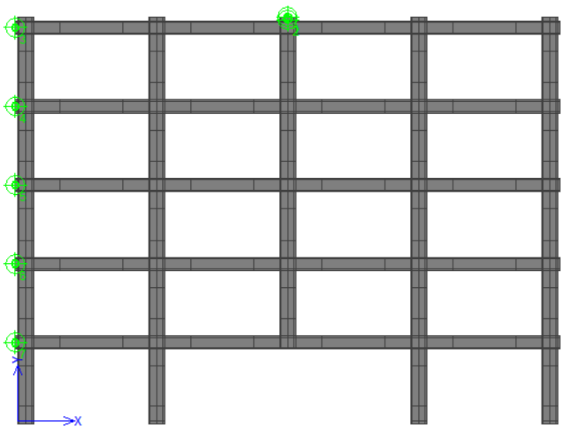

Figure 6.19: Disposition of monitoring points

6.5 Push-down analysis results

Each of the 100 different structural models produced a single capacity curve, representing a particular structural behaviour influenced by the combination of the sampled material properties. This means that obviously each simulation and thus each derived result, represent a hypothetical aleatory situation that could potentially represents a realistic structural system. The set of results, hence, can be analyzed with a probabilistic approach.

6.5.1 Representative capacity curves

On figure 6.20 three particular capacity curves are reported; looking at them the global behaviour shown by all the 100 different capacity curves can be analysed as follows:

- in the first stage, which is that before the first peak, the plane frame undergoes a certain vertical displacement in the linear elastic field until a certain point where non-linear material behaviour became dominant. In the last phase of this stage the compressive membrane effect governed by concrete properties and due to cracks openings, guarantee a certain resistance reservoir which is capable to bear the load until the maximum flexural behaviour is reached;
- the first peak stage represents the condition in which the maximum flexural resistance is reached. The value of the corresponding load can be directly detected from each capacity curves, otherwise a simplified analytical approach can be exploited using equations (2.4), (2.5)) and (2.6);
- after this first peak, plastic hinges are formed and the tensile membranal effects governed by reinforcement properties, ensure still a resistance against the imposed displacement which continues even if the corresponding acting load remain more or less constant. This plateaux stage, continues until the second and last peak is reached;
- the second peak is the catenary peak. The corresponding load can be obtained from the graph, in alternative for an approximate approach, equation (2.7) can be used. This point represents the final moment in which the equilibrium conditions can be still satisfied, after that indeed, failure happens;
- the last stage is represented by the critical resistance drop, it defines a no more realistic situation in which static equilibrium can no longer be achieved and therefore what is obtain from the analysis are no more realistic data but only numerical approximation founded by the software trying to reach the numerical convergence.

These just explained stages can be easily detected in Figure 6.20a, 6.20b and 6.20c. More in detail, the figures represent three particular cases among the 100 different models. Figure 6.20a represents the capacity curves of the case “21” in which the maximum flexural peak $P_{\max}$ is registered (1554 kN). Figure 6.20b, which results from case “23”, is the case where the maximum value of the catenary peak P_{ult} is registered (1518 kN). The explanation of this singular behaviours can be understood looking at the material properties of the models under consideration shown in Table 6.4. The case reported in Figure 6.20c represents the case “11” with both minimum $P_{\max}$ (1198 kN) and P_{ult} (1151 kN). In this case the material characteristics define a structural system with poorer structural characteristics, Table 6.4.

case	f_c [N/mm^2]	ρ [N/mm^3]	E_s [MPa]	f_y [N/mm^2]	f_u [N/mm^2]	ε_u [$-$]
11	25.71	26.52	218540.7	435.56	498.04	0.162
21	33.72	24.81	206523.1	573.74	611.51	0.119
23	34.19	25.39	209416.9	525.80	661.36	0.127

Table 6.4: Material properties of case "11", "21" and "23".

As it is possible to see, material properties of case “21” and “23” define better combinations in terms of resistances of both concrete and steel. While for case “11” the situation is the opposite, since the higher concrete density, together with the poorer properties of

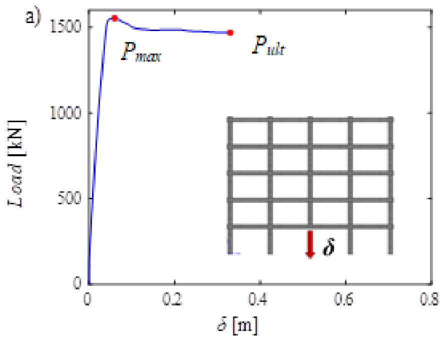

(a) Capacity curve of case "21"

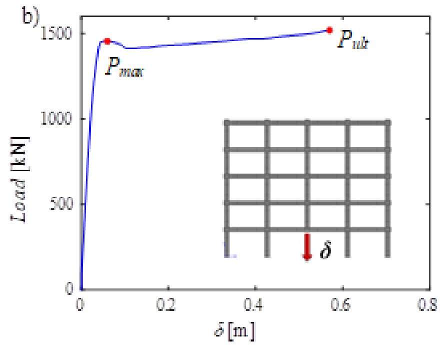

(b) Capacity curve of case "23"

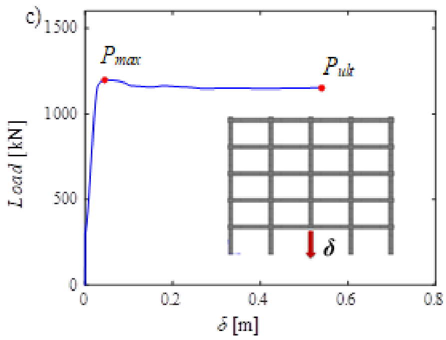

(c) Capacity curve of case "11"

Figure 6.20: Plots for cases "21", "23" and "11"

construction materials define a more critical situation for the eventual collapse of the structure. Moreover, the higher ultimate stress both of steel and concrete in case “23” produce a higher ultimate peak. Finally, although case “11” represent a model with poor material properties, the high ultimate strain of steel ensure as well an high value of deformation corresponding to the second peak, suggesting a better ductile behaviour that indeed can be seen from the capacity curves of Figure 6.20c, looking at the distance between the two peaks.

On Figure 6.21 the 100 different capacity curves are reported all together in the same graphs. Figure 6.21a and 6.21b present the curves stopped at the first step after collapse begins, while Figure 6.21c and 6.21d report the curves stopped at the value of P_{ult}, in these two graphs moreover, the peaks are reported with red dots for each simulation. In Figure 6.21a and 6.21c the curves are reported with their real values; is possible to see directly that the general behaviour defined by the previously described stages, is reflected in all of them. For all the simulations the three phases are clearly visible even if with different characteristics. In particular, the initial displacement necessary to reach the flexural peak are similar but, the value of the corresponding peak load changes ranging from 1198 kN of model “11” to 1554 kN of model “21”.

The amplitude of the second stage, that in between the two peaks, is more varying, indeed it strongly depends on the material properties of each single model. Consequently,

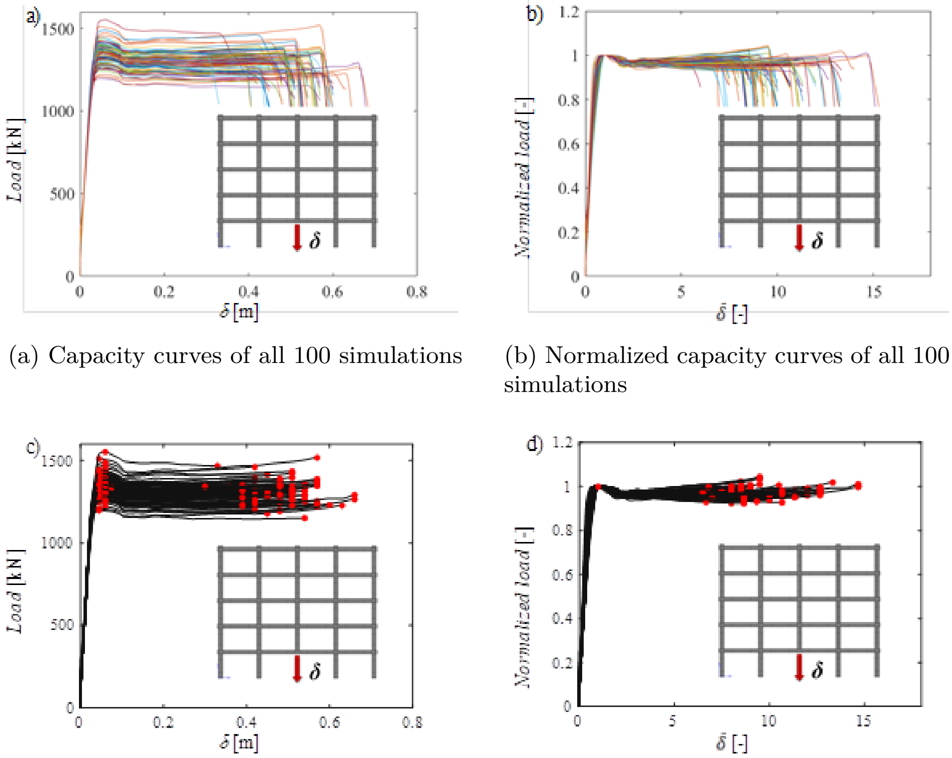

(a) Capacity curves of all 100 simulations

(b) Normalized capacity curves of all 100 simulations

(c) Capacity curves of all 100 simulations with peaks

(d) Normalized capacity curves of all 100 simulations with peaks

Figure 6.21: Plots for all 100 simulations

also the displacement value at which the catenary peak is reached varies as well. The second peak ranges from 1151 kN of model "11" to 1518 kN of model "23". Moreover, is possible to understand that generally the flexural peak has a value slightly higher that the catenary one. However there are particular situations like case "23", Figure 6.20b for which the catenary peak is higher then the first one, this means that for these cases the catenary behaviour is fully exploited by the structural system that thus, behaves like a robust structure.

Finally on Figure 6.21b and 6.21d the same capacity curves normalized are reported; the loads have been normalized with respect to the value of the first peak, while the displacements have been normalised with respect to the value that it assumes at the flexural peak. As demonstration is possible clearly to see that all the curves pass from the point of coordinate (1;1).

6.5.2 Probabilistic analysis of peaks resistances

The two peaks which physical meaning was just explained are now analyzed with a probabilistic approach. For each variable the graphs representing the probability distribution functions 6.22a, the histogram with the fitted *PDF* 6.22b, the probability plot of the logarithm of the variable 6.22c and the scatter plot 6.22d are reported in Figure 6.22 Figure 6.22. For both $P_{\max}$ and P_{ult} it was found that a lognormal distribution exactly fits the data how is possible to check looking at the figures.

The mean values and the standard deviations are reported in Table 6.5.

Variable	Mean	Standard deviation
P_{max}[kN]	1346.52	63.05
P_{ult}[kN]	1311.18	63.65

Table 6.5: $P_{\max}$ and P_{ult} data

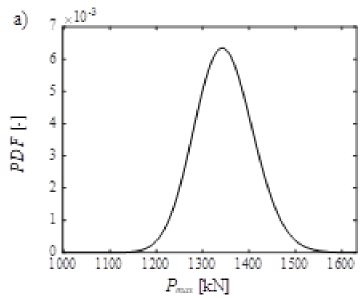

(a) Probability density function of $P_{\max}$

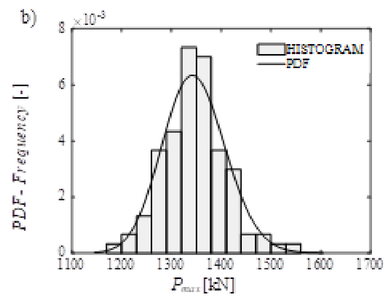

(b) Histogram and probability density function of $P_{\max}$

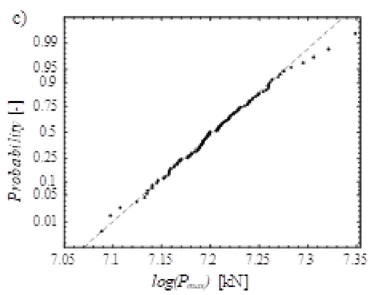

(c) Probability plot of $\log(P_{\max})$

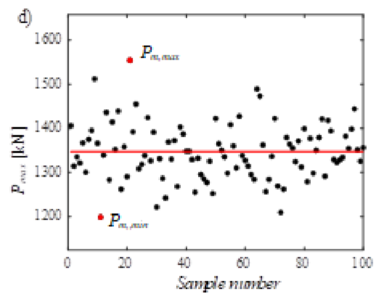

(d) Scatter plot of $P_{\max}$

Figure 6.22: Plots of $P_{\max}$

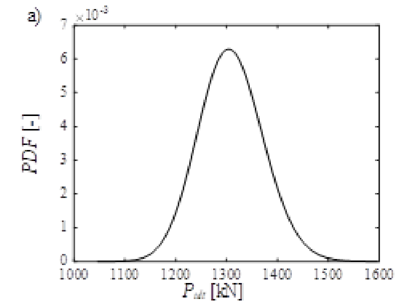

(a) Probability density function of $P_{\rm ult}$

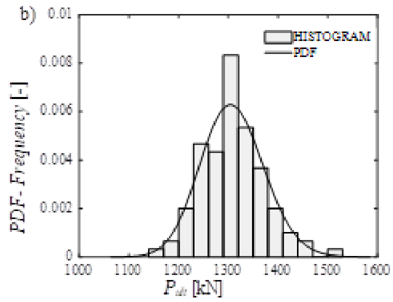

(b) Histogram and probability density function of $P_{\rm ult}$

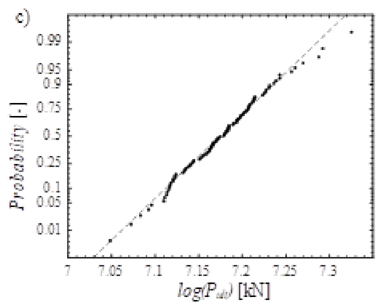

(c) Probability plot of $\log(P_{\rm ult})$

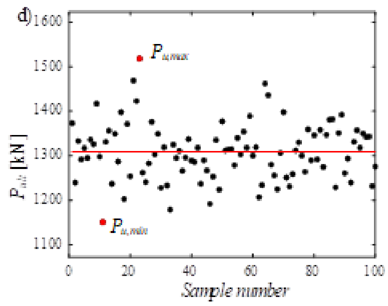

(d) Scatter plot of $P_{\rm ult}$

Figure 6.23: Plots of $P_{\rm ult}$

Chapter 7

Capacity curves to assess the dynamic amplification factor

Capacity curves detection opens several directions of work in studying structural phenomena from different points of view. Although the results obtained from capacity curves seem to be very simple in their interpretation, often they represent a simple but very efficient instrument for structural analysis. Indeed, the analysis of such results can widely help engineers and researchers in performing different structural analysis aimed to many different purposes, with the final goal to obtain the best refined description of structural system. An example, can be the determination of the *dynamic amplification factor* (DAF) which makes possible the study of structural behaviour subjected to dynamic stress conditions. In this chapter in particular, the theory formulated by Izzuddin and others [34] based on an energetic approach, to find the DAF is exposed and then applied to the plane frame. Extended to the probabilistic analysis field, the statistic information obtained constitute the starting point of a *reliability analysis*, which starts properly from a simple but efficient description of the global resistance of the building. In this sense insights will be finally given regarding further probabilistic analysis appliable to the multistorey plane frame.

7.1 Dynamic amplification factor

The concept of *dynamic amplification factor* (DAF) has born to compensate for the approximation made when a structural non-linear analysis is performed. Indeed, although this approach guarantees to take into account geometrical and material non linearities, it must be stressed that the dynamic behaviour involved in particular analysis conditions are not taken into account; therefore, to obtain consistent results trying to better simulate the real behaviour of a building, dynamicity has to be taken into account. In particular, the sudden removal of an element of a structure to perform progressing collapse analysis, causes an immediate geometric change in the structure; the results are a release of potential energy and rapid alteration of internal static dynamic forces, including the inertial one [30].

The application of the DAF allows thus to perform correctly non-linear analysis, ensuring a correct interpretation of the global behaviour of the structure simulating the dynamic consequences that exceptional event can reflect on the structural system.

When a base column of a frame is seriously damaged by an accidental action, an instantaneous downward loading equal to the vertical load supported by the lost column is transferred to the remaining building. The alternative load path method allows the structure to redistribute the stress trying to find a new equilibrium condition. This may be described by a step force function that is shown in Figure 7.1, where the rise time t_r is taken as an infinitesimal value [29].

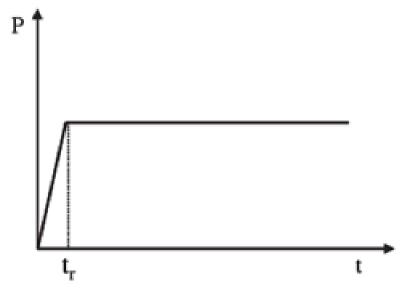

Figure 7.1: The step force function for dynamic analyses

The displacement-based (see next) elastic DAF under the step force can be computed trough the formula suggested by Chopra [35]:

$$DAF = 1 + \frac{|\sin(\pi t_r/T_n)|}{\pi t_r/T_n} \tag{7.1}$$

where T_n is the structural natural period in the force direction. When the sudden removal of a base column is simulated, the value of t_r/T_n tends to zero. Hence, the DAF is approximated to 2.0 and it is therefore the maximum possible amplification that the structure can undergo; moreover, in this case the *displacement-based* DAF is equal to the *force-based* one.

In fact, two different formulations of the DAF can be defined:

- The *displacement-based* DAF defined as the ratio of the dynamic displacement response (Δ_{dy}) of an elastic single-degree-of-freedom (SDOF) system to its static displacement response (Δ_{st}) under an equal applied loading P. It can be expressed by the following expression:

$$DAF = \frac{\Delta_{dy}}{\Delta_{st}} = \frac{P/k_{dy}}{P/k_{st}} = \frac{k_{st}}{k_{dy}} \tag{7.2}$$

  where k_{st} and k_{dy} represent the equivalent static and dynamic stiffness of the SDOF system, respectively [29].

- The *force-based* DAF expressed as the ratio of the static force response to the dynamic force response under an equal displacement demand. In this case it is defined as:

$$DAF = \frac{P_{st}}{P_{dy}} \tag{7.3}$$

where P_{st} and P_{dy} are the required static and dynamic force under the same deflection.

The two definitions coincide only in the elastic field.

Codes like [36] and [37], suggest to use a DAF equal to 2 in performing linear structural analysis. The non-reliability of linear approach has been discussed yet, the use of an amplification factor equal to 2 in addition, make the analysis result even more unrealistic, since such amplification entity is strongly not recommended in literature by [38], [39] and others. Indeed, according to them, the DAF can change under different conditions and with different force demand, meaning that using a DAF equal to 2.0 generally lead to highly conservative estimates and inconsistent results.

7.2 Simplified framework for progressive collapse assessment

Referring to the robustness evaluation of a multistorey building considering a column loss scenario, a valid alternative has been presented by [34], which defined a new simplified framework for progressive collapse assessment. The main advantage in using this method is the possibility to carry out reliable estimation of structural robustness, even from non-linear static analysis without the need to resort to dynamic non-linear analysis but considering dynamic effects trough a simplified approach.

7.2.1 Method workflow

The method is organized in three phases, each of them is necessary for the final evaluation of structural robustness:

- *non-linear static response*: in this stage the structural non-linear analysis under gravity loading is carried out. This analysis has as main goal to define the response curve of the damaged structure under increasing loads;

- *simplified dynamic assessment*: in this second stage the maximum dynamic response under sudden column loss is established. A simplified mathematical approach based on the energy based virtual work principle is used in this phase;

- *ductility assessment*: in this last phase the potential alternative load paths are examined to understand if connections above all, can bear the new loads determined by the new equilibrium conditions. The system pseudo capacity as measure of the ductility limit is also computed.

Finally, thanks to the multilevel approach discussed, the system pseudo capacity obtained cam be compared with the originally applied gravity load defining a measure of the structural robustness.

According to authors, this approach can be applied to different structural scheme of different complexity, whether it is a complex structural system like an entire building or a simpler one like an individual floor or a single beam system.

7.2.2 Application to the multistorey plane frame and mathematical formulation

The theory just exposed can be adopted for the analysis of the multistorey plane frame under analysis. In particular, the first stage of the proposed simplified framework can be resumed in the results just obtained from the study of the probabilistic capacity curves determined in the previous chapter. The resistance assessment of the structural system, by mean of a non-linear analysis, therefore, has been just carried out and is possible to use the obtained capacity curves as starting point to move on with the second step.

In this stage the DAF is determined by mean of a simplified dynamic assessment. The importance of determine such coefficient with maximum possible reliability was as well discussed in this chapter. Also, the physical meaning of the application of such coefficient was explained. In the formulation that follows the DAF is recalled in its mathematical form as λ_d.

The basic concept behind this approach, is that sudden column removal is similar in effect to sudden application of the gravity loads on the interested sub-structure. In the initial stages of the dynamic response, the gravity load exceeds the static structural resistance, and the external work done over the increasing deformations is transformed into additional kinetic energy, generating an increment of velocities. As the deformations increase, the static resistance exceeds the gravity loading, and the differential energy absorbed accounts for a reduction in the kinetic energy, thus the velocities decrease. The maximum dynamic response is achieved when the kinetic energy is zeroed, and hence when the external work done by the gravity loads becomes identical to the energy absorbed by the structure [34]. These concepts are illustrated in Figure 7.2a and 7.2b for two different dynamic amplification of the initial gravity load P_0; u_{di} define the maximum dynamic displacements corresponding to the nonlinear static load-deflection response evaluated on the capacity curve.

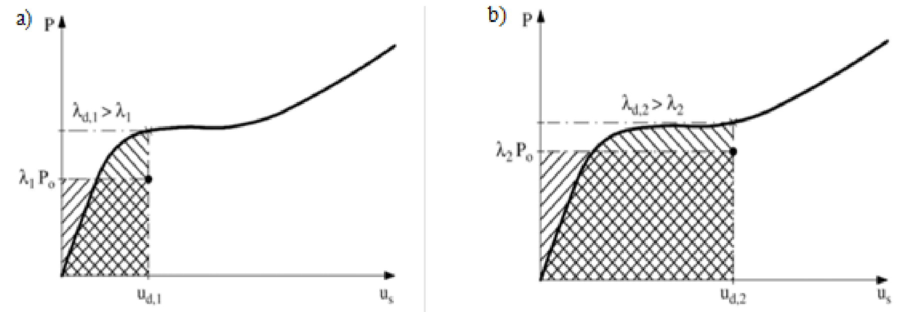

(a) Dynamic response $P_{d1} = \lambda_1 P_0$ (b) Dynamic response $P_{d2} = \lambda_2 P_0$

Figure 7.2: Dynamic responses for P_{d1} and P_{d2} [34].

The following expression for the external work W_e and internal energy W_i can be given:

$$W_e(u) = P_0 u \tag{7.4}$$

$$W_i(u) = \int_0^u P(u)du \tag{7.5}$$

In both cases of Figure 7.2, the equivalence between external work W_e and internal energy W_i is obtained when the two depicted hatched areas become identical. This means that the two functions, in this new equilibrium state, have an interception point defined by the condition $u = u_d$; explicating the equation:

$$P_0 u_d = \int_0^{u_d} P(u)du \tag{7.6}$$

From which the value of u_d can be determined. Thus, the dynamic response P_d can be computed as:

$$P_d = P(u_d) \tag{7.7}$$

Therefore, the dynamic amplification factor λ_d writes:

$$\lambda_d = \frac{P_d}{P_0} \tag{7.8}$$

It must be specified that this approach remain valid until a new equilibrium condition is reached by the system; in the next section this problem will be better stressed.

7.3 Probabilistic assessment of the DAF

The theory just explained, consisting in the second stage of the Simplified framework for progressive collapse assessment and, as just said, it can be adopted for the probabilistic assessment of the DAF also for the case of the multistorey plane frame.

The calculation of the DAF according to (7.8), needs for the estimates of the two terms, the original reaction P_0 and the dynamic response P_d.

7.3.1 Calculation of P_0

Therefore, the first step consists on the computation of the reaction at the point in which the column removal has been simulated during the push-over analysis. This step has been made for all the 100 different cases, to remain consistent with the probabilistic approach used. Therefore the reactions can be calculated considering the loads sampled through the *LHS* procedure which obtained results have been discussed in 6.2.3 of this thesis. After sampling, loads are multiplied for the influence area of each floor considering a width equal to the sum of half of the two central spans (5 m) and a depth equal to 5 m (it must be remembered that the sampled loads have been just computed considering the depth of 5 m thus they will be multiplied only fort the width of the influence area). At these distributed loads, the self-weight of the beams and the columns included in the considered influence area must be added taking as computational density that sampled in 6.2.1. This analysis can be resumed in the following expressions:

$$G_{1,\text{beams}} = \rho \cdot 0.4\,\text{m} \cdot 0.5\,\text{m} \cdot 4.4\,\text{m} \cdot 5 \tag{7.9}$$

where 0.4 m and 0.5 m are respectively the width and the height of the beams and 4.4 m is the total length of the two half beams excluding the node width;

$$G_{1,\text{columns}} = \rho \cdot 0.6\,\text{m} \cdot 0.6\,\text{m} \cdot 12.5\,\text{m} \tag{7.10}$$

where 0.6 m and 0.6 m are respectively the width and the depth of the columns and 12.5 is the total length of the four central remaining columns included the nodes; thus, the value of the reaction P_0 writes:

$$P_0 = G_{1,\text{beams}} + G_{1,\text{columns}} + (G_1 + G_2 + Q_f) \cdot 5\,\text{m} \cdot 4 + (G_1 + G_2 + Q_r) \cdot 5\,\text{m} \tag{7.11}$$

where 5 m is the aforementioned width of the influence area.

The obtained values of the reactions can be statistically analysed; a lognormal distribution is shown to well fit the data set, the graphs representing the probability distribution functions, the histogram with the fitted *PDF*, the probability plot and the scatter plot are reported in Figure 7.3. The value of the reaction ranges from a maximum value of 1210.65 kN, to a minimum value of 998.56 kN, the arithmetic mean is equal to 1085.33 kN.

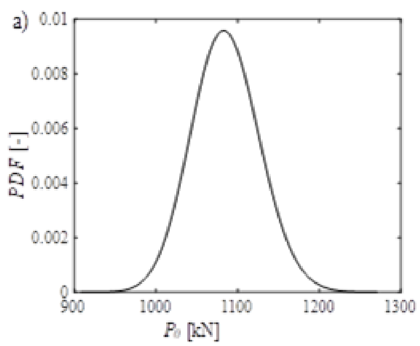

(a) Probability density function of P_0

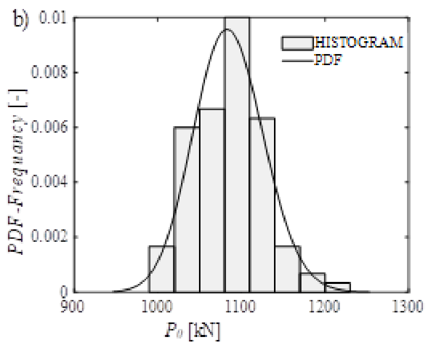

(b) Histogram and probability density function of P_0

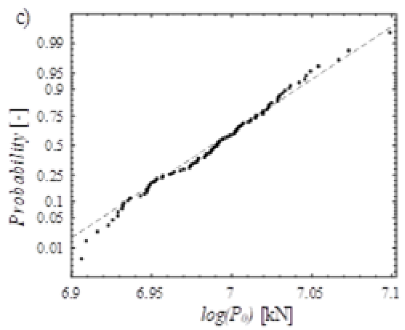

(c) Probability plot of $\log(P_0)$

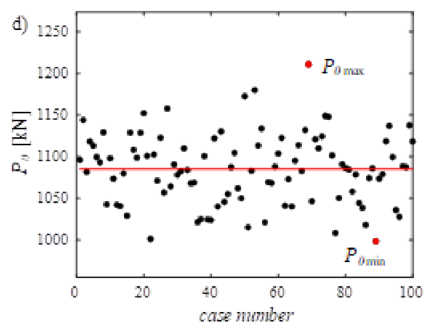

(d) Scatter plot of P_0

Figure 7.3: Plots of P_0

7.3.2 Calculation of P_d

Once that the P_0 values are obtained, the dynamic response needs. To compute the 100 different values, the equivalence between the external work and the internal energy must be found in terms of correspondent dynamic displacement. To detect the u_d, equations (7.4) and (7.5) are computed and plotted on the same graph. On Figure 7.4 and Figure 7.5 two cases, "11" and "21" are presented, repurposing the just seen capacity curve together with the energetic plot of W_i and W_e.

A graphical approach is therefore used to compute the searched solution in each of the 100 cases. From the intersection point between the two curves the corresponding abscissa u_d is then estimated. After, it is used to compute the equivalent dynamic response P_d by entering in the capacity curves and searching for the corresponding value on the ordinate axis. Now both terms are available to compute λ_d according to equation 7.8.

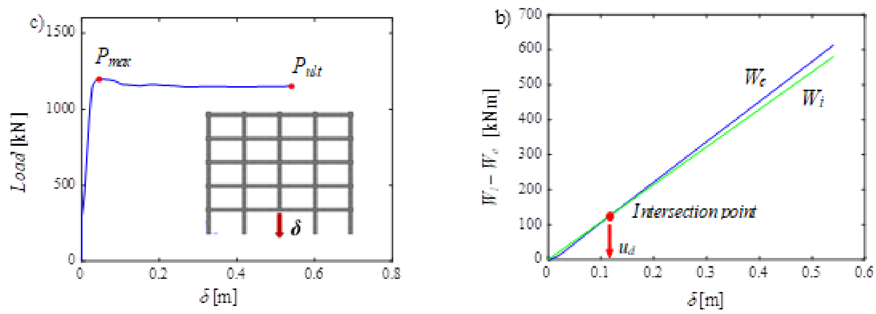

(a) Capacity curve (b) Energy plot

Figure 7.4: Case "11"

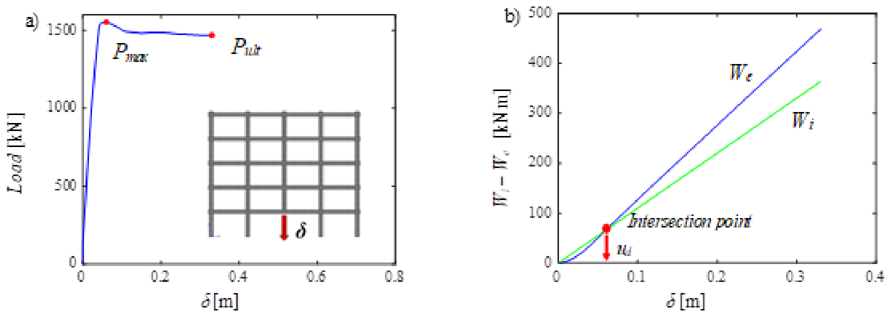

(a) Capacity curve (b) Energy plot

Figure 7.5: Case "21"

7.3.3 Probabilistic estimation of the DAF (λ_d)

The estimate of λ_d leads to a set of 100 different values ranging from a maximum of 1.448 to a minimum of 1.053. The mean value is equal to 1.229 and the representation of all the values are reported in Figure 7.6d where the red line represents the mean value.

Finally, also in this case, the obtained values of the dynamic amplification factor can be statistically analysed; a lognormal distribution is shown to well fit the data set, the graphs representing the probability distribution functions, the histogram with the fitted *PDF*, the probability plot and the scatter are reported in Figure 7.6.

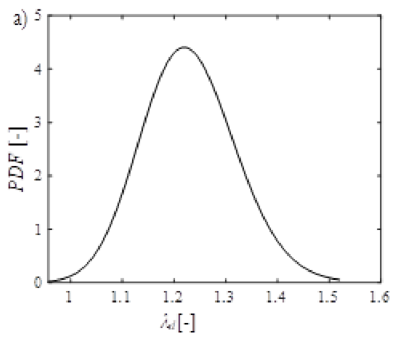

(a) Probability density function of λ_d

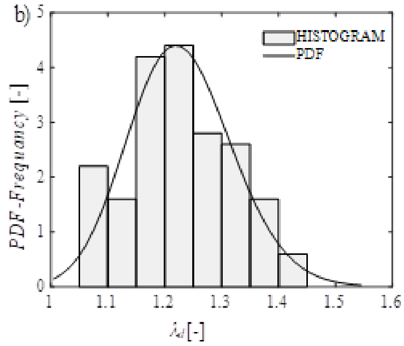

(b) Histogram and probability density function of λ_d

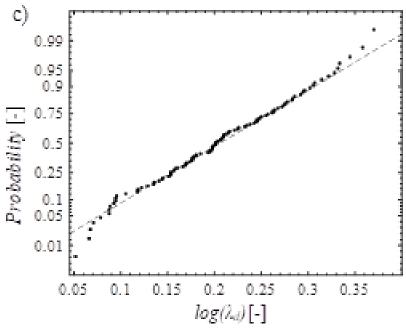

(c) Probability plot of λ_d

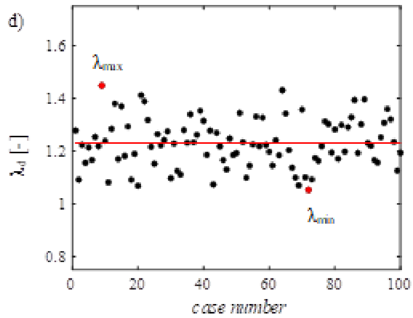

(d) Scatter plot of λ_d

Figure 7.6: Plots of λ_d

Chapter 8

Conclusion and future works

8.1 Conclusions

In this Master's Thesis the probabilistic capacity curves of a R.C. multistorey plane frame have been analysed as main goal. The structure considered for the analysis was a frame with a particular reinforcement arrangement derived by previous robustness analysis. The analysis had the objective to study the resistance of such structural system against a suddenly removal of a bearing element able to trigger a disproportioned collapse.

A probabilistic sampling has been carried out both on material and actions. The procedure followed for this purpose have implied the adoption of the Latin hypercube simulation; therefore 100 different models have been created with different characteristics and properties. The main attention has been focused on the push-down analysis, the consequent results and their possible application.

The push-down analysis have been carried out to simulate the column removal, and to understand the behaviour of the structure under this condition. The resulting displacement-force diagrams, one for each different case, define the ranges by which flexural and catenary structural behaviour can ensure a certain equilibrium condition, avoiding a disproportioned collapse. In particular, the value of the flexural peak ranges from 1198 kN to 1554 kN. While the catenary peak ranges from 1151 kN to 1518 kN.

Moreover, it can be added that the displacement value corresponding to the first peak remain almost constant while the value of the second peak change strongly for all the different 100 cases. This suggests that the maximum flexural capacity of the system involves linear elastic stage of material behaviour, being not much influenced by the sampled properties. On the contrary the catenary peak is strongly interested by the non-linear properties of materials that have been sampled; indeed the intermediate stage of the capacity curves, that in between the two peaks, is influenced by the yielding of steel, as well as the second peak itself is governed by ultimate strain and stress of materials.

Finally, capacity curves have been adopted to exploit one stage of the simplified framework for progressive collapse assessment. In particular by using the proposed simplified dynamic assessment the dynamic amplification factors λ_d have been probabilistic determined thanks to the virtual work principle and the capacity curves previously defined. Analysis have led to a set of 100 different values ranging from a maximum of 1.448 to a minimum of 1.053. these values represent the hypothetic dynamic amplification that loads can show if a column loss scenario would happen.

8.2 Future developments

The results obtained up to this point constitute only the starting point of more complex probabilistic robustness analysis. Indeed, capacity curves found in chapter 6 give information regarding the global behaviour of the structure under a column removal condition, while from the dynamic amplification factors computed in this chapter, it possible to understand which could be the dynamic response of the structure under the same exceptional event.

However, the DAF as just suggested, could be used to simulate the dynamic effect of the column removal, applying it directly on the loads in a set of probabilistic non-linear structural analysis, in which, through some expedient such an a temporally fictitious reaction, the column removal can be simulated. This approach might produce a set of probabilistic simulations from which the behaviour of the structural system against a disproportioned collapse could be directly analysed.

Moreover, the aforementioned simulation results, in terms of deformation due to amplified loads, might be the starting point of a reliability analysis conducted with the aim to find the probability of failure P_f of such structure and consequently the reliability index β according to expression (2.11) which could express finally a measure of the structural safety and robustness of the structure under analysis.

All this procedure, conducted with a probabilistic approach could represent the basis of a new path work for the future of the structural design procedure, producing more accurate results, but less conservative and therefore economically advantageous.

Bibliography

[1] JCSS. *Probabilistic Model Code, Part 1 - Basis of Design*. 2000. URL: https://www.jcss-lc.org/publications/jcsspmc/desbasis2a.pdf.

[2] Seung-Kyum Choi, Ramana Grandhi, and Robert A. Canfield. *Reliability-based Structural Design*. Springer London, 2007. DOI: 10.1007/978-1-84628-445-8.

[3] CNR. *Istruzioni per la valutazione della robustezza delle costruzioni*. 2018. URL: https://www.cnr.it/it/node/9625.

[4] MIT. Aggiornamento delle «Norme tecniche per le costruzioni». In: *Gazzetta Ufficiale della Repubblica Italiana* (Feb. 18, 2018), pp. 1–198. URL: https://www.gazzettaufficiale.it/eli/gu/2018/02/20/42/so/8/sg/pdf.

[5] *Eurocode 1 - Actions on structures - Part 1-7: General actions - Accidental actions*. Tech. rep. European Committee for Standardization, July 19, 2006.

[6] *Recommendations for Designing Collapse-Resistant Structures*. Tech. rep. Structural Engineering Institute, 2010.

[7] *fib Model Code for Concrete Structures 2010*. Ernst W. + Sohn Verlag, Nov. 1, 2013. ISBN: 3433030618. URL: https://www.ebook.de/de/product/20594378/fib_model_code_for_concrete_structures_2010.html.

[8] *Eurocode - Basis of structural and geotechnical design*. Tech. rep. European Committee for Standardization.

[9] *Minimum Design Loads for Buildings and Other Structures*. American Society of Civil Engineers, Nov. 2005. DOI: 10.1061/9780784408094.

[10] Diego Gino. "Advances in reliability methods for reinforced concrete structures". PhD thesis. Politecnico di Torino, Sept. 19, 2019. URL: http://hdl.handle.net/11583/2754713.

[11] M. D. Mckay, R. J. Beckman, and W. J. Conover. "A Comparison of Three Methods for Selecting Values of Input Variables in the Analysis of Output From a Computer Code". In: *Technometrics* 42.1 (Feb. 2000), pp. 55–61. DOI: 10.1080/00401706.2000.10485979.

[12] C. Allin Cornell. "A Probability-Based Structural Code". In: *Journal Proceedings* 66 (12 Dec. 1, 1969). Ed. by American Concrete Institute, pp. 974–985.

[13] Abraham M. Hasofer and Niels Lind. "An Exact and Invariant First Order Reliability Format". In: *Journal of Engineering Mechanics* 100 (Jan. 1974), pp. 111–121.

[14] G. Koenig and D. Hosser. *The simplified level II method and its application on the derivation of safety elements for level I. Bullettin no. 147.* Tech. rep. CEB, 1982.

[15] *Partial factor methods for existing concrete structures. Bulletin no. 80.* Tech. rep. International Federation for Structural Concrete, 2016.

[16] MIT. Istruzioni per l'applicazione dell'«Aggiornamento delle "Norme tecniche per le costruzioni"» di cui al decreto ministeriale 17 gennaio 2018. In: *Gazzetta Ufficiale della Repubblica Italiana* (Feb. 11, 2019), pp. 1–337. URL: `https://www.gazzettaufficiale.it/eli/gu/2019/02/11/35/so/5/sg/pdf`.

[17] *Eurocode 2 - Design of concrete structures - Concrete bridges - Design and detailing rules.* Tech. rep. European Committee for Standardization, Oct. 12, 2005.

[18] *Calcestruzzo - Specificazione, prestazione, produzione e conformità, UNI EN 206:2016.* Tech. rep. UNI - Ente Italiano di Normazione, Dec. 1, 2016.

[19] Fortunato Mauro. "Robustezza strutturale di edifici intelaiati in calcestruzzo armato: analisi parametrica e nuove proposte progettuali". PhD thesis. Politecnico di Torino, 2019.

[20] Luca Giacomo Capri. "Robustezza strutturale di opere multipiano in calcestruzzo armato: analisi parametrica di telai 2D per mezzo di modelli globali e locali". PhD thesis. Politecnico di Torino, 2019.

[21] Silvia Caprili and Walter Salvatore. "Mechanical performance of steel reinforcing bars in uncorroded and corroded conditions". In: *Data in Brief* 18 (June 2018), pp. 1677–1695. DOI: `10.1016/j.dib.2018.04.072`.

[22] Arthur Slobbe et al. "On the value of a reliability-based nonlinear finite element analysis approach in the assessment of concrete structures". In: *Structural Concrete* 21.1 (June 2019), pp. 32–47. DOI: `10.1002/suco.201800344`.

[23] Yong Lu and Xiaoming Gu. "Probability analysis of RC member deformation limits for different performance levels and reliability of their deterministic calculations". In: *Structural Safety* 26.4 (Oct. 2004), pp. 367–389. DOI: `10.1016/j.strusafe.2004.01.001`.

[24] Andreas J Kappos, Marios K Chryssanthopoulos, and C. Dymiotis. "Uncertainty analysis of strength and ductility of confined reinforced concrete members". In: *Engineering Structures* 21.3 (Mar. 1999), pp. 195–208. DOI: `10.1016/s0141-0296(97)00181-8`.

[25] JCSS. *Probabilistic Model Code, Part 2 - Load Models.* 2001. URL: `https://www.jcss-lc.org/publications/jcsspmc/part_ii.pdf`.

[26] JCSS. *Probabilistic Model Code, Part 3 - Resistance Models.* 2002. URL: `https://www.jcss-lc.org/publications/jcsspmc/part_iii.pdf`.

[27] M. Saatcioglu and S. R. Razvi. "Strength and Ductility of Confined Concrete". In: *Journal of Structural Engineering* 119.10 (Oct. 1993), pp. 3109–3110. DOI: `10.1061/(asce)0733-9445(1993)119:10(3109)`.

[28] Vladimír Červenka, Libor Jendele, and Jan Červenka. *ATENA Program Documentation Part 1 Theory.* Ed. by Cervenka Consulting Ltd. 2012.

[29] Meng-Hao Tsai and Bing-Hui Lin. “Dynamic amplification factor for progressive collapse resistance analysis of an RC building”. In: *The Structural Design of Tall and Special Buildings* 18.5 (Aug. 2009), pp. 539–557. DOI: 10.1002/tal.453.

[30] S. M. Marjanishvili. “Progressive Analysis Procedure for Progressive Collapse”. In: *Journal of Performance of Constructed Facilities* 18.2 (May 2004), pp. 79–85. DOI: 10.1061/(asce)0887-3828(2004)18:2(79).

[31] Taewan Kim, Jinkoo Kim, and Junhee Park. “Investigation of Progressive Collapse-Resisting Capability of Steel Moment Frames Using Push-Down Analysis”. In: *Journal of Performance of Constructed Facilities* 23.5 (Oct. 2009), pp. 327–335. DOI: 10.1061/(asce)0887-3828(2009)23:5(327).

[32] Kapil Khandelwal and Sherif El-Tawil. “Pushdown resistance as a measure of robustness in progressive collapse analysis”. In: *Engineering Structures* 33.9 (Sept. 2011), pp. 2653–2661. DOI: 10.1016/j.engstruct.2011.05.013.

[33] Shalva Marjanishvili and Elizabeth Agnew. “Comparison of Various Procedures for Progressive Collapse Analysis”. In: *Journal of Performance of Constructed Facilities* 20.4 (Nov. 2006), pp. 365–374. DOI: 10.1061/(asce)0887-3828(2006)20:4(365).

[34] B. A. Izzuddin et al. “Progressive collapse of multi-storey buildings due to sudden column loss — Part I: Simplified assessment framework”. In: *Engineering Structures* 30.5 (May 2008), pp. 1308–1318. DOI: 10.1016/j.engstruct.2007.07.011.

[35] Anil K. Chopra. *Dynamics of structures: Theory and applications to earthquake engineering*. International Series in Civil Engineering and Engineering Mechanics. Prentice-Hall, 1995, p. 729.

[36] *Alternate Path Analysis & Design Guidelines For Progressive Collapse Resistance*. Tech. rep. US GSA, 2016.

[37] *UFC 4-023-03 Design Of Buildings To Resist Progressive Collapse, With Change 3*. Tech. rep. US Department of Defense, 2016.

[38] Griengsak Kaewkulchai and Eric B. Williamson. “Beam element formulation and solution procedure for dynamic progressive collapse analysis”. In: *Computers & Structures* 82.7-8 (Mar. 2004), pp. 639–651. DOI: 10.1016/j.compstruc.2003.12.001.

[39] A. J. Pretlove, M. Ramsden, and A. G. Atkins. “Dynamic effects in progressive failure of structures”. In: *International Journal of Impact Engineering* 11.4 (Jan. 1991), pp. 539–546. DOI: 10.1016/0734-743x(91)90019-c.